Funded by
the European Union

ACCREU
Assessing
Climate Change
Risk in EUrope

ACCREU

Assessing Climate Change Risk in EUrope

GA number: 101081358, Funding type: HORIZON-CL5-2022-D1-07-two-stage

Deliverable number	**D 4.4**
Milestone name:	*Integrated Policy Assessment of adaptation, mitigation and residual damages: planned scenario-experiments in the IAMs*
WP / WP number:	4
Delivery due date:	Project month 39 (31/08/2026) Postponed to 30/09/2026
Actual date of submission:	09/11/2026
Dissemination level:	[confidential/public]
Lead beneficiary:	UU
Responsible scientist/administrator:	Matthias Van der Heyden
Contributor(s):	Matthias Van der Heyden, Laurent Drouet, Ramiro Parrado, Franziska Piontek, Paul Watkiss, Pieter Sayer, Andries Hof & Kaj-Ivar van der Wijst
Internal reviewer:	Francesco Bosello

Funded by the European Union. Views and opinions expressed are however those of the author(s) only and do not necessarily reflect those of the European Union. Neither the European Union nor the granting authority can be held responsible for them

1. Changes with respect to DoA

A note on Deliverable 4.1 vs Deliverable 4.4.

Deliverable 4.1 details the model improvements necessary for the work in this deliverable (D4.4). However, since D4.1 was published, we have had to make several adjustments, mainly in how the adaptation functions and damage functions have been calculated. This is explained in detail in section 2.1 of this deliverable. For all intents and purposes, this deliverable supersedes the results from D4.1.

2. Dissemination and uptake

This text serves to consolidate the results of the scientific work carried out by the IAM modellers within the framework of ACCREU and to make them accessible in a clear and structured manner to stakeholders and the interested public. It will be disseminated through ACCREU's usual channels. In addition, the IAM models employed are publicly accessible on GitHub.

3. Short summary of results

This text describes how the new damage and adaptation functions that follow from the work of WP2 were implemented in the three IAMs, and what CBA-optimal results they lead to under various conditions and constraints.

4. Evidence of accomplishment

Successful model implementation in three IAMs: New, sector-specific damage and adaptation functions (for sea-level rise, riverine flooding, labour productivity, and mortality) have been developed and implemented in three independent Integrated Assessment Models.

Generation of robust, cross-model results: The models have produced consistent, quantifiable output regarding temperature pathways, emission reductions, sectoral damage, and adaptation costs up to 2100.

Table of content

1. Introduction **3**
2. Methodology **4**
2.1. Creating the Damage and Adaptation Effectiveness Functions **4**
2.2. Integrated assessment modelling scenarios protocol **16**
2.3. Channels, relationships and drivers of damages and costs **18**
2.4. IAM-specific implementation **21**
2.3.1. MIMOSA 21
2.3.2. WITCH 22
2.3.3. REMIND 24
3. Results **25**
3.1. Temperature outcomes in 2100 ..... **26**
3.2. Damages **28**
3.3. Adaptation costs **32**
3.4. Adaptation efficiency **33**
3.5. Mortality 35
4. Discussion **37**
5. Conclusion **40**
6. Bibliography **42**
7. Appendix **51**
7.1. Appendix A: Gross damage functions and adaptation functions for REMIND and WITCH **51**
7.2. Appendix B: Distribution of damages, adaptation costs and mortality costs **61**
7.2.1. REMIND 61
Gross damages 61
Adaptation costs 64
Mortality costs 65
7.2.2. WITCH 67
Gross damages 68
Adaptation costs 70
Mortality costs 71
7.2.3. MIMOSA 73
Damages 73
Adaptation 75
Mortality 75
7.3. Appendix C: Adaptation protection level under successful adaptation (ADA) vs. an implementation gap (ADA_impl_gap) **76**
7.4. Appendix D: 78
Reduced-form climate change damage functions. A robustness test with ACCREU insights 78
7.5. Appendix E: 98
Identifying differences between direct and indirect damages in economic assessments with IAMs and CGEs 98

1. Introduction

A cost-benefit analysis (CBA) of climate change provides insight into the economic implications of various climate policy strategies. The outcomes of such CBAs are determined to a considerable extent by the damage functions used, the reliability of the underlying data on mitigation and adaptation costs, the effectiveness of adaptation assumed, and the overall model characteristics. In this deliverable, we implement new damage and adaptation functions in three different Integrated Assessment Models (IAMs) in order to provide an updated assessment of CBA-optimal pathways.

Within the literature, various approaches have been adopted to modelling the economic impact of climate change. Top-down studies are macro-level analyses that seek to estimate aggregate climate damage to GDP directly and to establish global damage functions for the economy as a whole. Bottom-up studies, by contrast, focus on specific sectors, regions or countries, employing detailed empirical methods (Howard & Sterner, 2017). In the COACCH project[1]significant steps were taken to improve damage functions relative to earlier bottom-up models (van der Wijst et al. 2023); in ACCREU, we build upon COACCH and introduce further improvements.

COACCH represented a major advance on earlier Integrated Assessment Models (IAMs) in that (a) it employed separate damage functions for different sectors, namely sea level rise (SLR) and other climate effects; (b) it employed separate damage functions for different regions; and (c) it used updated damage estimates (van der Wijst et al., 2021). ACCREU goes further in several respects: (i) the non-SLR damage functions have been further disaggregated by impact sector; (ii) updated damage estimates from Work Package 2 of ACCREU are used[2]; (iii) adaptation is included globally in the analysis, rather than only for three countries; and (iv) mortality has been added as an additional impact channel. As in COACCH, these improvements are implemented in three different IAMs - MIMOSA, WITCH and REMIND - so that our results do not depend on the particularities of a single model but instead allow us to test the sensitivity of our findings to model choice.

Chapter 2 of this deliverable explains how the new damage and adaptation functions were developed, which scenarios were run, how the damage and adaptation variables are related, and how these were implemented in each IAM. Chapter 3 discusses the key results, namely the outcomes regarding temperature, emissions pathways, sectoral damage and adaptation

[1] https://www.coacch.eu/

[2] It should be noted that the set of impact drivers employed in ACCREU is more limited than that used in COACCH. This is a deliberate methodological choice, justified by the fact that only those impact drivers for which explicit adaptation functions are available can be included in the analysis. Since the central objective of ACCREU is precisely to integrate adaptation into the modelling framework, restricting the analysis to this subset of drivers ensures consistency between the adaptation functions and the impact channels considered. The reduction in the number of impact drivers relative to COACCH therefore reflects the specific purpose of ACCREU rather than an arbitrary narrowing of scope. To provide the context of the updated damages provided by ACCREU, Appendix D presents a comparison of the damage functions produced by the ACCREU and COACCH projects.

costs, and sectoral adaptation efficiency. In doing so, we consistently present results for a scenario without additional policy; for various optimisations, in which different constraints are imposed on the models; and for variations in adaptation efficiency.

2. Methodology

2.1. Creating the Damage and Adaptation Effectiveness Functions

Throughout the ACCREU project, impact models have been used to create new estimates of climate impacts and adaptation options and costs. In Work Package 4, we integrate these results in an integrated policy analysis. Specifically, in Work Package 2, new impact estimates have been created for several impact sectors: riverine flooding, labour productivity, sea-level rise, and agriculture. Since the available scenarios for the agriculture sector did not include global results for both low and high RCP's, and both with and without adaptation (which are needed to use them in this deliverable in a meaningful way), we will focus on the three impact sectors that have a global coverage: riverine flooding, labour productivity, and sea-level rise. For each of them, we create new reduced-form damage functions for the economic damages without adaptation (called gross damages from now on), drawn from WP2 model runs without or with minimal adaptation (see deliverables D2.1, D2.2, D2.3 and D2.5). Then, for each impact sector, we use the results from Work Package 3 on adaptation costs and effectiveness (D3.4), also relying on input from WP2 models, but with different levels of adaptation, to create adaptation effectiveness functions. In this section, we detail how both the gross damage functions and the adaptation functions have been constructed.

A note on temperature values

The impact models in Work Package 2 used CMIP6 input data for climate drivers, but they do not provide temperature pathways directly as output. Therefore, to derive temperature-dependent damage functions we draw directly from the IPCC AR6 scenario database for RCP-specific global mean temperature pathways. Specifically, we use the median values of the variable "AR6 climate diagnostics|Surface Temperature (GSAT)|MAGICCv7.5.3|50.0th Percentile" for the scenarios matching the following filters:

RCP	**Scenario name matches…**
RCP 2.6	*-26
RCP 4.5	*-45
RCP 6.0	*-60
RCP 7.0	SSP3-Baseline
RCP 8.5	SSP5-Baseline

Table 1: Filters used to calculate temperature outcomes per RCP.

This gives the following temperature series:

Year	2020	2030	2040	2050	2060	2070	2080	2090	2100
RCP									
RCP 2.6	1.22	1.46	1.65	1.75	1.79	1.79	1.75	1.69	1.63
RCP 4.5	1.21	1.46	1.73	1.96	2.17	2.34	2.44	2.53	2.56
RCP 6.0	1.20	1.46	1.76	2.07	2.37	2.64	2.88	3.09	3.25
RCP 7.0	1.20	1.49	1.85	2.23	2.60	3.00	3.37	3.78	4.21
RCP 8.5	1.22	1.55	1.94	2.40	2.89	3.43	3.99	4.53	5.04

Table 2. Temperature outcomes per RCP as used throughout this deliverable.

2.1.1. Riverine flooding

The impacts of riverine flooding are estimated using the GLOFRIS model (see Deliverable 2.1). For the gross damage function, the low-adaptation scenario is used, for RCP 2.6, RCP 4.5, RCP 6.0 and RCP 8.5. GLOFRIS provides EAD in 2030, 2050 and 2080 which have been inflated from 2005 USD to 2017 USD and expressed as % of GDP.

The resulting GDP impacts, as a function of global mean temperature, are shown in Fig. 1. While the impacts vary strongly per region, a consistent almost-linear or quadratic response to global mean temperature can be observed. For each region, we fit the following function:

$$EAD(T) = a + b * T + c * T^2, \; where \; c \geq 0.$$

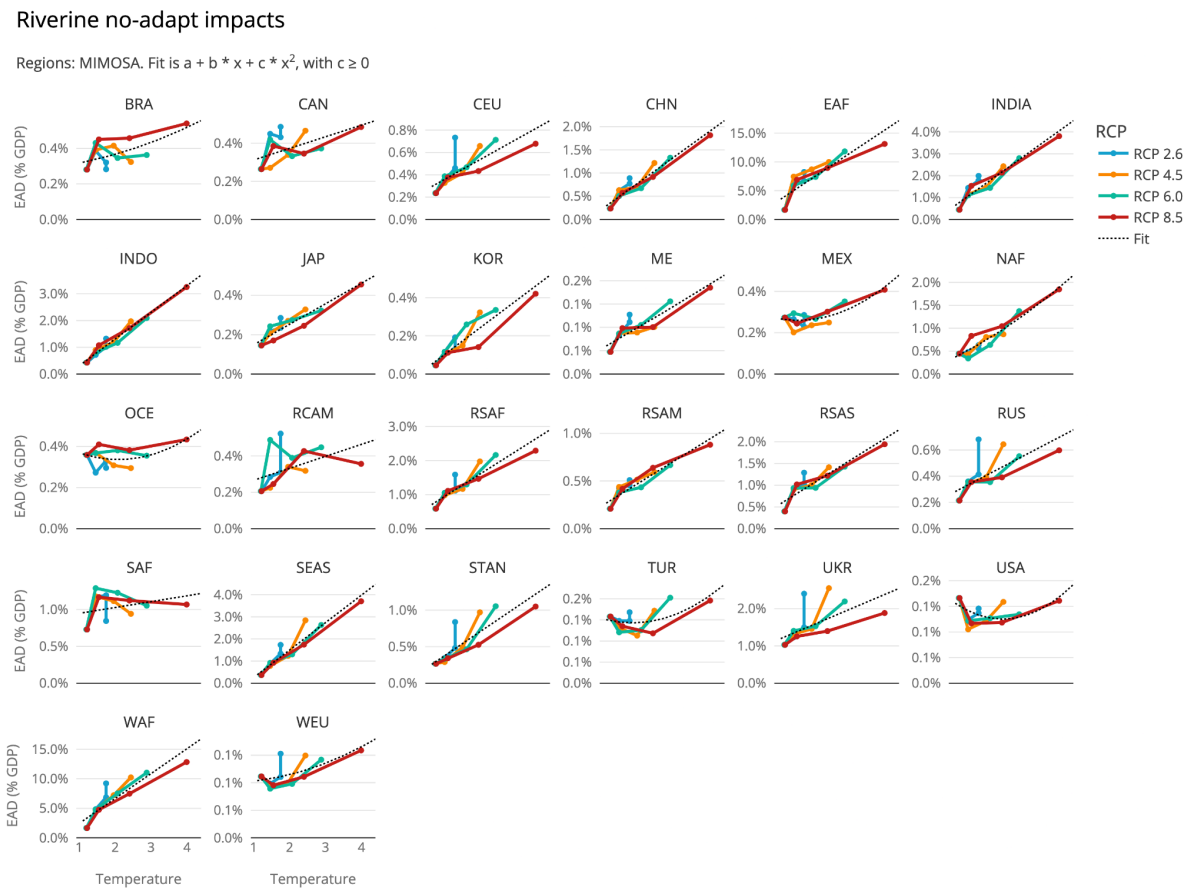

Fig. 1. Gross damages for riverine floodings as a function of GMT (°C above pre-industrial). The coloured lines represent the direct results from GLOFRIS (annualised). The dotted line is the best fit of a quadratic function. Regional aggregation is shown here for the MIMOSA regions. See appendix A. for fitted coefficients for each IAM.

GLOFRIS also provides various levels of adaptation, with associated adaptation costs: constant dike height ("constant"), constant expected annual damages ("EAD constant") and optimal adaptation ("optimal"). The model estimates costs as a present value over a 2020-2050 investment period in 2005 USD. It was therefore necessary to convert this to an annual adaptation cost which was done by first converting the present value into an annuity using the 5% discount rate used in GLOFRIS modelling. This annuity was then inflated to 2017 USD and finally, maintenance costs were added as 1% of cumulative investment in line with GLOFRIS modelling assumptions. The annual adaptation costs used to develop the adaptation functions was the sum of the annual investment and maintenance costs.

The result of this annualisation process was that the only variation in adaptation costs over time were those driven by the maintenance costs which, by design, were a small proportion of total costs. It was therefore deemed that the relationship between adaptation costs and damage was most faithfully modelled by only using the last timestep (2080).

The resulting adaptation costs, and associated effectiveness, are shown in Fig. 2. Throughout this section, *effectiveness* is defined as the percentage of avoided gross damages through adaptation. These are assumed to be yearly values: spending *x* dollars on adaptation leads to *y* % of reduced damages, in a single year.

The adaptation estimates are fitted with the following function:

$$eff(adaptcosts) = a * (1 - e^{-b*adaptcosts}), \; with \; a \leq 1.$$

Here, a is the maximum effectiveness (value between 0 and 1), and b the cost parameter, expressed in (trillion US$2017)$^{-1}$. This functional form leads automatically to marginally decreasing impact of adaptation: it becomes increasingly more expensive to reach higher adaptation effectiveness, with an asymptote of a, the maximum effectiveness.

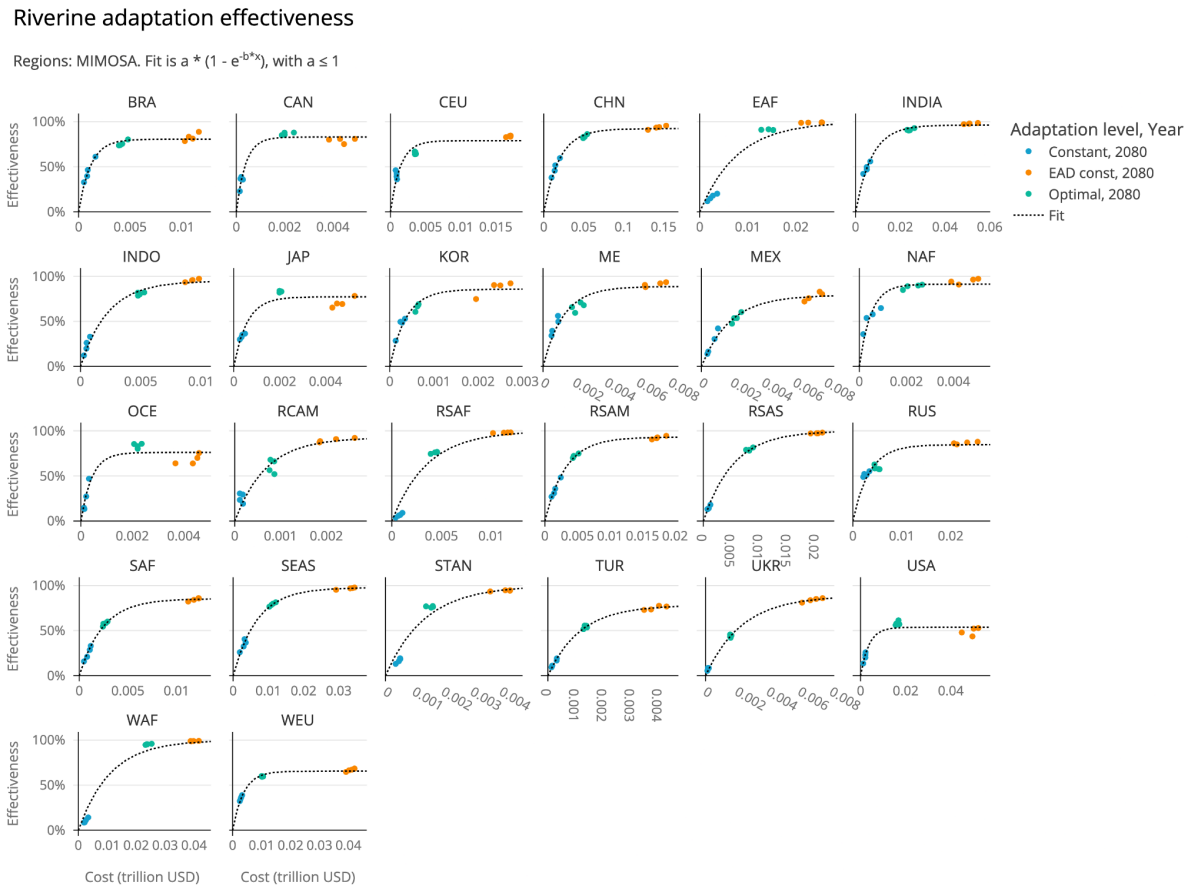

Fig. 2. Adaptation effectiveness (in % of avoided gross damages) for riverine floodings as a function of regional adaptation costs (in trillion US$2017 MER). See appendix A. for fitted coefficients for each IAM.

2.1.2. Labour productivity

The impact of climate change on labour productivity (see Deliverable 2.3) can be decomposed in two types: heat-related expected annual costs due to warming (e.g. hot regions get hotter, leading to reduced labour productivity), and cold-related expected annual benefits due to less cold days (especially relevant for currently cold regions).

First, the heat-related EAD shows a near-linear response to GMT, as shown in Fig. 3. The fitted function is:

$$EAD(T) = a + b * T$$

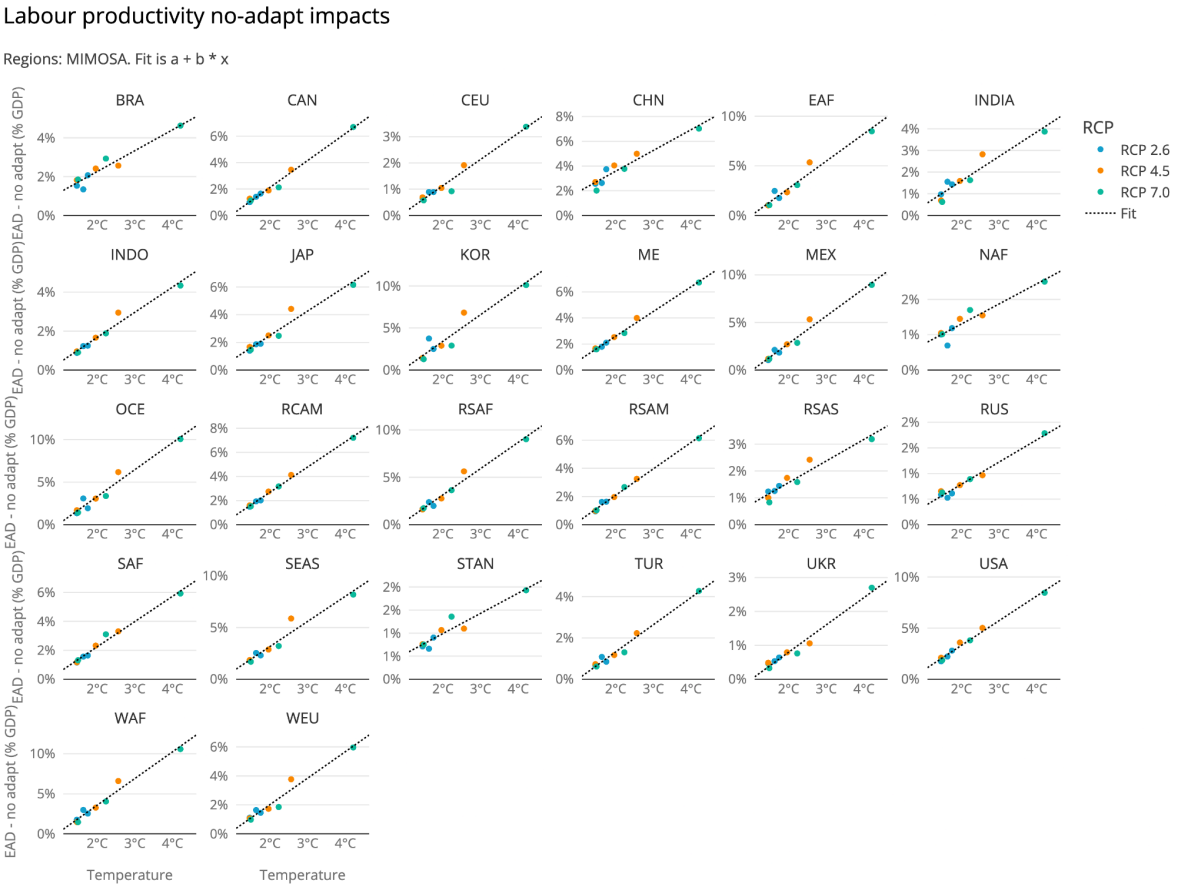

Fig. 3. Gross damages for heat-related labour productivity impacts, as a function of GMT (°C above pre-industrial). See appendix A. for fitted coefficients for each IAM.

Second, cold-related labour productivity benefits are shown in Fig. 4, together with the net impacts (heat-related costs + cold-related benefits). This also shows a linear relation. While it is interesting to see the net impacts from heat and cold related impacts, it is important to keep them separate, since adaptation will only reduce the heat-related costs, and not the cold-related benefits.

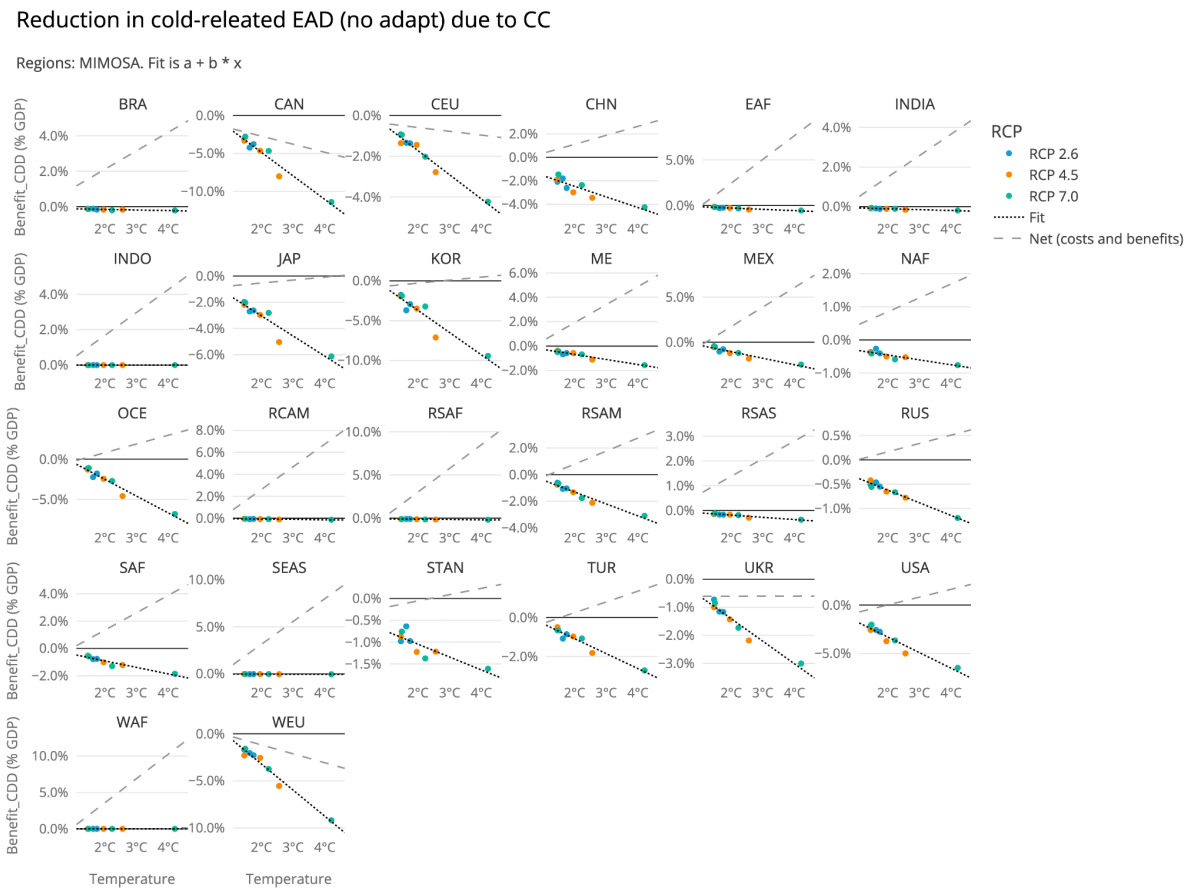

Fig. 4. Cold-related labour productivity benefits (dotted lines), and net costs and benefits (dashed line), as a function of GMT (°C above pre-industrial). See appendix A. for fitted coefficients for each IAM.

Adaptation to labour productivity impacts is modelled as cooling expenditure (see D2.2 and D2.3 (Colleli 2026). See Fig. 5. for the resulting adaptation effectiveness functions. Since a large part of labour happens in places where air conditioning is ineffective, the maximum effectiveness is 15-20%, much less than for riverine flooding.

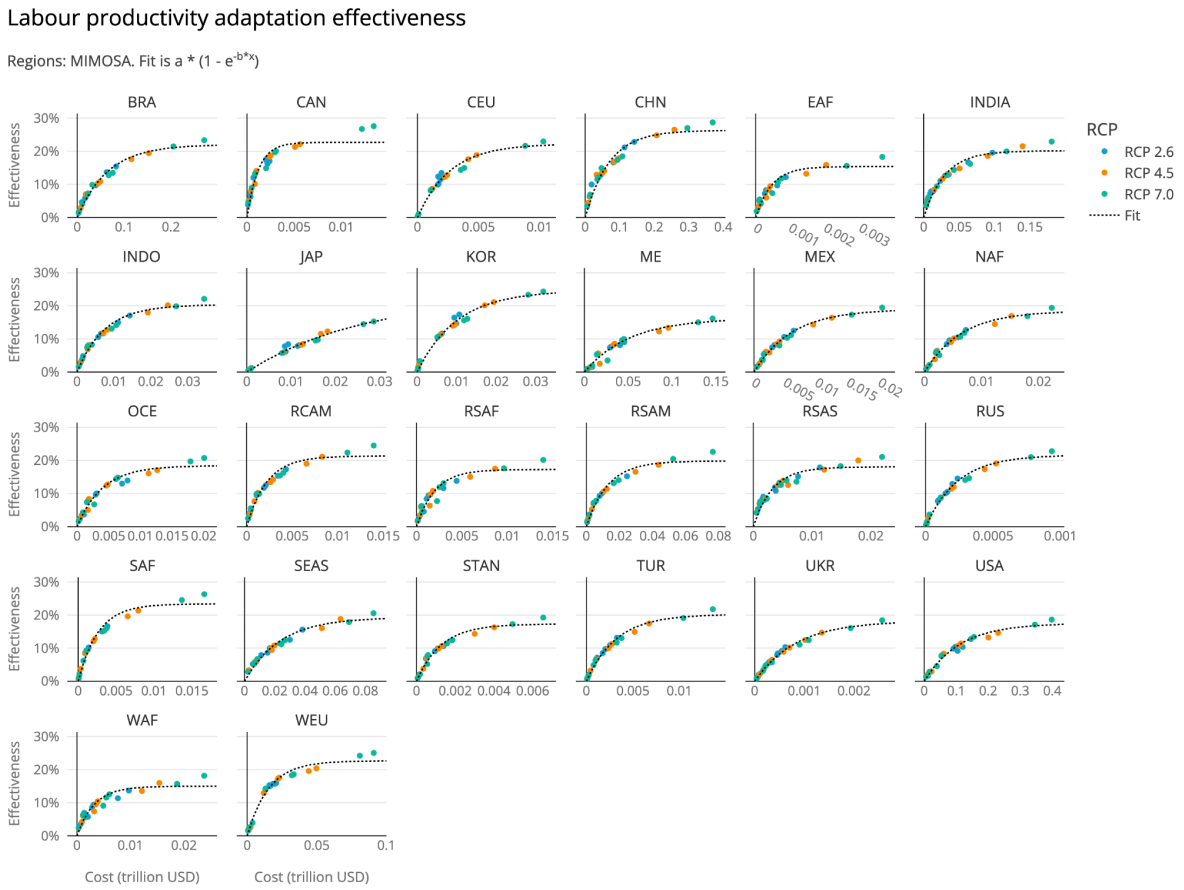

Fig. 5. Adaptation effectiveness (in % of avoided gross damages) for the heat-related labour productivity costs as a function of regional adaptation costs (in trillion US$2017 MER). See appendix A. for fitted coefficients for each IAM.

2.1.3. Sea-level rise

The sea-level rise impacts are calculated using the DIVA model (see Deliverable 2.1). Specifically, for this purpose, we compare the Constant Dike Height scenario ("low-adaptation / CDH") with three adaptation scenarios: Constant flood protection standards, Doubling flood protection standards, and Quadrupling flood protection standards. Importantly, we do not use the "optimal adaptation" scenario from DIVA, to avoid double optimisation in the IAMs.

The low-adaptation gross damages are shown in Fig 6, as a function of sea-level rise relative to 2020 (in meters), for RCP 2.6, RCP 4.5, and RCP 7.0. We fit a power function to the data:

$EAD(SLR) = a + b * (SLR)^c$.

For numerical stability when determining the best fit, we constraint the power coefficient c between 0.2 and 3.

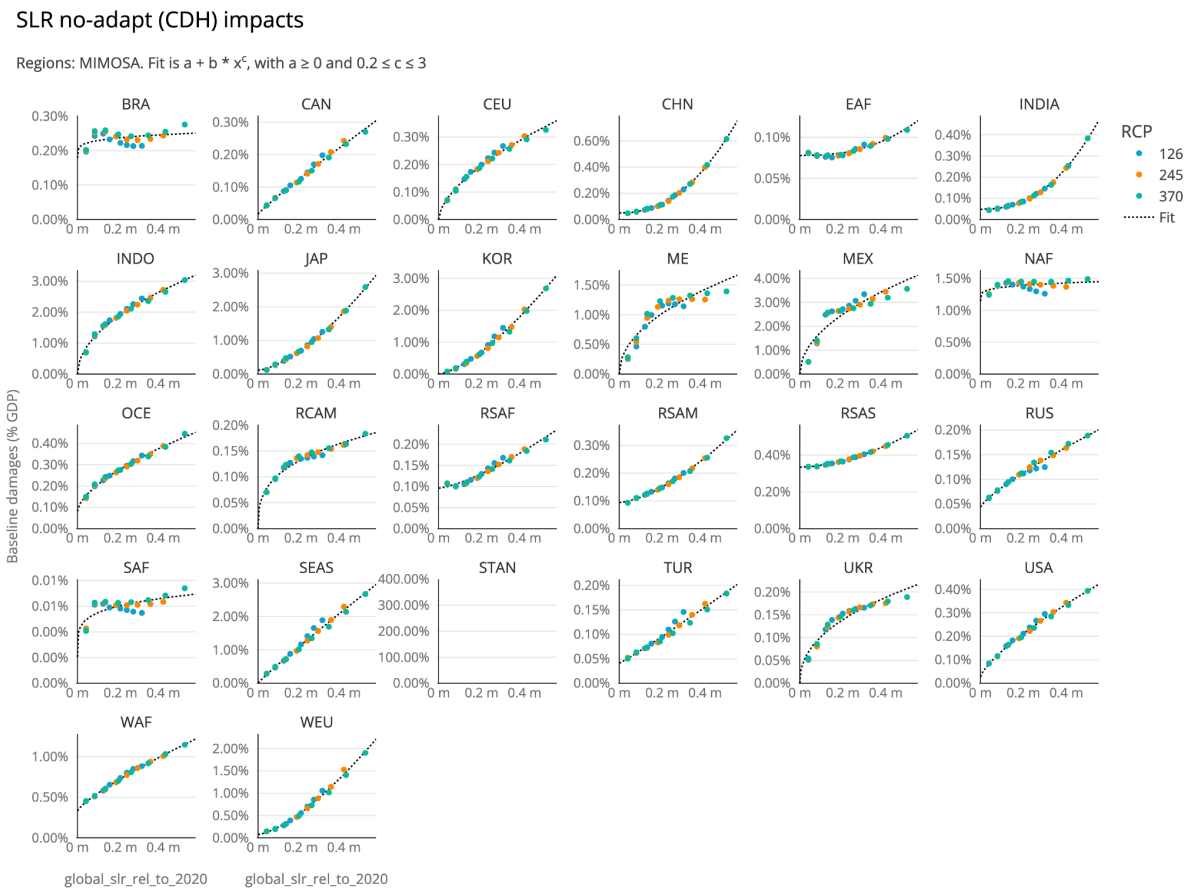

Fig. 6. Gross sea-level rise impacts (constant dike height scenario, see D4.1) as a function of global sea-level rise (in meters, relative to 2020 level). See appendix A for fitted coefficients for each IAM.

Adaptation data is again fitted with the same negative-exponential saturation fit as for riverine flooding and labour productivity, as shown in Fig 7. This leads to a maximum effectiveness of 80-100%.

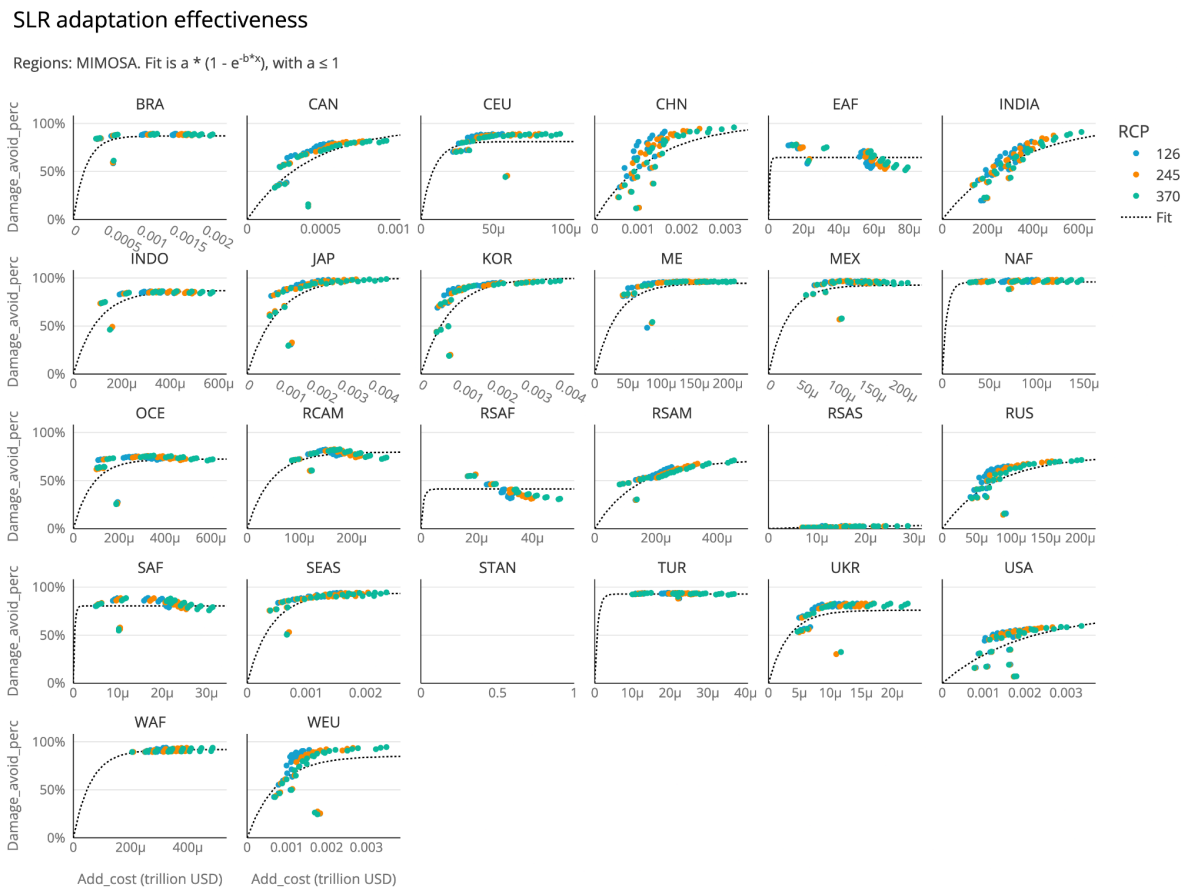

Fig. 7. Adaptation effectiveness (in % of avoided gross damages) for sea-level rise impacts as a function of regional adaptation costs (in trillion US$2017 MER). See appendix A. for fitted coefficients for each IAM.

2.1.4. Combined riverine flooding and labour productivity impacts

Since the REMIND model is not able to have two separate control variables for the riverine flooding adaptation costs and the labour productivity adaptation costs, we also create a combined adaptation effectiveness function, combining adaptation costs and effectiveness of the two impact sectors.

There is no straightforward analytical solution for this function, a given amount A of adaptation costs can be split in many ways between adaptation for riverine flooding, and adaptation for labour productivity. For every region, temperature level, and total adaptation budget A, we allocate the expenditure between riverine flooding adaptation and labour productivity adaptation, such that the total residual damages are minimised. Specifically, if A_i is adaptation costs in sector i ($i = R$ for riverine and $i = L$ for labour productivity), E_i the adaptation effectiveness function for sector i, and $D_i(T)$ the gross damages for sector i at temperature T, we calculate:

$$\max_{A_R, A_L} E_R(A_R) \cdot D_R(T) + E_L(A_L) \cdot D_L(T)$$

subject to $A_R + A_L = A$, and $A_R, A_L \geq 0$. Combining the optimal sectoral expenditures A^*_R and A^*_L, we can calculate the resulting effectiveness of the total amount A. As shown in Fig. 8, there is only very little influence of the temperature parameter. For this reason, we made the combined adaptation function temperature-independent, using a central value T=2.5°C. Through the optimised values, we fit the same negative-exponential saturation curve as the other sectors.

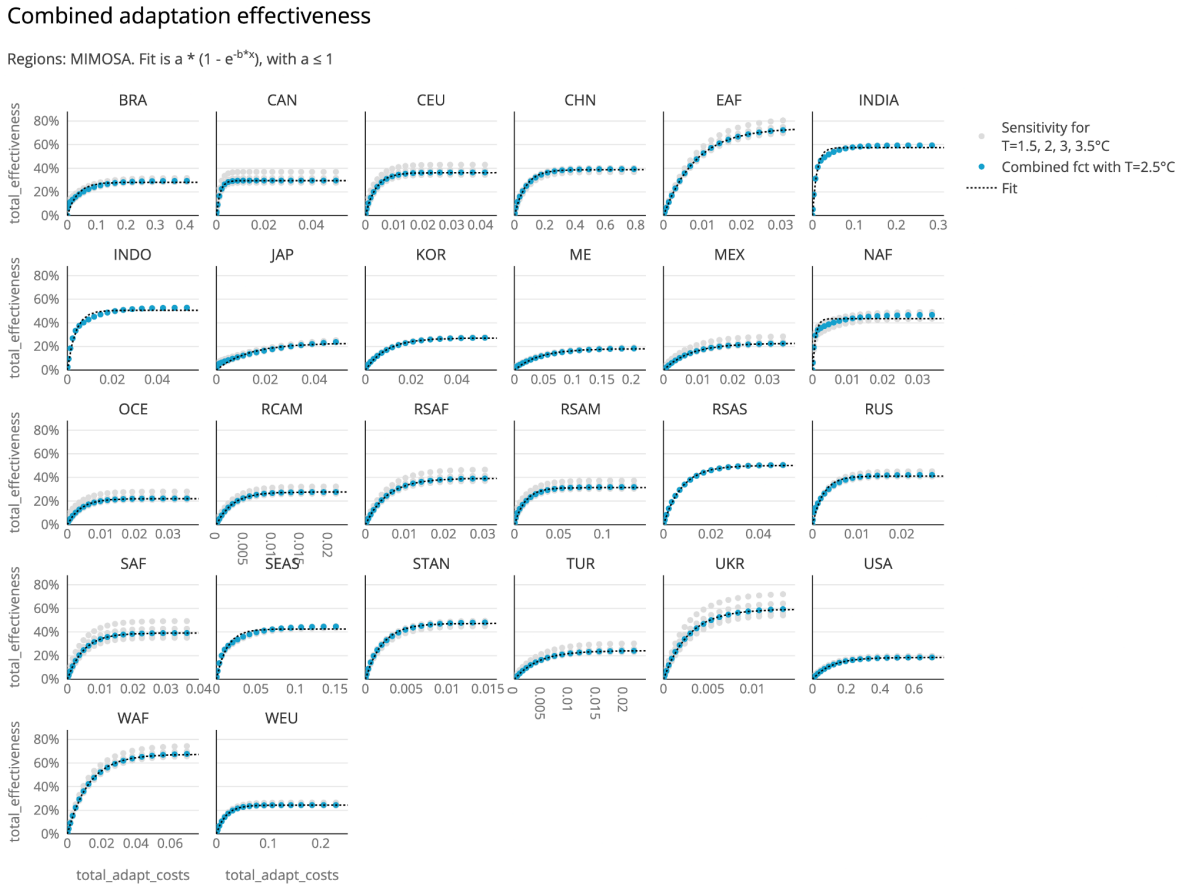

Fig. 8. Combined adaptation effectiveness (in % of avoided gross damages) for riverine and labour productivity impacts combined, as a function of regional adaptation costs (in trillion US$2017 MER). See appendix A. for fitted coefficients for each IAM. The blue dots are the result of the optimisation routine for 20 values of the total adaptation costs, where the gross damages are calculated with T=2.5°C. The dotted black line is the fit through those points of the negative-exponential saturation curve. The light grey dots represent the sensitivity optimisation runs, with different temperature values between 1.5°C and 3.5°C.

Fig 9 shows how the total adaptation costs would have been distributed between riverine and labour productivity adaptation costs if the two sectors were modelled separately. The strong non-linearities and different behaviours per region show why it is important to do this optimisation per region and per level of adaptation costs, and not simply add the two underlying functions.



Fig. 9. Share of how the total adaptation costs (x-axis) are split between adaptation in riverine flood protection (yellow) vs in labour productivity adaptation (blue). The x-axis is expressed in trillion US$2017 MER.

2.1.5. Mortality

ACCREU aims to extend impact analyses to non-market impacts. In the IAM analyses we therefore also include temperature-related mortality impacts, though without accounting for explicit adaptation. Like labour productivity, there is a heat-related and cold-related component, varying strongly between regions. As global mean temperature increases, the heat-related mortality increases, while the cold-related mortality decreases.

The mortality forecasts are sourced from Bressler et al. (2021). The paper forecasts the change in future heat-related and cold-related mortality rates under RCP 2.6, RCP 4.5, RCP 6.0 and RCP 8.5 scenarios. It does so for the 2040-59 and 2080-99 periods. For this analysis, the estimates for these ranges are assigned to the years 2050 and 2090 respectively. In order to convert the forecasted change in the mortality rate into an estimate of excess mortality, the Bressler forecasts were combined with mortality rate forecasts from the World Bank (2025).

Excess mortality$_{trcp}$ (% of population) = % change in mortality rate$_{trcp}$ (%) * mortality rate$_{t}$ (% of population)

where t is the year and RCP is the RCP scenario.

The resulting values, as % of population, for both heat-related and cold-related mortality are shown in Fig. 10. The heat-related mortality was fitted with a quadratic function. Given that they represent additional mortality relative to 2010, the fit was relative to temperature in 2010: 1.1°C:

$$mortality_{heat,r}(T) = a + b * (T - 1.1)^2$$

Cold-related mortality showed a linear relation with temperature, accounting for the fact that reductions in cold-related mortality don't become marginally larger when temperatures become very high. In fact, at some point we expect to see a plateau. However, the data doesn't show this behaviour for the assessed temperature range, where a linear fit throughout is the best fit.

$$mortality_{cold,r}(T) = a + b * (T - 1.1)$$

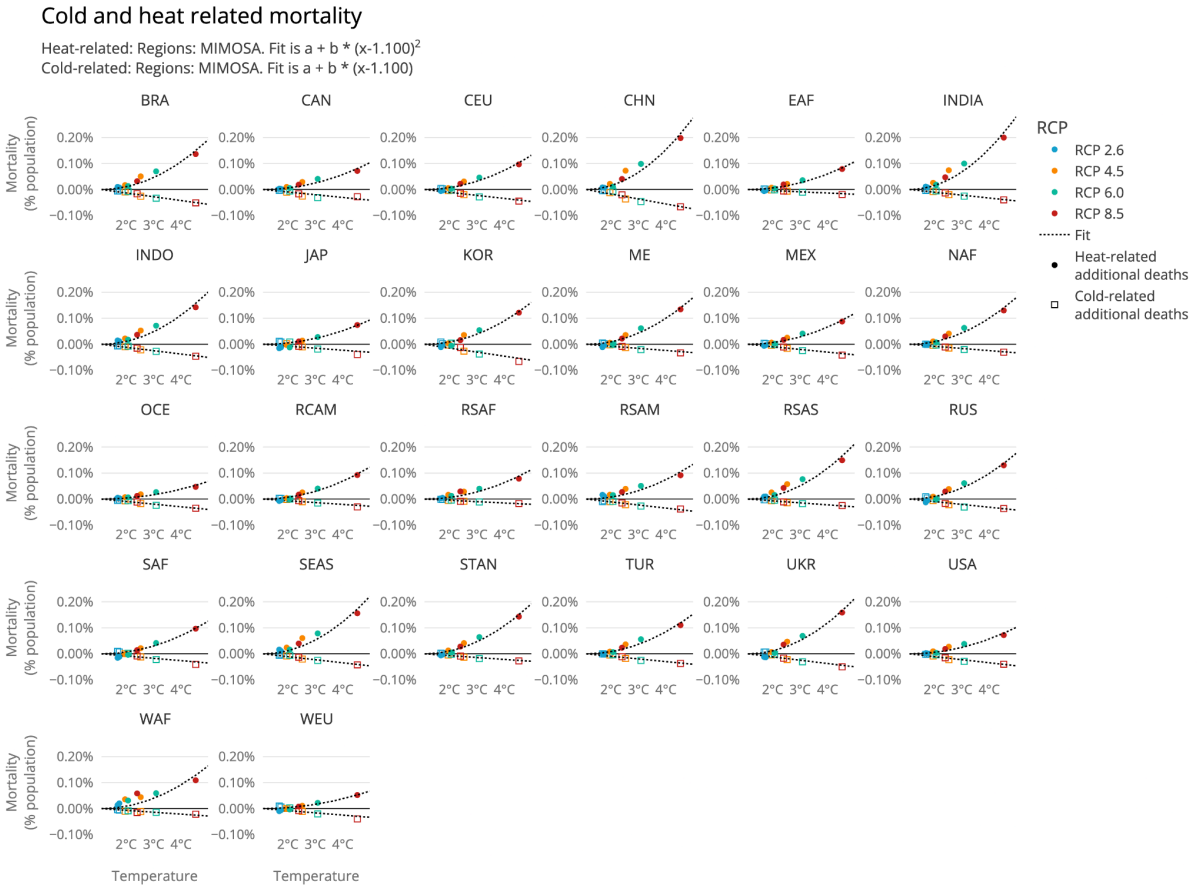

Fig. 10. Mortality damage functions, expressing mortality in % of regional population as a function of global mean temperature. The solid circles represent additional heat-related mortality, while the open squares represent the reduction in cold-related mortality. See appendix A. for fitted coefficients for each IAM.

2.1.6. Valuing the cost of mortality

The net temperature-related mortality is monetised to be taken into account in the welfare functions of the Integrated Assessment Models. This is done only for a subset of the scenarios, given the challenges around such a monetization.

Valuation of mortality in monetary units can be done using values of statistical life (VSL) or values of statistical life years (VSLY) multiplied by the expected life years lost. The main difference between these valuation methods is that the VSLY approach gives relatively lower values to mortality of people with a lower remaining life expectancy, while the VSL approach values mortality in all age classes equally. As the largest mortality change from climate change occurs in the elderly population, using a VSLY approach would result in a lower valuation of mortality than VSL. As discussed in Botzen et al. (2020), one could argue that preventing deaths of younger people is more valuable than preventing deaths of older people with fewer remaining life years - but whether giving lower values to mortality of older people is desirable or ethically justified may be debated. Here, we follow the recommendation by the OECD to not adjust valuation according to the age of the population as this would imply that public policy and cost-benefit analysis outcomes could differ solely based on differences in the age of the populations studied. Moreover, little is known about the expected life years lost due to climate change impacts (Toulemon & Barbieri, 2008).

We therefore use the VSL approach for valuing the cost of mortality. Throughout this deliverable, we use the recommended estimates of the VSL from the OECD (2025). They provide a weighted world value of the VSL of $2.4 million, in 2022 USD PPP. We compare this value to the world GDP per capita of 2022 (also expressed in PPP dollars, given by the World Bank) of $20 409 per capita, leading to the following value:

$$VSL = 117.59 \times GDP_{cap}$$

This value therefore scales with the GDP per capita of a region. However, the value 117.59 is constant for all the regions (see graphs B7-B-10, B16-B18 and B-26-B-26 in annex B for the differing regional effects of this valorisation).

2.2. Integrated assessment modelling scenarios protocol

We have developed eight scenarios to simulate different policy choices and assess their effects on temperature rise, damage and potential adaptation costs. The ‘No Policy’ run assumes no additional mitigation or adaptation policies, whereas in all other scenarios such policies are implemented. In the latter scenarios, a cost-benefit-optimal outcome is always sought, but different constraints are imposed on the models. We have implemented the scenarios across the three models. All eight scenarios are implemented across the three models and are described below, along with a short explanation of their relevance.

1. No Policy
In this scenario, no adaptation or mitigation is undertaken. We adopt the SSP-2 assumptions regarding economic growth and emissions, and do not implement any climate policy beyond what is currently in place. This scenario is set against all other scenarios in which some form of additional policy is implemented.

2. ADA
This scenario is a cost-benefit analysis in which adaptation is the only form of response. There is no explicit mitigation.

3. MIT
This scenario is a cost-benefit analysis in which mitigation is the only form of climate policy. There is no adaptation.

4. MIT_then_ADA
This is the optimal scenario, in which damage is minimised as much as possible. First, a cost-benefit analysis is carried out in which only mitigation measures are considered (this is identical to the MIT scenario). This emissions pathway is then used as the basis for a second analysis, in which the optimal level of additional adaptation is calculated. This scenario explicitly avoids the weighing of adaptation against mitigation given the current lack of robustness and the incompleteness of the adaptation costs and effectiveness estimates.

5. MIT_ADA
This is a cost-benefit analysis in which adaptation and mitigation policies are implemented simultaneously. As such, the models weigh expenditures and effectiveness on adaptation and mitigation against one another. While this will lead to higher economic output than the previous scenario, it relies heavily on the assumptions that all regions will adapt optimally to climate change in all time periods and that this optimal adaptation, based on models and assumptions from the Holocene, will be successful under Anthropocene conditions. As these assumptions may be too optimistic, especially given, among other things, the difficulty in estimating cost-effectiveness parameters (cf. supra), we include the MIT_then_ADA scenario above. We included this scenario as well, as in previous CBA studies with explicit adaptation, this type of optimisation has been used (Amirmoeini et al., 2026; Bahn et al., 2019; de Bruin et al., 2009).

6. MIT_late_ADA
For the period up to 2045, it is a cost-benefit analysis in which adaptation is the sole form of response and no mitigation policy is pursued. Starting in 2050, this is a cost-benefit analysis in which adaptation and mitigation policies are implemented simultaneously. This scenario serves to illustrate what would happen if policymakers postpone investments in mitigation further and focus solely on adaptation in the short term, whilst. This scenario is plausible because policymakers are confronted with three opposing forces: (1) budgetary constraints, (2) climate disasters that will intensify the public's demand for government protection, and (3) political forces opposed to mitigation policy within and between countries. This scenario serves to illustrate the long-term effects of such policy choices.

7. ADA_red_eff

This scenario is a cost-benefit analysis in which adaptation is the sole form of response to climate impacts. There is no mitigation. The difference compared with the ADA scenario is that we assume an unexpected failure of adaptation policy. We reduce the effectiveness of adaptation by 50 per cent. We do this to take into account the possibility that the assumptions underlying our adaptation functions are too optimistic.The data underlying these functions are, after all, model-based, aggregate and incomplete, and they are likely to miss many real-world issues that drive up costs and reduce effectiveness. Furthermore, this data is based on a world that is only in the early stages of global temperature increase. Consequently, it is uncertain whether these functions can be extrapolated to a future with prolonged climate change.

8. ADA_impl_gap

This scenario is a cost-benefit analysis in which adaptation is the sole form of response to climate impacts. There is no mitigation. The difference compared with the ADA-scenario is that this scenario takes into account the institutional capacity of different countries. Rich, developed countries are more likely to be able to successfully implement adaptation policies than poor, underdeveloped countries. We use the quantification of differentiating adaptive capacity from Andrijevic et al. (2020) and apply it to the adaptation cost estimate.

2.3 Channels, relationships and drivers of damages and costs

Figure 11 illustrates how the relevant variables in the IAMs relate to one another and how their outputs are derived in terms of adaptation costs, adaptation effectiveness and climate damage.

2.1.1. Direct damages

2.1.1.1. Sea Level Rise and Riverine Flooding

The climate impact of both Sea Level Rise and Riverine Flooding operate in the same fashion. Global mean temperature is determined by greenhouse gas emissions (which, in turn, is determined by the presence or absence of mitigation policies) and subsequently affects the Gross Damages caused by climate damage. In scenarios where adaptation policies are in place, a certain amount is spent on adaptation measures at each time step, leading to a reduction in damage. The residual damage that remains after adaptation is what will actually be experienced as loss to GDP, while total costs also include the costs of adaptation.

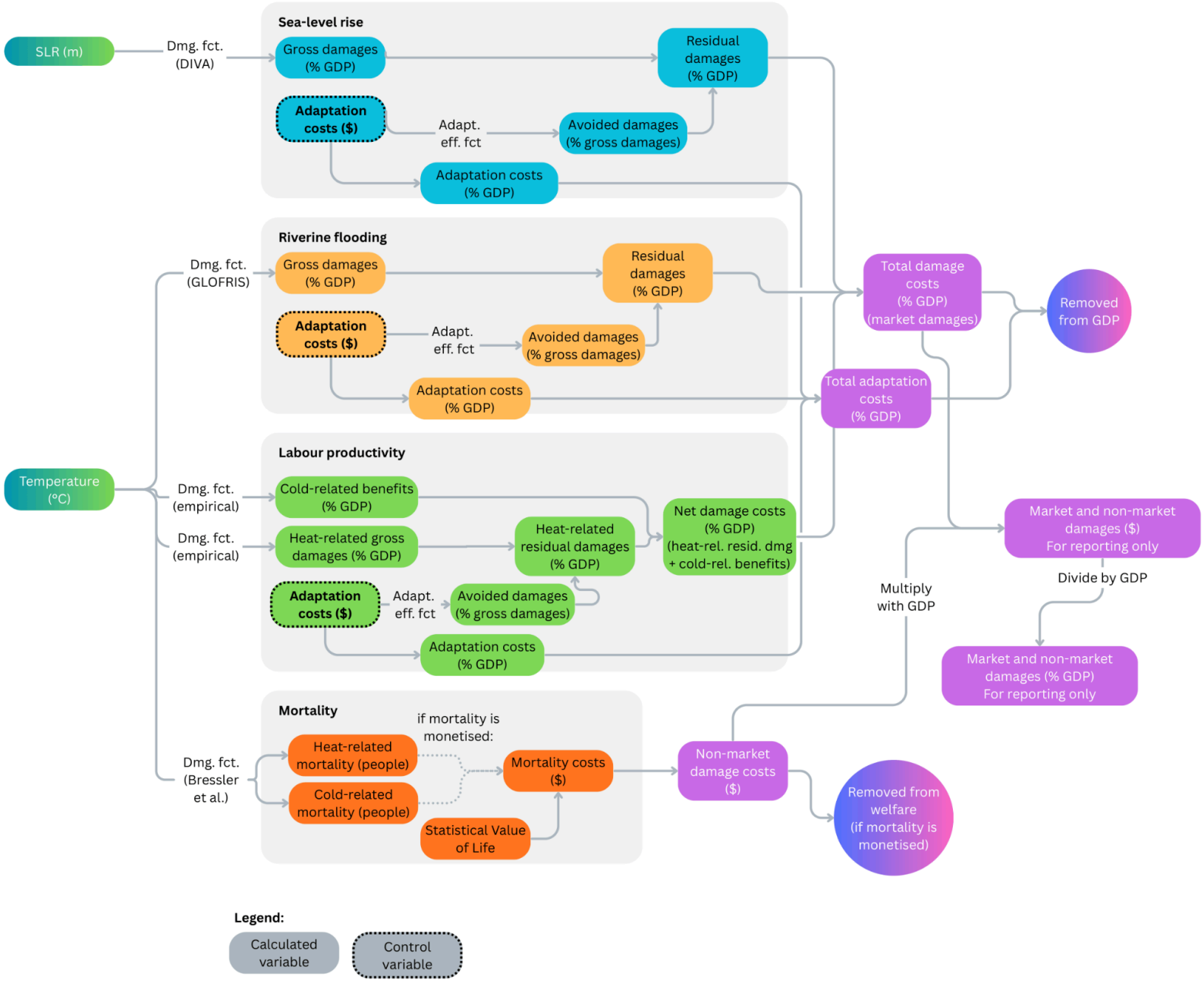

Figure 11: Flowchart with relationship of damage and adaptation variables in IAMs.

2.1.1.2. Labour Productivity

Certain climatic conditions are optimal for labour productivity, while it is decreased in colder as well as hotter conditions (with humidity also playing an important role in interaction with heat). This is already true in present day conditions. Consequently, rising global temperatures will cause the negative effect of heat on labour productivity to become more prevalent and wide-spread, whilst the losses due to cold temperatures will decrease. As a result, our models include two separate functions that express the effect of weather conditions on labour productivity:

- The heat function works in a similar way to the effects of sea-level rise and riverine flooding described above: gross damage is a consequence of global temperature increase, whilst expenditure on adaptation reduces the remaining, residual damage.
- The cold function works in the opposite way: increasing temperature results in benefits.

As with SLR and riverine flooding, the damage is deducted from Gross GDP, and the costs of mitigation and adaptation are deducted from GDP, which leads to lower investments.

2.1.1.3. Mortality

In addition to the effect of changing weather conditions on labour productivity, there is also an effect on mortality. Indeed, we observe excess mortality during both heatwaves and cold spells. Hence, two effects are again taken into account: an increase in heat-related deaths and a decrease in cold-related deaths. With increasing global mean temperature in colder regions, the net effect can be positive, but in most regions this leads to an increase in excess mortality compared with present-day conditions.

Since this form of losses, unlike the economic consequences of sea-level rise, river flooding and loss of labour productivity, has no direct impact on the supply side of the economy, or even on GDP: it is included in the modeling as a loss of welfare driven by reduced consumption. Note that this means that its economic effects are modelled as a reduction in demand and that any potential additional temperature reduction in scenarios with mortality result from the fact that it is cheaper to increase the amount of mitigation and adaptation than to permit the knock-on effects of this structural demand reduction as a result of an increase in the number of deaths. It is important to note that the supply side of the economy is exogenous with respect to the level of demand. The effect therefore affects the welfare function alone; it exerts no influence on the development of the production function.

As explained in 2.1.6, we use a global average value of 117 times GDP per capita to quantify the additional excess mortality within a cost-benefit framework. Since regions have different GDP per capita, this results in not every death being valued at a nominally equal amount. We do not wish to imply that one person's moral value is greater than another's, but neither do we wish to simulate unrealistic behaviour on the part of governments by assigning exactly the same value to every individual. Alternative approaches can be easily implemented by selecting a different Statistical Value of Life (SVL) as an input parameter.

2.1.2. Indirect damages

All of the above forms of damage have a direct impact on investment or consumption. However, climate damage, mortality and expenditure on mitigation and adaptation all cause the economic trajectory to deviate further from a baseline in which the economy can grow unchecked, as there is

less scope for productive investment. As a result of this decline in investment, the model also accumulates indirect damage.

2.4 IAM-specific implementation

2.4.1 MIMOSA

For this deliverable, we use MIMOSA version 1.4. Compared to the previous COACCH project, several general aspects have been updated in MIMOSA: the baseline values have been recalibrated using the latest SSP updates, the starting year is now 2025 instead of 2020, the sea-level rise module has been replaced by a more detailed version, calibrated to the latest IPCC AR6 report, and a variable timestep has been introduced to allow for better finetuning of the timesteps.

Specifically for this project, the damage module has been fully replaced. The total damage costs are calculated as

$$D_{r,t}^{tot} = D_{r,t}^{SLR}(1 - P_{r,t}^{SLR}) + D_{r,t}^{riverine}(1 - P_{r,t}^{riverine}) + D_{r,t}^{heat_labourprod}(1 - P_{r,t}^{heat_labourprod}) + L_{r,t}^{benefit},$$

where $D_{r,t}^{i}$ are the gross damage costs in impact sector i, at region r and timestep t, $P_{r,t}^{i}$ is the protection level (between 0 and 1), and $L_{r,t}^{benefit}$ is the benefits of reduced cold-related labour productivity impacts.

Consequently, the adaptation costs are:

$$AC_{r,t}^{tot} = AC_{r,t}^{SLR} + AC_{r,t}^{riverine} + AC_{r,t}^{heat_labourprod}.$$

Since the adaptation effectiveness functions in this deliverable are given as a function of adaptation costs in 2017 dollars MER, they are first converted to MIMOSA's default currency unit: 2010 dollars PPP.

MIMOSA can be run in optimisation mode or in simulation mode. In optimisation mode, the model tries to find values for the control variables (typically the amount of regional mitigation and the amount of adaptation costs) such that the welfare function is maximised. The welfare function used here is the *regional welfare-loss minimising* function, where utility is calculated for every region. The global welfare is calculated as the sum of the regional utility values weighted by population. Then, the sum of the discounted yearly global welfare is maximised. Here, we use a medium pure rate of time preference of 1.5%/year.

In simulation mode, the values of the control variables are given as input. For example, a baseline run is a run in simulation mode where mitigation and adaptation values are set to 0.

Given the nature of the adaptation functions, it is possible to calculate the optimal amount of adaptation analytically. Since the adaptation effectiveness is given by:

$$eff(AC) = a * (1 - e^{-b*AC}),$$

the optimal amount of AC is taken such that the sum of adaptation costs and residual damages is minimised. This leads to the following analytical solution:

$$AC_{opt,r,t} = log(a_r \cdot b_r \cdot D^i_{r,t} \cdot GDP_{r,t}).$$

nopolicy	Simulation run with mitigation and adaptation control variables set to 0
ADA	Simulation run with mitigation set to 0, but adaptation set to analytical optimal solution
MIT	Optimisation run where mitigation is optimised, but adaptation forced to 0
MIT_then_ADA	Sequential run. First a MIMOSA optimisation run is done with adaptation set to 0 (exactly MIT). Then a simulation run is done with the mitigation control values from MIT, and adaptation set to analytical optimal solution.
MIT_ADA	Joint optimisation run, where mitigation and adaptation control variables are optimised at the same time
MIT_late_ADA	Same as MIT_ADA, but with mitigation forced to 0 until and including 2045. Adaptation is optimised from the start year (2025)
ADA_red_eff	Simulation run. Mitigation is set to 0. Adaptation control variable values are taken from ADA run. The effectiveness of adaptation (parameter a in the adaptation function) is reduced by 50%, leading to 50% lower protection level.
ADA_impl_gap	Simulation run. Mitigation is set to 0. Adaptation control variable values are taken from ADA run, and are multiplied by the regional adaptive capacity value (value between 0 and 1). The simulation is then run with the reduced adaptation cost values.

2.4.2 WITCH

The ACCREU damage and adaptation functions have been implemented in a dedicated damage module of WITCH, which replaces the default COACCH-based damage function. The model is run with its 17-region aggregation. The regional coefficients, estimated for the native 18 WITCH regions (Section 2.1), are aggregated to these regions using GDP weights for the damage and adaptation parameters and population weights for the mortality parameters. WITCH runs in five-year time steps. The period up to 2025 is fixed to a common current-policy run, so that all scenarios share the same history, and damages and adaptation are active from 2030 onwards.

The total damage costs are calculated as

$$D^{tot}_{r,t} = D^{SLR}_{r,t}(1 - P^{SLR}_{r,t}) + D^{riverine}_{r,t}(1 - P^{riverine}_{r,t}) + D^{heat_labourprod}_{r,t}(1 - P^{heat_labourprod}_{r,t}) + L^{benefit}_{r,t}$$

and the total adaptation costs as

$$AC^{tot}_{r,t} = AC^{SLR}_{r,t} + AC^{riverine}_{r,t} + AC^{heat_labourprod}_{r,t}$$

where $D^i_{r,t}$ are the gross damages in impact sector i, region r and period t, $P^i_{r,t}$ is the protection level (between 0 and 1), $AC^i_{r,t}$ are the adaptation costs and $L^{benefit}_{r,t}$ is the benefit of reduced cold-related labour productivity losses, which is not subject to adaptation. The total costs of climate change are the sum of both. All terms are in % of GDP. As in MIMOSA, WITCH uses the separate

adaptation effectiveness functions for sea-level rise, riverine flooding and heat-related labour productivity; the combined riverine and labour productivity function is implemented as an option but not used here.

All damage functions are anchored to the base year 2025: each fitted function is evaluated at time t minus the same function evaluated in 2025,

$$D^{i}_{r,t} = f^{i}_{r}(x_{t}) - f^{i}_{r}(x_{2025})$$

so that damages are zero in 2025 and the fitted constant cancels out. For riverine flooding and labour productivity, x is the global mean temperature above pre-industrial levels; for sea-level rise, x is global mean sea-level rise relative to 2020, which is the reference used in the fit.

The adaptation expenditures of each sector, region and period are decision variables of the model. They determine the protection level through the adaptation effectiveness functions of Section 2.1,

$$P^{i}_{r,t} = a^{i}_{r}(1 - e^{-b^{i}_{r} AC^{i}_{r,t}})$$

Adaptation expenditures are deducted from GDP in the same way as other costs, and thus compete with consumption and investment. Residual damages are deducted from gross GDP. Since the adaptation effectiveness functions take adaptation costs in trillion 2017 USD, while WITCH uses 2005 USD, the cost parameter b^{i}_{r} is rescaled with the 2005–2017 GDP deflator (a factor of about 1.23).

Net additional mortality combines the heat- and cold-related mortality functions of Section 2.1, again relative to 2025, and multiplies them by population:

$$M_{r,t} = pop_{r,t}[(h_{r}(T_{t}) - h_{r}(T_{2025}))(1 - P^{heat_labourprod}_{r,t}) + c_{r}(T_{t}) - c_{r}(T_{2025})]$$

where h_{r} and c_{r} are the heat- and cold-related mortality functions (as a fraction of the population). The reduction in cold-related mortality is a benefit that is obtained without adaptation. Since the ACCREU database does not provide an adaptation effectiveness function for mortality, WITCH applies the protection level of heat-related labour productivity, the other heat-driven adaptable impact, to heat-related mortality. This is why, unlike in the other two models, adaptation reduces additional mortality in WITCH. In the scenario variants that include mortality, net additional mortality is monetised with a value of a statistical life of 117.6 times the regional GDP per capita (Section 2.1.6). This cost is subtracted from consumption in the welfare function only; it does not enter the budget constraint, and therefore does not directly affect GDP, investment or the energy system.

WITCH is solved as a non-cooperative game between its 17 regions: each region maximises its own intertemporal welfare, defined over per capita consumption and discounted with a pure rate of time preference of 1%/year, taking the decisions of the other regions as given. The equilibrium is found by iterating over the regional optimisations until convergence. Global mean temperature is computed with WITCH's reduced-form carbon-cycle and climate module, calibrated to MAGICC, and global mean sea-level rise with a semi-empirical module based on Li et al. (2020). In the cost-benefit scenarios (MIT, MIT_ADA, MIT_late_ADA), temperature and sea-level rise are computed inside each regional optimisation, so that each region accounts for the effect of its emissions on its own damages (but not on those of other regions). In the other scenarios, temperature and sea-level rise are recomputed between iterations from the emissions of all regions: damages affect GDP, but emissions are not chosen to reduce them. All scenarios follow SSP2 population and GDP projections.

We now describe the implementation of the different scenarios.

No policy: Current policies are continued, using the same constraints as the WITCH current-policy scenario. There is no adaptation. Damages affect GDP but are not internalised in emission decisions.

ADA: As No policy, but adaptation expenditures are optimised.

MIT: Cost-benefit scenario without adaptation: each region chooses its level of mitigation by internalising its own damages. Current-policy constraints are removed.

MIT_then_ADA: The regional social cost of carbon from the MIT scenario (the shadow value of CO2 emissions divided by the marginal value of output) is imposed as a carbon tax on all taxed greenhouse gases, with negative values set to zero. Adaptation is then optimised on top. To avoid counting the damages twice, once through the tax and once through their internalisation, temperature and sea-level rise are computed outside the regional optimisation, as in the No policy scenario.

MIT_ADA: Cost-benefit scenario in which mitigation and adaptation are optimised jointly against the same damages.

MIT_late_ADA: All variables are fixed to the No policy scenario up to and including 2045. From 2050 onwards, the scenario is identical to MIT_ADA, i.e. mitigation and adaptation are optimised jointly.

ADA_red_eff: Adaptation expenditures are fixed to those of the ADA scenario, while the maximum effectiveness of adaptation is halved: $P^{i}_{r,t} = 0.5a^{i}_{r}(1 - e^{-b^{i}_{r}AC^{i}_{r,t}})$.

ADA_impl_gap: Adaptation expenditures are fixed to those of the ADA scenario, multiplied by the regional adaptive capacity $cap_{r,t}$ (between 0 and 1), based on the SSP2 governance index of Andrijevic et al. (2020): $AC^{i}_{r,t} = AC^{i,ADA}_{r,t} \cdot cap_{r,t}$. The avoided damages follow from the adaptation effectiveness functions.

2.4.3 REMIND

The total costs of climate change are calculated as

$$D^{tot}_{r,t} = D^{nonSLR}_{r,t}(1 - P^{nonSLR}_{r,t}) + L^{benefit}_{r,t} + AC^{nonSLR}_{r,t} + D^{SLR}_{r,t}(1 - P^{SLR}_{r,t}) + AC^{SLR}_{r,t}$$

where $D_{r,t}$ is the direct damage, $P_{r,t}$ is the protection level from adaptation and $AC_{r,t}$ are the adaptation costs. The total costs consist of the contribution from sea level rise (SLR) and the combined impacts of riverine floods and labor productivity (nonSLR). The positive impact of increased labor productivity is included separately, as it is not subject to adaptation. All is in % of GDP. The damage and adaptation cost functions are those described in Section 2.1. The monetized net mortality impact $M_{r,t}$ is included in the welfare function as a reduction in consumption

$$W_r = \sum_t (1 + \rho_r)^{-(t-t_0)} P_{r,t} \left\{ \left(\frac{C_{r,t} - M_{r,t}}{P_{r,t}} \right)^{1-1/\eta} - 1 \right\}^{1-1/\eta}$$

where ρ_r is the pure rate of time preference and η is the intertemporal elasticity of substitution.

Global mean temperature change and sea level rise, which drive the damage functions, are taken from MAGICC 7.5.3 (see Nauels et al. 2025). Impacts are endogenized through the social cost of carbon which takes into account the marginal effects of an additional ton of CO2 emissions on all components of the residual damage.

We now describe the implementation of the different scenarios, following an SSP2 pathway and using the most recent SSP2 GDP and population scenarios (IIASA, 2026). For the damage

calculations we assume a pure rate of time preference of 1.5% and . Starting year of the optimization is 2030, until then all is determined by historic data.

No policy: In REMIND the baseline is a current policy scenario, i.e. a scenario assuming the continuation of all currently implemented climate policies into the future, but no new additions. The emission trajectories reflect both near-term feasibility constraints and bottom-up studies on the effectiveness of the policies. Emissions remain at a high level under this scenario.

ADA: This scenario uses the same policy setting but allows an optimization of adaptation levels based on the regional adaptation cost functions.

MIT: The cost-optimal level of mitigation is determined based on the damages implemented, while no adaptation is allowed.

MIT_then_ADA: The level of mitigation is fixed to that of the MIT scenario by using the resulting carbon price as exogenous input. The optimization then allows for the free determination of the level of adaptation as in the ADA scenario.

MIT_ADA: The level of mitigation and adaptation are both determined through the optimization of welfare. The outcome is driven by the damage and adaptation cost functions.

MIT_late_ADA: While adaptation is part of the optimization from the start year, mitigation is only allowed starting in 2050. For that carbon pricing is fixed to the no policy scenario until 2045 (REMIND operates in 5-year time steps until 2060), and is set to the social cost of carbon starting in 2050.

ADA_red_eff: No mitigation is allowed, adaptation is implemented similarly to the ADA scenario, but with half the effectiveness, which is implemented in the adaptation cost function: $P_{r,t} = 0.5\gamma_{1,r}(1 - e^{-\gamma_{2,r}AC_{r,t}})$

where $\gamma_{1,r}$ and $\gamma_{2,r}$ are the regional parameters of the adaptation cost function.

ADA_impl_gap: No mitigation is allowed. The adaptation investment is fixed to that found to be optimal in the ADA scenario but reduced based on regionally varying limited adaptive capacity ($cap_{r,t}$), parameterized based on Andrijevic et al. (2020):

$$AC_{r,t} = AC_{r,t}^{ADA} * cap_{r,t}.$$

3. Results

In what follows, we will discuss the output of the three IAMs, in which the new damage and adaptation cost functions have been implemented. We will show the temperature, sectoral damage, sectoral adaptation costs, and sectoral adaptation efficiency in 2100, as well as the emission pathways throughout the 21st century.

We have run the models according to the previously described scenarios in 2.2, but not all scenarios are always displayed, as this is not always meaningful—for example, the different adaptation-only scenarios will show no difference in emissions and temperature.

We note that overall the models respond in a similar way to the damages, losses and adaptation options, though magnitudes differ due to underlying model differences.

3.1. Temperature outcomes in 2100

Scenarios without additional mitigation policy lead to a temperature rise of approximately 3°C in all models (No policy and ADA in Figure 12). The MIT and MIT_then_ADA scenarios result in the lowest temperatures in all models: between 1.9°C and 2.2°C across the IAMs. Both are CBA scenarios in which mitigation is optimised under the assumption that no adaptation is undertaken. Since adaptation is not available to offset climate impacts during the mitigation optimisation, the models pursue more ambitious mitigation, resulting in lower temperatures than in scenarios where adaptation is considered alongside mitigation (MIT_ADA). In MIT_then_ADA, adaptation is optimised in a separate second stage, while keeping the mitigation effort as in MIT, which therefore leads to practically the same temperature.

Figure 12 also shows that a delayed start to mitigation, modelled in MIT_late_ADA, cannot be fully compensated in any model. The reason for this becomes clear in Figure 13, namely that the models already undertake large-scale mitigation before 2050 in all scenarios that permit this. In MIT_ADA and MIT, the emissions reductions taking place before 2050 amount to, respectively, more than half and nearly three-quarters of the starting year's emissions. It is worth noting that these emissions also continue to decline thereafter. A delayed start means that the model subsequently has no room left to compensate for this, and consequently results in a lock-in of a higher temperature at the end of the century.

Valuing heat- and cold-related mortality leads to increased mitigation effort, with cost-optimal temperatures dropping by 0.1-0.15°C in the MIT, MIT_then_ADA, and MIT_ADA scenarios (panels d, e and f in Figure 2). This is to be expected, since an additional impact category is taken into account.

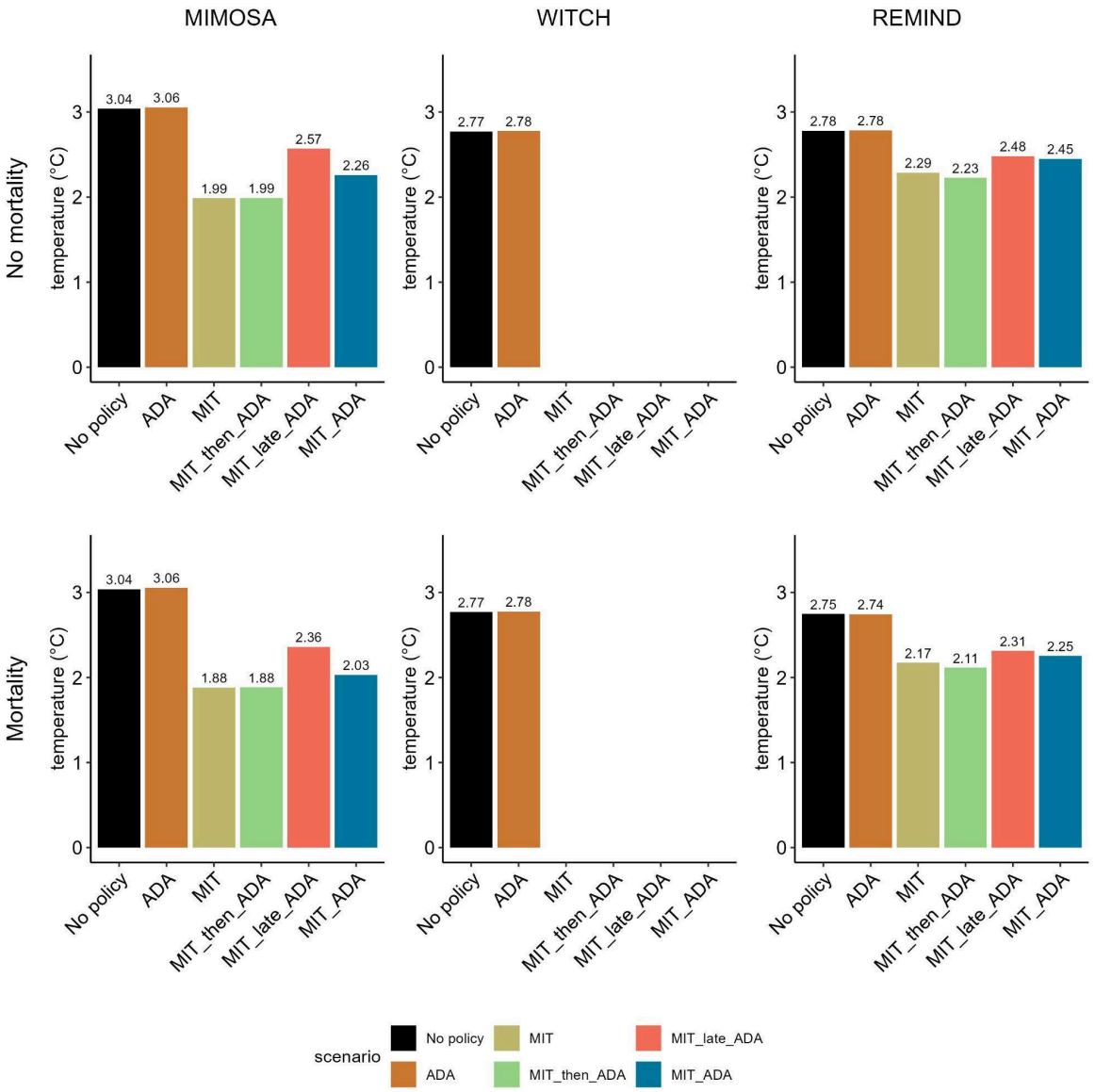

Figure 12: Global mean temperature increase with respect to pre-industrial in 2100 in 3 IAMs across multiple scenarios.

REMIND shows a lower variation than MIMOSA between the scenarios. This pattern persists throughout the results. One reason for this is that REMIND already has lower emissions in the scenario without additional policy, and, as a result, a lower end-of-century temperature because it includes more current policy measures than MIMOSA. A second reason is that REMIND has a more detailed representation of the energy sector, capturing better constraints on how quickly emissions can be reduced.

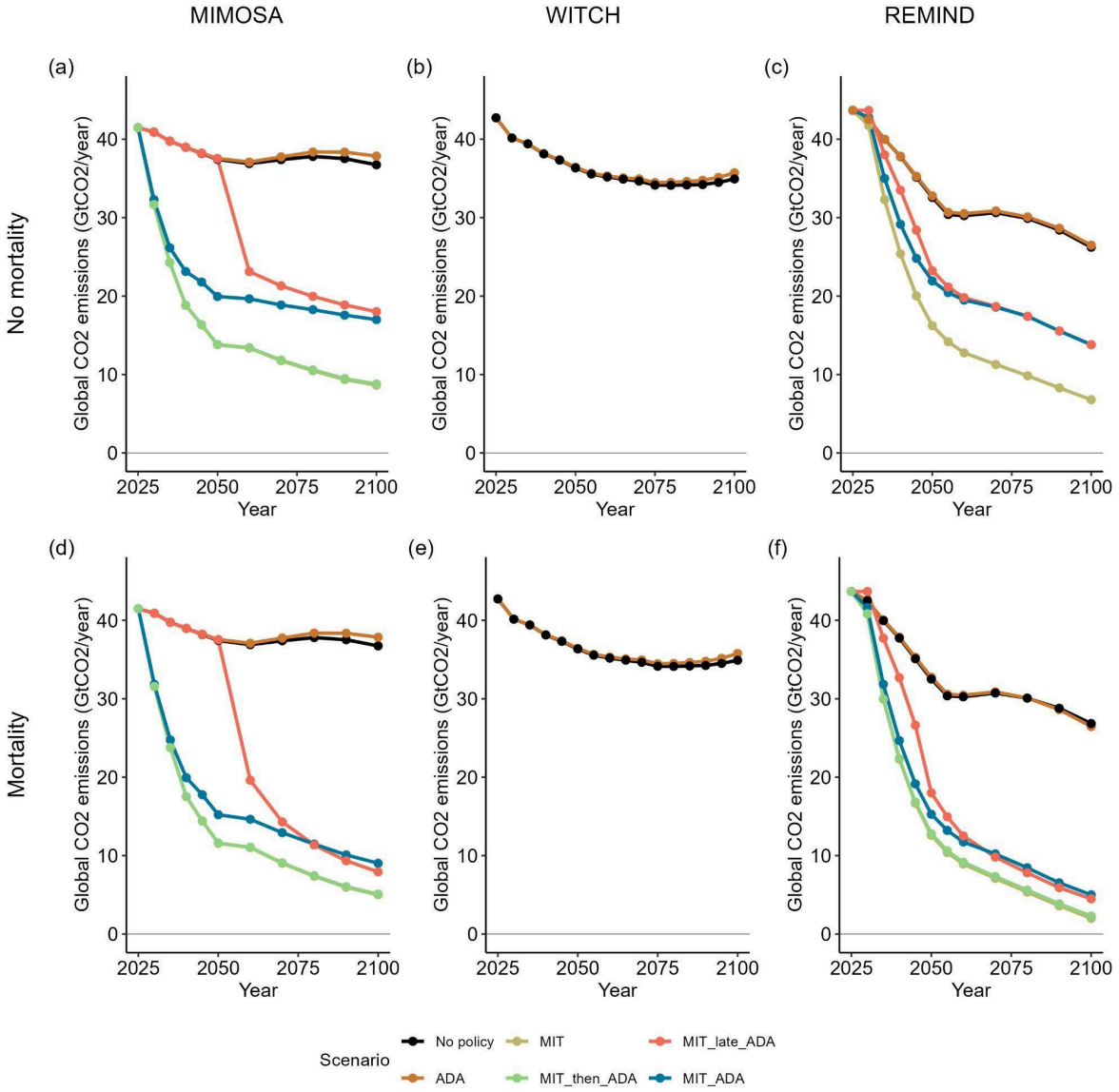

Figure 13: Emission paths in 3 IAMs across multiple scenarios.

3.2. Damages

In Figure 14, we observe that the scenario without additional mitigation and adaptation policy measures ("No policy") leads to the highest damage in all models, whilst MIT_then_ADA consistently leads to the lowest damage. This is a logical consequence of the fact that these are the scenarios in which, respectively, the least and the most is invested in damage reduction. In the no policy scenario, the total damages consist of roughly one fifth of sea-level rise damages, two fifths of riverine flooding and two fifths of labour productivity impacts. Mitigation reduces the total damages by 35-50%, where sea-level rise damages take a much larger share, because of the slower process of sea-level rise compared to temperature related damages. In contrast, adaptation without mitigation (ADA) leads to very large reductions (85-95%) in sea-level rise and riverine impacts, despite the temperature still being almost 3°C. The labour productivity impacts experience much less reduction from adaptation: these can only be substantially reduced through mitigation. In our modelling, if only optimal adaptation can be implemented (ADA), total sectoral damages are

lower than if only mitigation can be implemented (MIT), since in our input data, adaptation is inexpensive, and highly efficient in the sea-level rise and riverine flooding impact sectors. However, when mortality costs are also taken into account, this picture is reversed, and MIT becomes a considerably more attractive scenario. Almost all mortality is averted in that scenario, whereas ADA proves highly unsuccessful in reducing mortality-related damage.

Furthermore, the low sectoral damages are contingent on the functional forms and parameterisations of the adaptation modules employed, and warrant a critical reading. The adaptation functions in our models are stylised, smooth representations that assume adaptation can be deployed cost-effectively once resources are allocated. The high efficiency reported for sea-level rise and riverine flooding adaptation (85–95%) is a direct consequence of the optimistic damage-reduction data supplied by the underlying impact models; the assumed shape and parameters of the efficiency curves simply follow from that input. In our models, these curves are concave and asymptotic: efficiency rises with spending but at a diminishing rate, and the parameterisation is such that high efficiency is attainable at relatively modest cost, but this reflects the impact-model data rather than an independent modelling choice on our part. Whether the impact models underlying these data provide a realistic picture under the more severe, compound, and potentially non-linear impacts projected at around 3°C of warming is uncertain (Burke et al., 2015; Steffen et al., 2018; Zscheischler et al., 2018). The impact models may be overly optimistic, as they do not fully account for the complexities and non-linearities of real-world adaptation under extreme conditions. Furthermore, the underlying impact data may still understate how quickly adaptation options become ineffective as wet-bulb temperatures approach physiological limits (Im et al., 2017; Kang & Eltahir, 2018; Pal & Eltahir, 2016; Raymond et al., 2020; Sherwood & Huber, 2010). The favourable outcomes of adaptation thus depend critically on the assumptions and set-up of the underlying impact models, and the magnitude of the reported damage reductions should be interpreted with that caveat in mind.

If we assume that adaptation is undertaken continuously, but mitigation only from 2050 onwards (MIT_late_ADA), then damage in 2100 is higher than in scenarios where both mitigation and adaptation is implemented from the present (MIT_ADA and MIT_then_ADA). Two points should be noted in this regard. First, this graph shows only damage in a single year, 2100, whereas cumulative damage is substantially larger in MIT_late_ADA. Second, damage in 2100 is nevertheless higher than in MIT_ADA or MIT_then_ADA, despite the fact that cost-optimal adaptation and mitigation may indeed take place from 2050 onwards in MIT_late_ADA. This implies that it is not possible to compensate at a later stage for delayed mitigation. This serves as a powerful reminder that mitigation policy must not be delayed.

In the scenarios where mortality impacts are monetised and included in the optimization through their welfare effect, damage reduction is, on average, 10 per cent greater than in the scenarios where this is not the case. As we already mentioned in 3.1, this is a logical consequence of increased mitigation since an additional impact channel is taken into account. This increases the need for mitigation as the costs of inaction become larger.

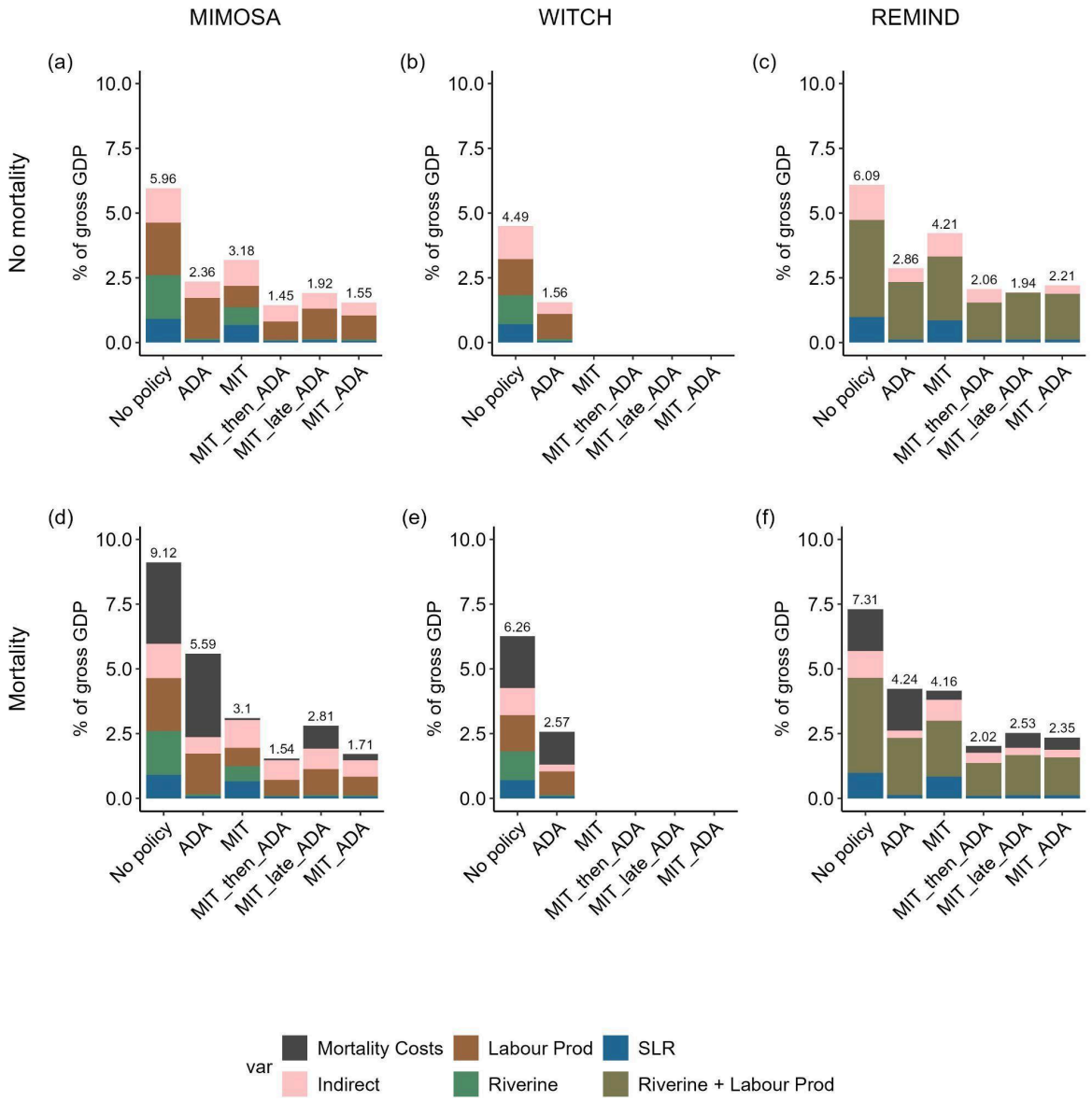

Figure 14: Damages in 2100 in 3 IAMs across multiple scenarios (variations regarding the goal of optimisation).

As expected, sectoral damages in the scenario where adaptation partially fails to deliver (ADA_red_eff) are substantially lower than in the No Policy scenario but still, on average, 80% higher than in the optimal adaptation scenario (Figure 15). This scenario illustrates what might happen if our expectations regarding the efficiency of adaptation do not materialise. Indeed, a damage reduction strategy based on adaptation will always be precarious to a certain extent. The extent to which adaptation succeeds in reducing climate damage is uncertain insofar as our assumptions regarding its effectiveness may, in practice, prove to be excessively optimistic. This is not the case for mitigation: lower CO_2 emissions invariably give rise to a reduction in damage. A dam may burst, but a molecule of CO_2 that is not emitted can never warm the planet.

We can also see that ADA_impl_gap has slightly higher damage levels than ADA across the board. Given that governments' institutional capacities vary in strength from place to place, this is a more realistic assessment of the best achievable adaptation scenario than ADA, See Figure C-1 in Annex C for an illustration of the considerable regional differences with regard to adaptation

efficiency when institutional limitations are taken into account. Note that in some regions and sectors (e.g., South Africa (SAF), SLR) there is initially increasing divergence, before convergence begins to occur towards the second half of the 21st century as a result of increasing economic growth, but that this is never completed within this century. Note moreover that in certain regions (e.g., Ukraine (UKR) and Central America excluding Mexico (RCAM)), for the Riverine sector, only increasing divergence occurs, which implies that this problem is not resolved by economic growth. It is worth noting that this takes place within SSP2 specifications, the middle-of-the-road scenario concerning conceivable developments in interregional inequality, which implies that this is not even a pessimistic scenario with respect to the limitations that such regions may experience in the implementation of adaptation.

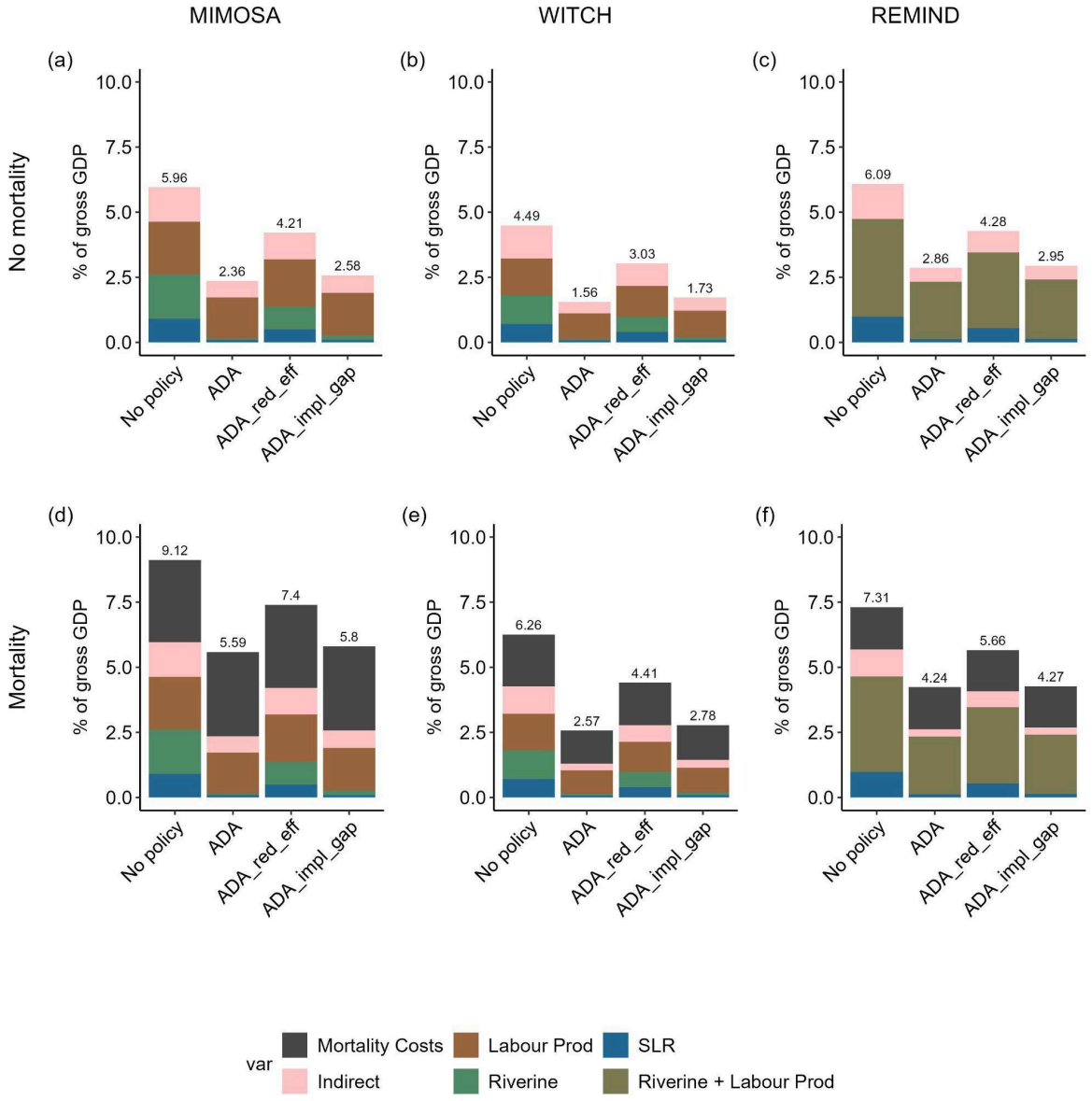

Figure 15: Damages in 2100 in 3 IAMs across multiple scenarios (variations of adaptation).

3.3. Adaptation costs

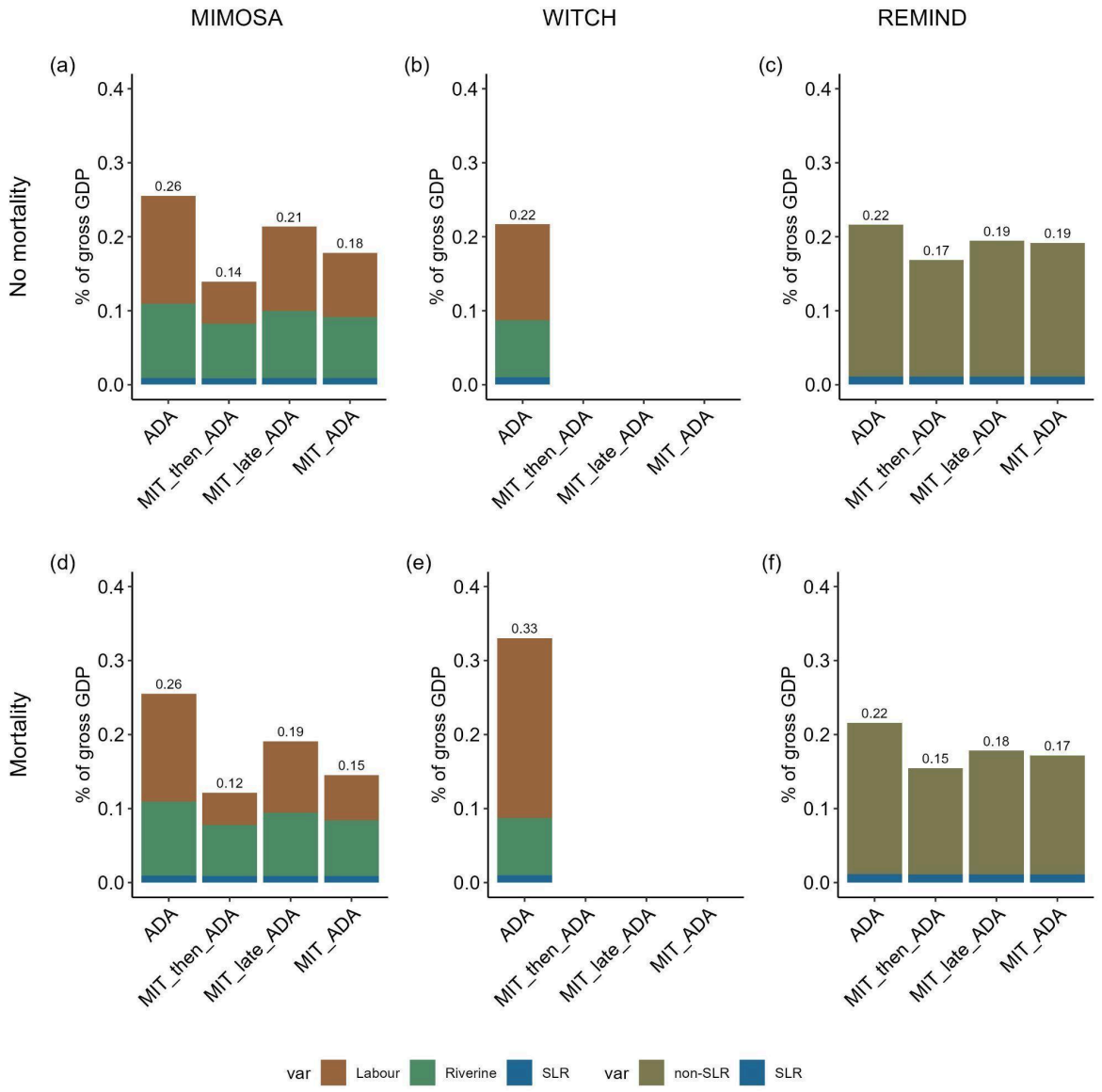

Figure 16: Adaptation costs in 2100 in 3 IAMs across multiple scenarios.

Figure 16 shows that adaptation expenditures are, as expected, the largest in the scenario with only adaptation: the high temperature of the ADA scenario leads to a need for the highest adaptation expenditure, of around 0.3% GDP. In Mit_then_ADA, the average expenditure on adaptation is 20% lower than in MIT_ADA. This becomes yet more apparent in Figure 17, in which adaptation and mitigation costs in MIMOSA are plotted over time. Given the differences between these two scenarios, this similarity is remarkable: if the models apply a second optimization focussed exclusively on adaptation, following a prior optimization based solely on mitigation, the outcome is one in which 80% as much adaptation effort is still undertaken as under a simultaneous optimisation of mitigation and adaptation. In other words, whether adaptation is applied post hoc, or is allowed to compete with mitigation for scarce resources, makes relatively little difference to how much cost-optimal expenditure is devoted to adaptation. This is a consequence of the fact that adaptation, in our input data from the other work packages, is cheap (cf. the consistently different

order of magnitude of expenditure on mitigation and adaptation in Figure 17), efficient, and that its effectiveness increases as nominal expenditures thereon increases (cf. the chapter on methodology). The fact that the models judge that it is still sensible to retain such a high amount of adaptation in a new optimization, in which the emission and mitigation path of MIT is imposed, shows that questions can be raised regarding how opportune it is to ask the model to make a trade-off between mitigation and adaptation, which happens in MIT_ADA and is standard in most IAM optimizations. It implies that MIT_then_ADA must be the standard for what ought to be considered as optimal.

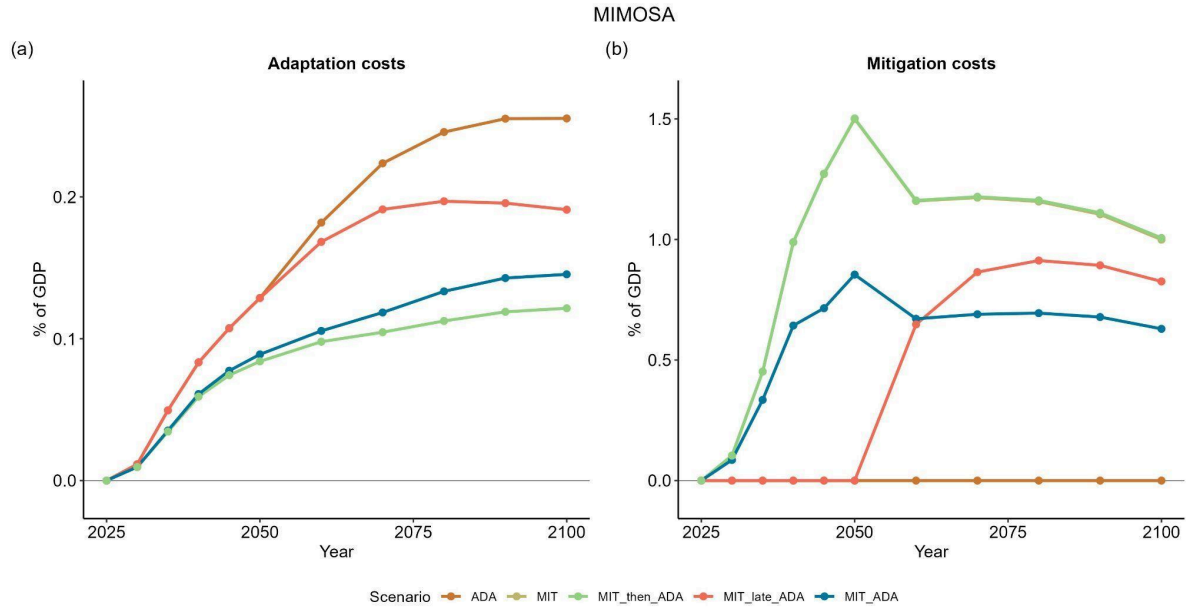

Figure 17: Expenditure on adaptation and mitigation in MIMOSA under different scenarios.

3.4. Adaptation efficiency

Figures 18 and 19 illustrate the point made earlier in Section 3.2 with regard to damage reduction across the different sectors: adaptation is highly effective for SLR and riverine flooding, but not in the labour productivity sector.

MIMOSA shows global effectiveness of over 95% for the riverine sector, and 10-15% for the labour productivity sector. Since REMIND models adaptation in the riverine and labour productivity sectors as one aggregated adaptation option, the combined adaptation effectiveness is also between the optimal effectiveness of both sectors separately: around 40%.

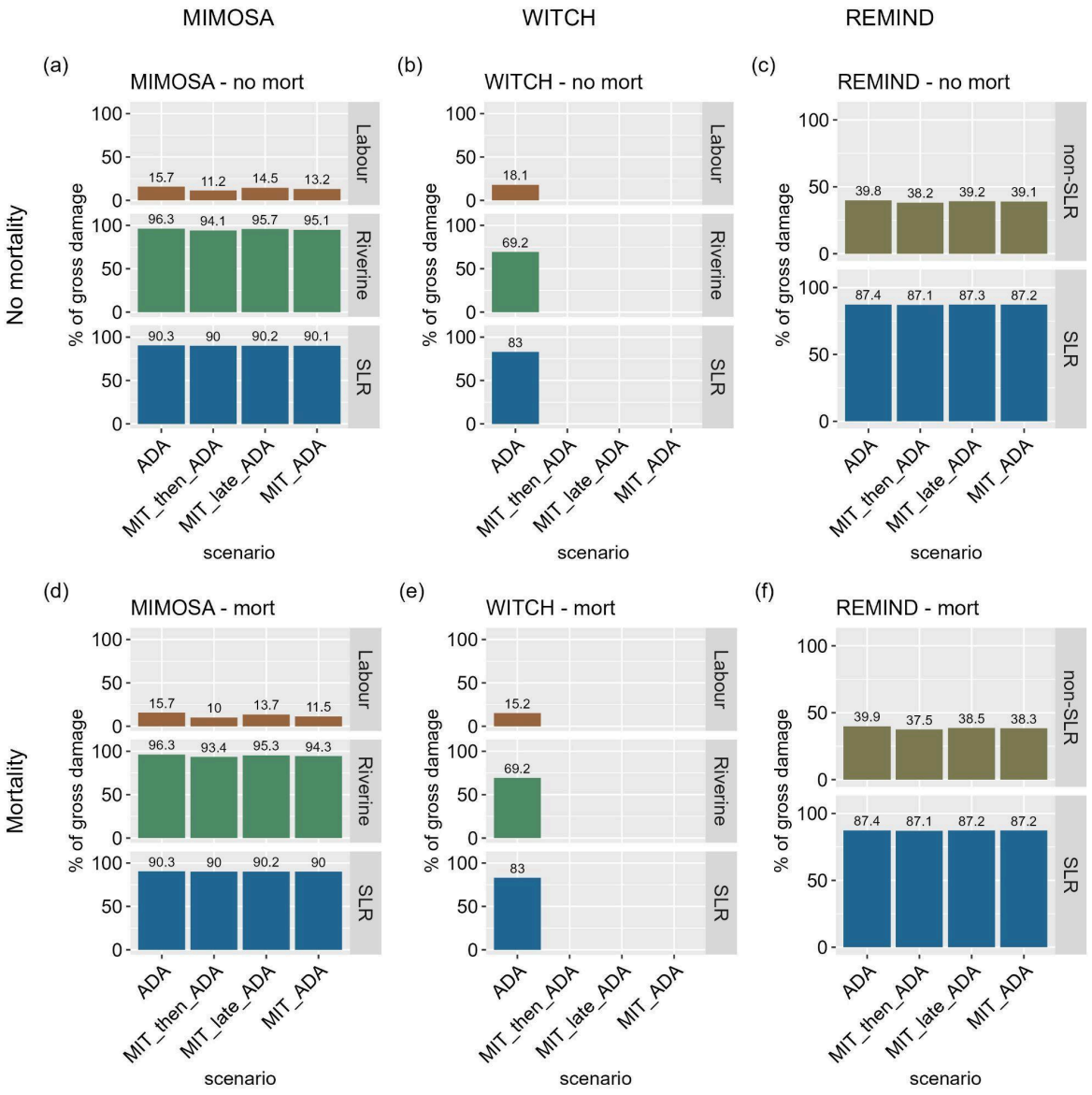

Figure 18: Adaptation efficiency in 2100 in 3 IAMs across multiple scenarios (variations regarding the goal of optimisation).

In ADA_impl_gap (the scenario in which adaptation expenditure is constrained on the basis of the empirically demonstrated institutional capacities of a region), adaptation efficiency is lower than in ADA, but only to a limited extent: whilst expenditure does decline, given the concave/asymptotic shape of the adaptation-efficiency curves, regions nevertheless remain situated on the flat portion of the curve (cf. Figure 19 for the reduced efficiency and figures 7 and 8 for the underlying reason). There are, however, large regional differences for this, depending on a region's assumed adaptive capacity, see figure C-1 in appendix C.

In a scenario that accounts for the possible failure of adaptation, ADA_red_eff, effectiveness is, by definition, half that of ADA.

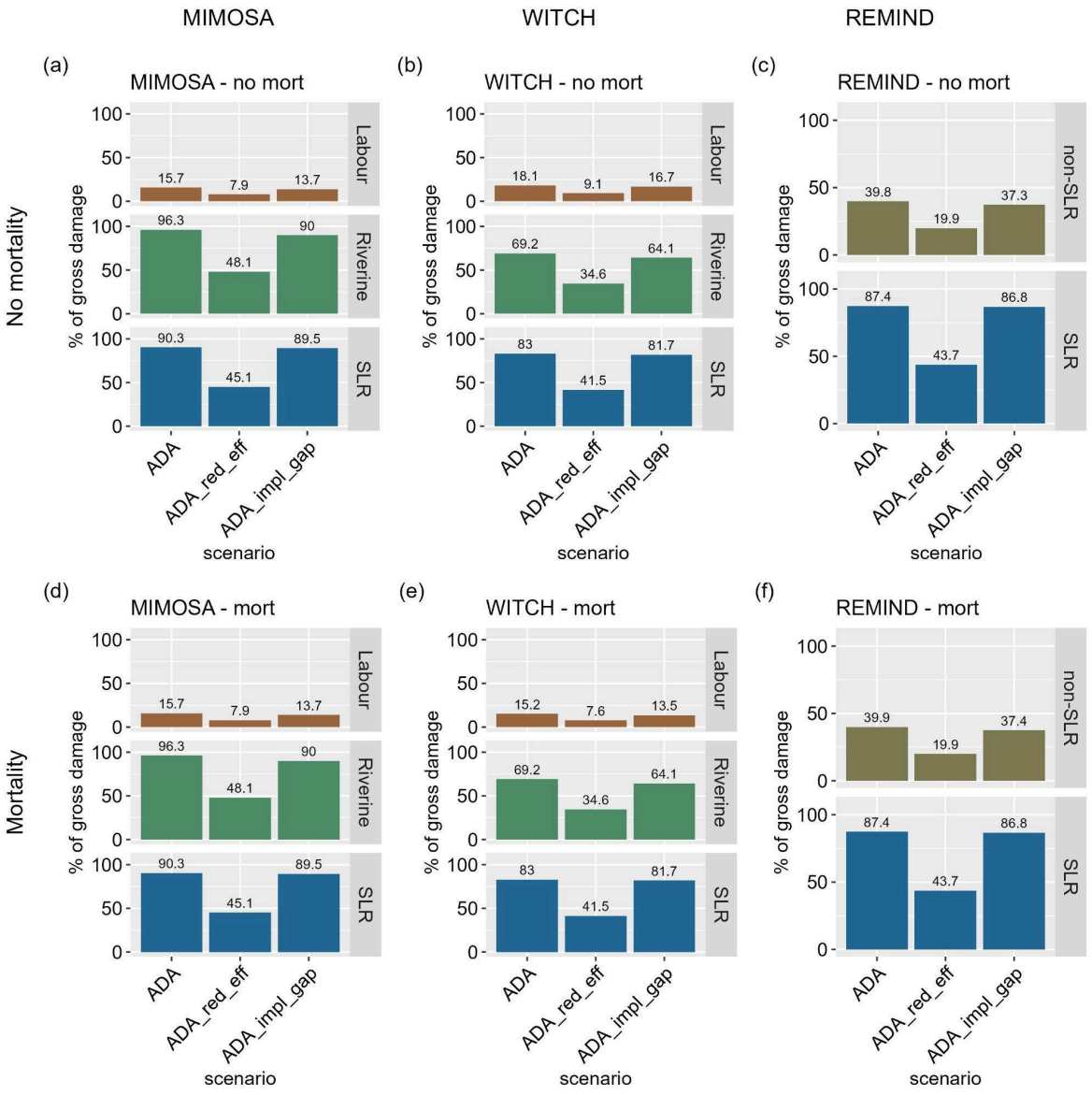

Figure 19: Adaptation efficiency in 2100 in 3 IAMs across multiple scenarios (variations of adaptation).

3.5. Mortality

Figure 20 shows first and foremost that mitigation can be particularly successful in limiting the annual additional mortality caused by climate warming. Limiting the temperature increase to 1.88°C (cf. Figure 11) ensures that only 0.1 million additional people die in MIMOSA, whereas in a No Policy scenario, in which the temperature rises to 3.04°C, this would amount to almost 3 million people. Scenarios that lie between these in terms of temperature have a corresponding figure that falls between the two most distinct scenarios. In REMIND, the difference is less pronounced, but the tendency is still very clear: whereas in the No Policy scenario almost 2 million additional people would die, in MIT this is only half a million: a reduction of more than 70%. The results are unequivocal: mitigation saves lives; more mitigation saves more lives.

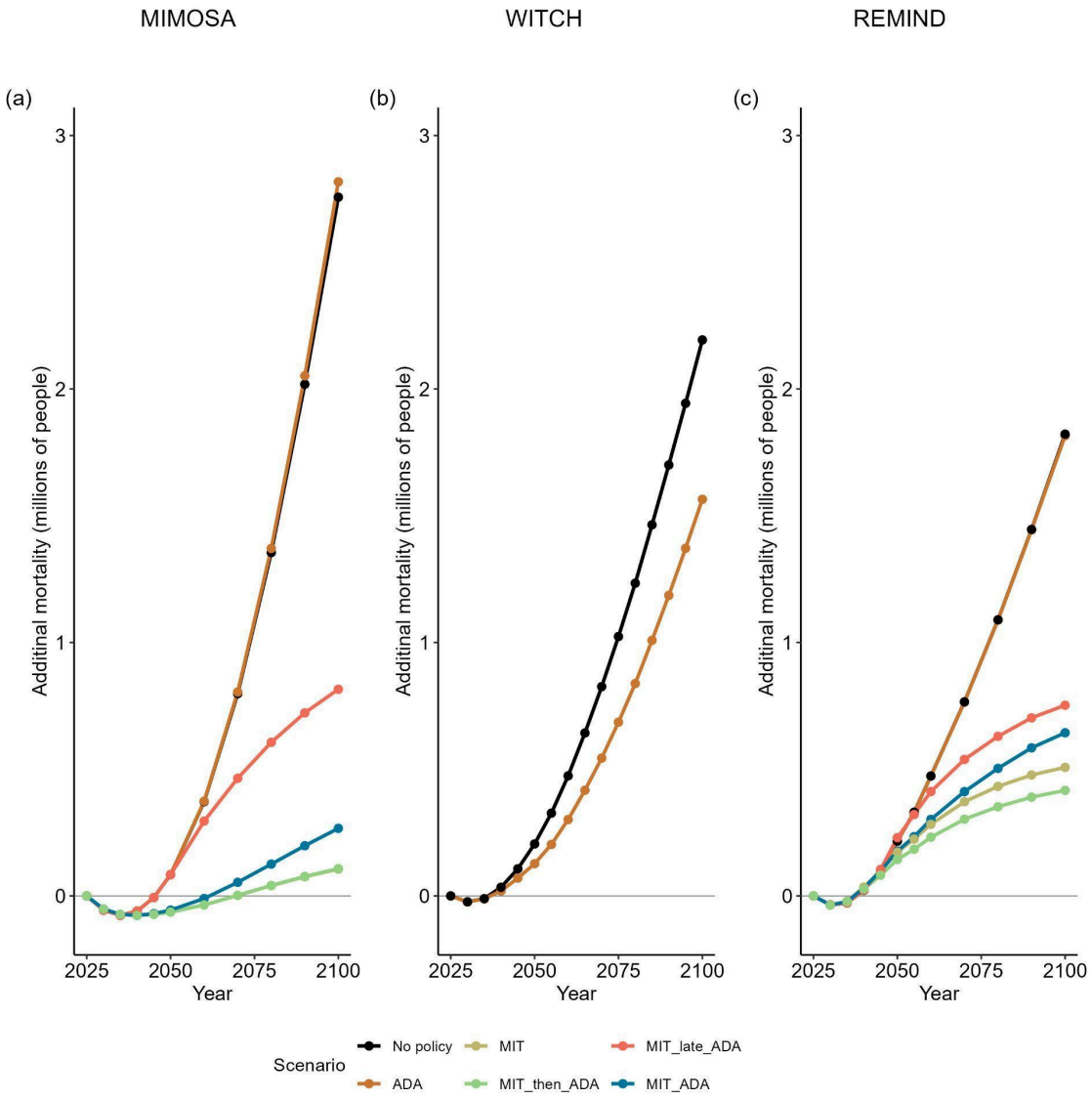

Figure 20: Additional mortality path in 3 IAMs across multiple scenarios.

The effect of adaptation on additional mortality with respect to the No Policy scenario is uncertain: in MIMOSA, there is slightly more annual additional mortality in ADA than in No Policy; in WITCH, by contrast, there is clearly a reduction; and in REMIND, there is exactly the same amount of annual additional mortality in both scenarios. The direction of the relationship thus differs owing to model uncertainty; however, if we consider the order of magnitude of the effect, the outcomes are robust: the models agree that a policy response consisting solely of adaptation fails to bring about a significant reduction in annual additional mortality.

Figure 20 also shows why damage in ADA is lower when mortality is not taken into account, but higher when it is taken into account (cf. Figures 14 and 15): all scenarios in which some form of mitigation is applied succeed in limiting mortality relative to the No Policy scenario, but if only adaptation is undertaken, annual additional mortality remains very close to the No Policy scenario. MIT_late_ADA confirms this picture, since it follows the scenarios without mitigation until 2050.

Our results should be nuanced because not all forms of excess mortality are included. As stated in Section 2.1.5, our excess mortality is based on Bressler (2021), in which DICE was extended with

a temperature-related mortality effect. It should be noted here that this study includes only mortality due to direct, temperature-related excess mortality, whilst other impact channels, such as air pollution, infectious diseases, food insecurity, conflicts and floods, were excluded. Other methodologies arrive at higher mortality. Carleton et al. (2022) find an empirical, U-shaped relationship between mortality and temperature that, if extrapolated to the end of the century, yields an increase in annual additional mortality of 73 persons per 100,000. In the SSP-2 population projections that we employ, this implies 7.3 million annual additional excess deaths at the end of the 21st century. Pozzer et al. (2024) combine climate simulations with epidemiological exposure-response functions and also take into account eight diseases and air pollution due to the burning of fossil fuels. This study finds that at the end of the century as many as 30 million annual additional deaths could occur due to climate change. The importance of our results concerning mortality therefore lies not primarily in the actual magnitude of the effect, but rather in the robust illustration they provide of the importance of mitigation, given its high success rate in drastically limiting mortality.

4. Discussion

4.1. Comparison to previous work

The results in this Deliverable build upon work previously undertaken in COACCH. Compared to COACCH, there are markedly lower damage curves. There are several reasons why this is the case.

First, fewer impact channels are used in ACCREU. This stems from the fact that we had usable input data at our disposal for only three direct impact sectors: labour productivity, riverine flooding and SLR. The most significant missing sector is agriculture.

Second, compared to COACCH, the damage of one of those three sectors is lower owing to a change in the model which created that input: the resolution in the DIVA model is finer, so that the construction of dikes in response to sea-level rise can be targeted at locations where they have the greatest economic effect, for example population centres, without automatically also protecting economically less valuable hinterland, such as agricultural land or nature, cf. WP2.

Third, and most significantly, the sectoral damage curves project lower damages as they were constructed with a fundamentally different methodology compared to COACCH: we incorporated the data from the models of WP2 in ACCREU directly into the IAMs, whereas in COACCH the raw data was processed by a CGE before being incorporated into the IAMs. Consequently, COACCH didn’t solely incorporate the immediate economic damage arising from the physical effects of climate change into the damage function, but also the way in which the market responded to these impacts. In ACCREU, by contrast, we have omitted this intermediate step, proceeding directly from physical impact models to IAMs. On the one hand, this approach does not take into account market effects; on the other hand, it might be clearer what causes the impacts. Our present results are easier to comprehend because the manner in which damage exerts an economic impact is more clearly described. However, this methodological choice, which implies the exclusion of market effects, reduces the economic impact.

Here, it should be noted that it is uncertain in which direction a market effect will operate. Does the market operate in a self-correcting manner, so that the damage becomes less intense, or do

initially small imbalances have the opposite outcome of creating a leverage effect that leads to greater economic damages? Both options are possible and, if they are to be modelled in an IAM, these countervailing effects should ideally be made explicit. Further research should focus on comparing the effects of, on the one hand, damage functions implemented directly in IAMs and, on the other hand, damage functions constructed via a CGE, with explicit attention to which market effects attenuate or amplify the initial damage. Appendix D presents the differences between direct and indirect damages within economic assessments considering IAMs and the propagation effects due to market interactions embedded in CGE assessments.

Nevertheless, despite the more finegrained impact model, the fact that fewer impact channels are included and the fact that market effects operating in CGEs are omitted, the resulting lower damage functions have not resulted in CBA-optimal temperatures that are substantially higher in ACCREU compared to COACCH. Depending on whether or not mortality is valorised, in 2100, ACCREU produces a CBA-optimal temperature increase of 1.9-2.2°C without adaptation (MIT) and of 2.0-2.5°C when adaptation is included (MIT_ADA), whereas COACCH attained 1.9°C of warming (van der Wijst et al., 2023).

Importantly, an increase in global mean temperature of 0.1°C to 0.6°C is not negligible at all. Every tenth of a degree represents enormous quantities of economic damage, as well as the potential disappearance of unique ecosystems and species that are irrevocably lost to future generations. Yet, it needs to be explained, what accounts for these outcomes?

First, as time has progressed, the scenarios are simply started later than those of COACCH, meaning less time is available and the initial level of warming is higher, this already renders mitigation more difficult.

Second, the relatively close optimal temperature to the one in COACCH is a consequence of the shape of the damage functions: although the damage function is lower in ACCREU, it is also more linear, whereas it was more convex in COACCH. Consequently, in COACCH it is very important to avoid the high points on the damage function, but variations at the beginning of the damage function are less important for optimization, since the differences remain on the flat part of the curve and thus result in relatively little difference in damage. In ACCREU, this is different: the linear shape implies that reducing damage is already impactful at the beginning of the damage function. This subsequently carries over into the emission path throughout the rest of the period under consideration. Note that MIT_late_ADA never managed to catch up on the cumulatively accumulated damage due to delays in mitigation policy. In the comparison between COACCH and ACCREU, a similar effect plays out in the opposite way: because it is sensible to start mitigation early, it is CBA-optimal to arrive at a mitigation effort which comes somewhat close to the one in COACCH, where much higher damage was assumed. In other words: it is not solely the total amount of damage that matters, but also whether the damage already has an impact early on.

Third, the relatively large damage reduction in ACCREU is a consequence of how the impacts of climate damage are distributed. In the input data used in ACCREU, damage is more unequally distributed than was assumed in COACCH: poor regions bear a relatively larger share of the impacts in ACCREU. In MIMOSA, for instance, West and East Africa each experience economic damage exceeding 12% of their GDP in 2100 as a result of riverine flooding under the No Policy scenarios. Since the marginal utility of additional income for welfare is diminishing, the damage experienced as a result of a reduction in income of the same quantity of dollars is greater in poorer

regions, and it is consequently worthwhile to undertake more damage reduction in an unequal world than in an equal one. In other words, it is not solely the total amount of damage that matters, but also its distribution and its consequent effect on welfare.

4.2. Do we project low damage in the future?

Firstly, we consider only three types of damage. Our results should not be interpreted as an estimate of the total damage that can be expected as a result of global warming. Many potentially significant channels remain outside the analysis. These include, among others, agricultural yield losses (Challinor et al., 2014; Hultgren et al., 2025; Rezaei et al., 2023, Yiwei et al., 2026) and food-price effects (Delincé et al., 2015; Sulser et al., 2011), changes in energy demand (van Ruijven et al., 2019), storm damage, (Radfar et al., 2026; Smiley et al., 2026), wildfire damage (Abatzoglou et al., 2025; Burton et al., 2024), ocean acidification (Cooley et al., 2015; Milazzo et al., 2014; Munday et al., 2013), unlivable wet-bulb temperatures (Im et al., 2017; Kang & Eltahir, 2018; Pal & Eltahir, 2016; Raymond et al., 2020; Sherwood & Huber, 2010), biodiversity loss and ecosystem degradation (Bastien-Olvera & Moore, 2022; Retsa et al., 2020), water scarcity (Unfried et al., 2021), the already locked-in extinction of O_2-generating phyto-plankton, which generates 50 to 70% of Athmosferic oxygen (Petrovskii et al., 2017; Sekerci & Petrovskii, 2015, 2018) and ecological tipping points such as AMOC-collapse (van Westen et al., 2024, 2026) or forest diebacks (Cox et al., 2004; Gatti et al., 2021; Parry et al., 2022). Furthermore, we do not capture indirect and cascading effects such as disruption of supply chains (Barata da Rocha et al., 2025), large-scale migration (Clement et al., 2021), or the risk of climate change acting as a potential threat multiplier for geopolitical friction, driven by increased competition for scarce resources (Global Water Security, 2011; NIC, 2021). Omitting these channels means that the damages reported here should be interpreted as a partial, and likely lower-bound, estimate of total climate-related economic damage, rather than as a comprehensive assessment of the costs of warming.

Secondly, the impact on labour productivity is defined as the reduction in a person's capacity to perform work. This capacity decreases in both excessively hot and excessively cold conditions, while an optimal, moderate temperature allows for the highest productivity. This explains why, in very cold regions such as Russia and Canada, there is an increase in labour productivity. However, productivity per person depends not only on their personal mental and physical state, but also on the infrastructure available to them. The consequences of global warming will lead to increased pressure on infrastructure such as additional corrosion (Stewart et al., 2011), drainage systems unable to cope with extreme rainfall (Pudyastuti & Nugraha, 2018), etc. It is precisely in those countries where an increase in labour productivity is expected, that this effect is anticipated to be particularly pronounced: in Canada and Russia, some important infrastructure has been built on permafrost, meaning that its foundations will become progressively more unstable, leading to further decrease in economic productivity which we did not account for (Cordier et al., 2025; Gartler et al., 2025; Hjort et al., 2018; Langer et al., 2023; Streletskiy et al., 2012). This concerns both the economic activity and settlements directly affected by this in several medium-sized cities such as Yakutsk, Surgut and Fairbanks, but also the energy infrastructure that forms the basis for economic activity in larger parts of these countries. Canada and Russia specifically are both strongly dependent on their energy sector for both their direct domestic activity and their net balance of payments position: the energy sector accounted for 21%, and 53% of exports in 2024 in these countries, respectively (Harvard Growth Lab, n.d.). That is to say, they can only afford their

current level of consumption thanks to energy exports which are vulnerable to the aforementioned type of damage.

Thirdly, regional damages can still be very high, for example: South-East Asia, West and East Africa each experience economic damage around 10% of their GDP in 2100 as a result of just one of the impact channels in the No Policy scenarios (cf. figures B-1, B-11 and B-19 in annex B for a representation of unequal damages across the three models). Such figures show that global averages can mask severe regional burdens. In this regard, it should be noted that our models feature large regions, each with a population of hundreds of millions. Smaller areas and communities, such as Small Island Developing States, densely populated river deltas, Arctic communities or the slum-dwellers of megacities in the Global South, face, in all likelihood, impacts which are even larger, but are concealed by the size of our regions.

Fourthly, even for low economic damages, societal impacts can be high in multiple ways. GDP-based damage estimates do not capture all dimensions of welfare, such as the stress of displacement; the loss of identity and self-worth as a result of lost livelihoods or the loss of cultural heritage; the alienation, resulting from the erosion of social cohesion; and the feelings of mourning as a result of losing ecosystems, a way of life or simply the reduced certainty and predictability of life. These impacts can be severe even when their monetized effect on aggregate output is modest.

But even if the monetized effect on aggregate output is modest, that does not imply that actually-experienced financial damages are low. They are often unequally distributed across socioeconomically unequal strata of the population within the same region. Heatwaves disproportionately harm outdoor and informal workers, the elderly and low-income households in poorly insulated housing or urban heat islands, while floods hit informal settlements on floodplains hardest; wealthier groups can more easily insure, relocate or absorb income losses. Consequently, a modest aggregate GDP effect can coincide with severe losses in income for disadvantaged groups, deepening existing inequalities. A modest figure of projected damage to GDP should therefore not be read as evidence that climate change will have only limited societal consequences.

5. Conclusion

In D4.4, the interaction between mitigation and adaptation was examined systematically by means of a scenario protocol in which adaptation, mitigation, their interplay and their timing were investigated through different modes of optimisation across various IAMs. Adaptation and mitigation were examined both in isolation and in interaction with one another. This leads to several conclusions.

First, the valorisation of mortality is important. Activating this impact channel leads to an additional temperature reduction of 0.1 to 0.15°C across the models. This is an important observation *an sich*, but it merits additional attention given that we model only a few damage channels here and nevertheless arrive at a CBA-optimal temperature increase around or even below 2°C. Taking additional channels into account can only imply a further reduction.

The adaptation effectiveness in our models is very high for riverine flooding and SLR, but lower for labour productivity. Mitigation policy, on the other hand, is highly efficient in limiting mortality: the scenarios with the highest mitigation effort succeed in limiting this by 70 to 95%.

Our input data assume a high adaptation efficiency, but account must be taken of the possibility that adaptation may in practice be less efficient than hoped and that states may lack the institutional capacity to implement adaptation at an optimal level. We therefore ran a scenario where adaptation fails to deliver, ADA_red_eff, and a scenario where the institutional capacity of different regions is taken into account, ADA_impl_gap.

In terms of damage reduction in the three modelled direct impact sectors, the most optimistic scenario with regards to adaptation-efficiency, ADA, is a highly efficient scenario with low residual damage. However, ADA_red_eff demonstrates that this policy choice can lead to a lock-in to a scenario with the second-highest damage of all runs. Although it is unlikely that policymakers would choose adaptation alone, this scenario is conceptually important in illustrating that adaptation always carries a greater risk than mitigation. This is an important consideration for policymakers when choosing an appropriate policy mix.

ADA_impl_gap does not lead to a large increase in damage globally, but it does so regionally: in regions with limited institutional capacities, this is indeed the case. Various African, Asian and American regions see a strong reduction in their adaptation effectiveness and consequently experience high damage. Given that these are precisely the regions in which the most severe poverty already prevails, this extensive damage leads to the greatest reductions in welfare. This ought to be prevented.

In ACCREU, a CBA-optimal temperature increase of approximately 1.9 to 2.2 degrees Celsius is obtained. Compared with the project on which this builds, COACCH, this represents 0 to 0.3°C more warming. We obtain a higher temperature because, first, the starting point is a higher initial temperature (since the models start at a later point in time), meaning that more warming must already be taken into account at the outset. Just as our MIT_late_ADA run demonstrated: starting mitigation at a later point in time implies that, as time progresses, it will no longer be possible to prevent all the damage which is caused thereby in a CBA-optimal manner. Here, we see a real-world example of what is simulated in this scenario: a higher initial temperature, that is, a postponement of mitigation policy, entails a poorer starting position, which reverberates throughout the entire period under consideration. It is not possible to compensate for these knock-on effects at a later stage. Consequently, MIT_late_ADA always exhibits higher damage than scenarios that begin mitigation earlier, and we observe that the optimisations in COACCH lead to a lower CBA-optimal temperature in 2100 than those in ACCREU.

In addition, fewer impact sectors are included than in COACCH. This, however, is not the full story: the damage functions in ACCREU assume lower damage than in COACCH. This is a consequence of the fact that our damage functions are direct implementations of the physical impact models, and were not first processed through a CGE. Consequently, no account is taken of the market effects that, in the case of COACCH, amplified the initial damage. Nevertheless, the final temperature is not that much higher compared to COACCH; this is a consequence of the fact that the damage curves are more linear in shape. As a result, the models begin emissions reductions earlier, which carries through the entire period considered. Just as delayed mitigation cannot be caught up later, early mitigation leads to long-term benefits. Furthermore, damage is more unequally distributed than in COACCH with the poorest regions sustaining the greatest damage impacts, meaning that a rational planner will also undertake emissions reductions sooner even at lower damages: after all, the welfare loss of a poor person is greater per dollar lost. Therefore, not only the magnitude of the damage matters, but also how it is distributed across time and space.

There is some difference between the models in the final outcomes. This reflects different modelling of the energy sector, different modes of optimisation and different assumptions regarding current policy. Such uncertainty is inevitable and should be considered as a bandwidth of the real-life impact. We employ multiple models specifically to avoid the pitfall of implying non-existing certainty by only using one model, as often unintentionally happens. That said, the general direction of the findings is consistently the same across the models, which is an indication of the robustness of our results.

Finally, the manner in which one optimises a combination of adaptation and mitigation has implications.Simultaneous optimisation of mitigation and adaptation implies that the model makes a trade-off between adaptation and mitigation. This inevitably leads to less mitigation and higher temperatures. Conversely, if one first optimises for mitigation and subsequently performs an additional optimisation for adaptation, one obtains only a relatively small decrease in the amount of adaptation, but a very large decrease in mortality. This admittedly leads to higher policy costs, but, if applied in practice, it also rules out the possibility that adaptation efficiency proves lower than desired. Modellers should take sufficient care when making and explaining this choice, in order to prevent readers of scientific research from being unwittingly steered in a direction by virtue of unexamined or perfunctory choices in this regard.

Our modelling of adaptation which partially fails (ADA_red_eff) and adaptation which cannot be fully implemented due to imperfect institutional capacity of states (ADA_impl_gap), demonstrates conceptually that adaptation efficiency can turn out to be much lower regionally or globally than is modelled in standard optimisations, meaning that a simultaneous optimisation of adaptation and mitigation may give an overly optimistic picture of the actual outcomes. This is an important consideration to be taken into account when making a choice regarding the appropriate manner of jointly optimizing or implementing adaptation and mitigation, since the aptness of accepting its resulting amount of damage, depends not only on the magnitude of that damage, but also on the likelihood of its successful realisation.

6. Bibliography

Abatzoglou, J. T., Kolden, C. A., Cullen, A. C., Sadegh, M., Williams, E. L., Turco, M., & Jones, M. W. (2025). Climate change has increased the odds of extreme regional forest fire years globally. *Nature Communications*, *16*(1), 6390. https://doi.org/10.1038/s41467-025-61608-1

Amirmoeini, K., Bahn, O., de Bruin, K., Everett, K., Kouchaki-Penchah, H., & Pineau, P.-O. (2026). AD-MERGE 2.0: An integrated assessment of the Nexus among energy transitions, climate impacts, and adaptation responses. *Geoscientific Model Development*, *19*(17), 8081–8113. https://doi.org/10.5194/gmd-19-8081-2026

Andrijevic, M., Crespo Cuaresma, J., Muttarak, R., & Schleussner, C.-F. (2020). Governance in socioeconomic pathways and its role for future adaptive capacity. *Nature Sustainability*, *3*(1), 35–41. https://doi.org/10.1038/s41893-019-0405-0

Bahn, O., Bruin, K. de, & Fertel, C. (2019). Will Adaptation Delay the Transition to Clean Energy Systems? An Analysis with AD-MERGE. *The Energy Journal*, *40*(4), 207–234. https://doi.org/10.5547/01956574.40.4.obah

Barata da Rocha, M., Grabbe, H., & Poitiers, N. (2025). *Climate risks to global supply chains* (Working Paper No. 20/2025). Bruegel. https://www.bruegel.org/working-paper/climate-risks-global-supply-chains

Bastien-Olvera, B. A., & Moore, F. C. (2022). Climate Impacts on Natural Capital: Consequences for the Social Cost of Carbon. *Annual Review of Resource Economics*, *14*(1), 515–532. https://doi.org/10.1146/annurev-resource-111820-020204

Botzen, W. J. W., Martinius, M. L., Bröde, P., Folkerts, M. A., Ignjacevic, P., Estrada, F., Harmsen, C. N., & Daanen, H. A. M. (2020). Economic valuation of climate change–induced mortality: Age dependent cold and heat mortality in the Netherlands. *Climatic Change*, *162*(2), 545–562. https://doi.org/10.1007/s10584-020-02797-0

Bressler, R. D. (2021). The mortality cost of carbon. *Nature Communications*, *12*(1), 4467. https://doi.org/10.1038/s41467-021-24487-w

Bressler, R. D., Moore, F. C., Rennert, K., & Anthoff, D. (2021). Estimates of country level temperature-related mortality damage functions. *Scientific Reports*, *11*(1), 20282. https://doi.org/10.1038/s41598-021-99156-5

Burke, M., Hsiang, S. M., & Miguel, E. (2015). Global non-linear effect of temperature on economic production. *Nature*, *527*(7577), 235–239. https://doi.org/10.1038/nature15725

Burton, C., Lampe, S., Kelley, D. I., Thiery, W., Hantson, S., Christidis, N., Gudmundsson, L., Forrest, M., Burke, E., Chang, J., Huang, H., Ito, A., Kou-Giesbrecht, S., Lasslop, G., Li, W., Nieradzik, L., Li, F., Chen, Y., Randerson, J., … Mengel, M. (2024). Global burned area increasingly explained by climate change. *Nature Climate Change*, *14*(11), 1186–1192. https://doi.org/10.1038/s41558-024-02140-w

Carleton, T., Jina, A., Delgado, M., Greenstone, M., Houser, T., Hsiang, S., Hultgren, A., Kopp, R. E., McCusker, K. E., Nath, I., Rising, J., Rode, A., Seo, H. K., Viaene, A., Yuan, J., & Zhang, A. T. (2022). Valuing the Global Mortality Consequences of Climate Change Accounting for Adaptation Costs and Benefits. *The Quarterly Journal of Economics*, *137*(4), 2037–2105. https://doi.org/10.1093/qje/qjac020

Challinor, A. J., Watson, J., Lobell, D. B., Howden, S. M., Smith, D. R., & Chhetri, N. (2014). A meta-analysis of crop yield under climate change and adaptation. *Nature Climate Change*, *4*(4), 287–291. https://doi.org/10.1038/nclimate2153

Clement, V., Rigaud, K. K., de Sherbinin, A., Jones, B., Adamo, S., Schewe, J., Sadiq, N., & Shabahat, E. (2021). *Groundswell Part 2: Acting on Internal Climate Migration* (10.1596/36248). World Bank. https://hdl.handle.net/10986/36248

Colelli, F. P. (2026). *Labour Productivity Shock Dataset*. https://doi.org/10.5281/zenodo.23390461

Cooley, S. R., Kite-Powell, H. L., & Doney, S. C. (2015). Ocean Acidification's Potential to Alter Global Marine Ecosystem Services. *Oceanography*, *22*(4), 172–181. https://doi.org/10.5670/oceanog.2009.106

Cordier, M., Vasilevskaya, A., Jungsberg, L., Vanderlinden, J.-P., Ramage, J., & Lantuit, H. (2025). Uncovering the economic impact of thawing arctic permafrost: Exploring GDP production in a changing landscape. *Polar Science*, *44*, 101203. https://doi.org/10.1016/j.polar.2025.101203

Cox, P. M., Betts, R. A., Collins, M., Harris, P. P., Huntingford, C., & Jones, C. D. (2004). Amazonian forest dieback under climate-carbon cycle projections for the 21st century. *Theoretical and Applied Climatology*, *78*(1), 137–156. https://doi.org/10.1007/s00704-004-0049-4

de Bruin, K. C., Dellink, R. B., & Tol, R. S. J. (2009). AD-DICE: An implementation of adaptation in the DICE model. *Climatic Change*, *95*(1), 63–81. https://doi.org/10.1007/s10584-008-9535-5

Delincé, J., Ciaian, P., & Witzke, H.-P. (2015). Economic impacts of climate change on agriculture: The AgMIP approach. *Journal of Applied Remote Sensing*, *9*(1), 097099. https://doi.org/10.1117/1.JRS.9.097099

Gartler, S., Scheer, J., Meyer, A., Abass, K., Bartsch, A., Doloisio, N., Falardeau, J., Hugelius, G., Irrgang, A., Haukur Ingimundarson, J., Jungsberg, L., Lantuit, H., Nymand Larsen, J., Lodi, R., Martin, V. S., Mercer, L., Nielsen, D., Overduin, P., Povoroznyuk, O., … Ingeman-Nielsen, T. (2025). A transdisciplinary, comparative analysis reveals key risks from Arctic permafrost thaw. *Communications Earth & Environment*, *6*(1), 21. https://doi.org/10.1038/s43247-024-01883-w

Gatti, L. V., Basso, L. S., Miller, J. B., Gloor, M., Gatti Domingues, L., Cassol, H. L. G., Tejada, G., Aragão, L. E. O. C., Nobre, C., Peters, W., Marani, L., Arai, E., Sanches, A. H., Corrêa, S. M., Anderson, L., Von Randow, C., Correia, C. S. C., Crispim, S. P., & Neves, R. A. L. (2021). Amazonia as a carbon source linked to deforestation and climate change. *Nature*, *595*(7867), 388–393. https://doi.org/10.1038/s41586-021-03629-6

Global Water Security (Intelligence Community Assessment ICA 2012-08). (2011). CIA, DIA, NSA, NGIA, BIR, FBI, DHS, NCS. https://archive.dni.gov/files/documents/Special%20Report_ICA%20Global%20Water%20Security.pdf

Harvard Growth Lab. (n.d.). *The Atlas of Economic Complexity*. Center for International Development at Harvard University (CID). Retrieved September 30, 2026, from https://atlas.hks.harvard.edu/countries/288

Hinkel, J., Lincke, D., Vafeidis, A. T., Perrette, M., Nicholls, R. J., Tol, R. S. J., Marzeion, B., Fettweis, X., Ionescu, C., & Levermann, A. (2014). Coastal flood damage and adaptation costs under 21st century sea-level rise. *Proceedings of the National Academy of Sciences*, *111*(9), 3292–3297. https://doi.org/10.1073/pnas.1222469111

Hjort, J., Karjalainen, O., Aalto, J., Westermann, S., Romanovsky, V. E., Nelson, F. E., Etzelmüller, B., & Luoto, M. (2018). Degrading permafrost puts Arctic infrastructure at risk

by mid-century. *Nature Communications*, *9*(1), 5147. https://doi.org/10.1038/s41467-018-07557-4

Howard, P. H., & Sterner, T. (2017). Few and Not So Far Between: A Meta-analysis of Climate Damage Estimates. *Environmental and Resource Economics*, *68*(1), 197–225. https://doi.org/10.1007/s10640-017-0166-z

Hultgren, A., Carleton, T., Delgado, M., Gergel, D. R., Greenstone, M., Houser, T., Hsiang, S., Jina, A., Kopp, R. E., Malevich, S. B., McCusker, K. E., Mayer, T., Nath, I., Rising, J., Rode, A., & Yuan, J. (2025). Impacts of climate change on global agriculture accounting for adaptation. *Nature*, *642*(8068), 644–652. https://doi.org/10.1038/s41586-025-09085-w

IIASA. (2026, February 12). *Shared Socioeconomic Pathways Scenario Database (SSP)*. International Institute for Applied Systems Analysis. https://iiasa.ac.at/models-tools-data/ssp

Im, E.-S., Pal, J. S., & Eltahir, E. A. B. (2017). Deadly heat waves projected in the densely populated agricultural regions of South Asia. *Science Advances*, *3*(8), e1603322. https://doi.org/10.1126/sciadv.1603322

Kang, S., & Eltahir, E. A. B. (2018). North China Plain threatened by deadly heatwaves due to climate change and irrigation. *Nature Communications*, *9*(1), 2894. https://doi.org/10.1038/s41467-018-05252-y

Langer, M., von Deimling, T. S., Westermann, S., Rolph, R., Rutte, R., Antonova, S., Rachold, V., Schultz, M., Oehme, A., & Grosse, G. (2023). Thawing permafrost poses environmental threat to thousands of sites with legacy industrial contamination. *Nature Communications*, *14*(1), 1721. https://doi.org/10.1038/s41467-023-37276-4

Li, C., Held, H., Hokamp, S., & Marotzke, J. (2020). Optimal temperature overshoot profile found by limiting global sea level rise as a lower-cost climate target. *Science Advances*, *6*(2), eaaw9490. https://doi.org/10.1126/sciadv.aaw9490

Milazzo, M., Rodolfo-Metalpa, R., Chan, V. B. S., Fine, M., Alessi, C., Thiyagarajan, V., Hall-Spencer, J. M., & Chemello, R. (2014). Ocean acidification impairs vermetid reef recruitment. *Scientific Reports*, *4*(1), 4189. https://doi.org/10.1038/srep04189

Munday, P. L., Pratchett, M. S., Dixson, D. L., Donelson, J. M., Endo, G. G. K., Reynolds, A. D., & Knuckey, R. (2013). Elevated CO2 affects the behavior of an ecologically and economically important coral reef fish. *Marine Biology*, *160*(8), 2137–2144. https://doi.org/10.1007/s00227-012-2111-6

National Intelligence Council. (2021, October 21). *National Intelligence Council, "National Intelligence Estimate: Climate Change and International Responses Increasing Challenges to US National Security Through 2040*. https://nsarchive.gwu.edu/document/33167-document-39-national-intelligence-council-national-intelligence-estimate-climate

National Intelligence Council [NIC]. (2021). *Climate Change and International Responses Increasing Challenges to US National Security Through 2040* (NIC-NIE-2021-10030-A; National Intelligence Estimate). https://nsarchive.gwu.edu/document/33167-document-39-national-intelligence-council-national-intelligence-estimate-climate

Nauels, A., Nicholls, Z., Möller, T., Hermans, T. H. J., Mengel, M., Kloenne, U., Smith, C., Slangen, A. B. A., & Palmer, M. D. (2025). Multi-century global and regional sea-level rise commitments from cumulative greenhouse gas emissions in the coming decades. *Nature Climate Change*, *15*(11), 1198–1204. https://doi.org/10.1038/s41558-025-02452-5

OECD. (2025, October 1). *Support Materials—Mortality Risk Valuation in Policy Assessment*. https://www.oecd.org/en/publications/mortality-risk-valuation-in-policy-assessment_76ca89a2-en/support-materials.html

Pal, J. S., & Eltahir, E. A. B. (2016). Future temperature in southwest Asia projected to exceed a threshold for human adaptability. *Nature Climate Change*, *6*(2), 197–200. https://doi.org/10.1038/nclimate2833

Parry, I., Ritchie, P., & Cox, P. (2022). Evidence of Amazon rainforest dieback in CMIP6 models. *Earth System Dynamics*, *13*(4), 1667–1675. https://doi.org/10.5194/esd-13-1667-2022

Petrovskii, S., Sekerci, Y., & Venturino, E. (2017). Regime shifts and ecological catastrophes in a model of plankton-oxygen dynamics under the climate change. *Journal of Theoretical Biology*, *424*, 91–109. https://doi.org/10.1016/j.jtbi.2017.04.018

Pozzer, A., Steffens, B., Proestos, Y., Sciare, J., Akritidis, D., Chowdhury, S., Burkart, K., & Bacer, S. (2024). Atmospheric health burden across the century and the accelerating impact of temperature compared to pollution. *Nature Communications*, *15*(1), 9379. https://doi.org/10.1038/s41467-024-53649-9

Pudyastuti, P. S., & Nugraha, N. A. (2018). Climate change risks to infrastructures: A general perspective. *AIP Conference Proceedings*, *1977*(1), 040030. https://doi.org/10.1063/1.5043000

Radfar, S., Foroumandi, E., Moftakhari, H., Moradkhani, H., Sen Gupta, A., & Foltz, G. R. (2026). Synergistic impact of marine heat waves and rapid intensification exacerbates tropical cyclone destructive power worldwide. *Science Advances*, *12*(15). https://doi.org/10.1126/sciadv.adu1733

Ravallion, M. (1997). Famines and economics. *Journal of Economic Literature*, *35*(3), 1205.

Retsa, A., Schelske, O., Wilke, B., Rutherford, G., & De Jong, R. (2020, August 28). *Biodiversity and Ecosystem Services: A business case for re/insurance* (L. Kelly, Ed.). Swiss RE. https://www.researchgate.net/publication/348729525_Biodiversity_and_Ecosystem_Services_A_business_case_for_reinsurance

Rezaei, E. E., Webber, H., Asseng, S., Boote, K., Durand, J. L., Ewert, F., Martre, P., & MacCarthy, D. S. (2023). Climate change impacts on crop yields. *Nature Reviews Earth & Environment*, *4*(12), 831–846. https://doi.org/10.1038/s43017-023-00491-0

Sekerci, Y., & Petrovskii, S. (2015). Mathematical Modelling of Plankton-Oxygen Dynamics Under the Climate Change. *Bulletin of Mathematical Biology*, *77*(12), 2325–2353. https://doi.org/10.1007/s11538-015-0126-0

Sekerci, Y., & Petrovskii, S. (2018). Global Warming Can Lead to Depletion of Oxygen by Disrupting Phytoplankton Photosynthesis: A Mathematical Modelling Approach. *Geosciences*, *8*(6), 201. https://doi.org/10.3390/geosciences8060201

Smiley, K. T., Díaz-García, O., Done, J. M., Hemmerling, S. A., Larrison, K., Mostafiz, R. B., Rahim, M. A., Ramos-Valle, A. N., & Yevuyibor, J. T. (2026). Advancing extreme event impact attribution: Attributing multi-hazard impacts of Hurricane Ida in south Louisiana to past, present, and future climates. *Environmental Research: Climate*, *5*(2), 025027. https://doi.org/10.1088/2752-5295/ae6889

Steffen, W., Rockström, J., Richardson, K., Lenton, T. M., Folke, C., Liverman, D., Summerhayes, C. P., Barnosky, A. D., Cornell, S. E., Crucifix, M., Donges, J. F., Fetzer, I., Lade, S. J., Scheffer, M., Winkelmann, R., & Schellnhuber, H. J. (2018). Trajectories of the Earth System in the Anthropocene. *Proceedings of the National Academy of Sciences*, *115*(33), 8252–8259. https://doi.org/10.1073/pnas.1810141115

Stewart, M. G., Wang, X., & Nguyen, M. N. (2011). Climate change impact and risks of concrete infrastructure deterioration. *Engineering Structures*, *33*(4), 1326–1337. https://doi.org/10.1016/j.engstruct.2011.01.010

Streletskiy, D., Shiklomanov, N., & Hatleberg, E. (2012, June). *Infrastructure and a Changing Climate in the Russian Arctic: A Geographic Impact Assessment*. 10th International Conference on Permafrost, Salekhard, Russia. https://www.researchgate.net/profile/Dmitry-Streletskiy/publication/259762572_Infrastructure_and_a_Changing_Climate_in_the_Russian_Arctic_A_Geographic_Impact_Assessment/links/00b7d52dbfcba55051000000/Infrastructure-and-a-Changing-Climate-in-the-Russian-Arctic-A-Geographic-Impact-Assessment.pdf

Sulser, T. B., Nestorova, B., Rosegrant, M. W., & van Rheenen, T. (2011). The future role of agriculture in the Arab region's food security. *Food Security*, *3*(1), 23–48. https://doi.org/10.1007/s12571-010-0100-5

The World Bank. (2025). *DataBank*. https://databank.worldbank.org/

Toulemon, L., & Barbieri, M. (2008). The mortality impact of the August 2003 heat wave in France: Investigating the 'harvesting' effect and other long-term consequences. *Population Studies*, *62*(1), 39–53. https://doi.org/10.1080/00324720701804249

Unfried, K., Kis-Katos, K., & Poser, T. (2021). *Water Scarcity and Social Conflict*. IZA - Institute of Labor Economics. https://www.jstor.org/stable/resrep63287

van der Wijst, K.-I., Bosello, F., Dasgupta, S., Drouet, L., Emmerling, J., Hof, A., Leimbach, M., Parrado, R., Piontek, F., Standardi, G., & van Vuuren, D. (2023). New damage curves and multimodel analysis suggest lower optimal temperature. *Nature Climate Change*, *13*(5), 434–441. https://doi.org/10.1038/s41558-023-01636-1

van der Wijst, K.-I., Bosello, F., Ignjacevic, P., Preinfalk, E., Dasgupta, S., Parrado, R., Standardi, S., Drouet, L., Emmerling, J., Hof, A., Leimbach, M., Piontek, F., van Vuuren, D., Kuik, O., Botzen, Z., Knittel, N., Bednar-Friedl, B., Sainz de Murieta, E., Tesselaar, M., & Bachner, G. (2021). *COACCH D4.3 Macroeconomic assessment of policy effectiveness. Deliverable of the H2020 COACCH project.* https://www.coacch.eu/wp-content/uploads/2018/03/D4.3_revMAR2022.pdf

van Ruijven, B. J., De Cian, E., & Sue Wing, I. (2019). Amplification of future energy demand growth due to climate change. *Nature Communications*, *10*(1), 2762. https://doi.org/10.1038/s41467-019-10399-3

van Westen, R. M., Börner, R., & Dijkstra, H. A. (2026). Failure to track a stable AMOC state under rapid climate change. *Nature Climate Change*, 1–12. https://doi.org/10.1038/s41558-026-02730-w

van Westen, R. M., Kliphuis, M., & Dijkstra, H. A. (2024). Physics-based early warning signal shows that AMOC is on tipping course. *Science Advances*, *10*(6), eadk1189. https://doi.org/10.1126/sciadv.adk1189

Yiwei, J., Xuhui, W., Jägermeyr, J., Ciais, P., Müller, C., Zscheischler, J., Tao, L., Kun, C., Pengfu, H., Jianliang, H., Yu, J., Bin, W., Zhenwei, S., Zuolin, Z., Peng, Z., & Feng, Z. (2026). Vulnerability to high temperature shapes global warming impacts on rice yield |

Science Advances. *Science Advances*, *12*(31). https://doi.org/DOI:%252010.1126/sciadv.aed9226

Zscheischler, J., Westra, S., van den Hurk, B. J. J. M., Seneviratne, S. I., Ward, P. J., Pitman, A., AghaKouchak, A., Bresch, D. N., Leonard, M., Wahl, T., & Zhang, X. (2018). Future climate risk from compound events. *Nature Climate Change*, *8*(6), 469–477. https://doi.org/10.1038/s41558-018-0156-3

7. Appendix

7.1. Appendix A: Gross damage functions and adaptation functions for REMIND and WITCH

In section 2.1, we show the gross damage functions and adaptation effectiveness functions for the MIMOSA regions. Since the IAMs don't have the same regional aggregation, we show here the functions for REMIND and WITCH as well.

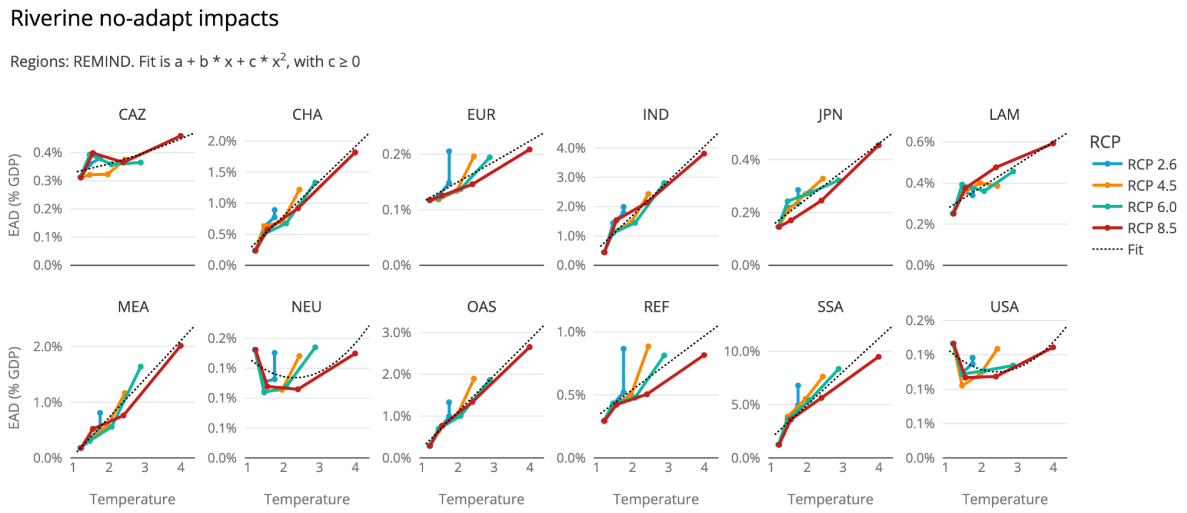

Fig. A-1. REMIND: Gross damages for riverine floodings as a function of GMT (°C above pre-industrial). The coloured lines represent the direct results from GLOFRIS (annualised). The dotted line is the best fit of a quadratic function.

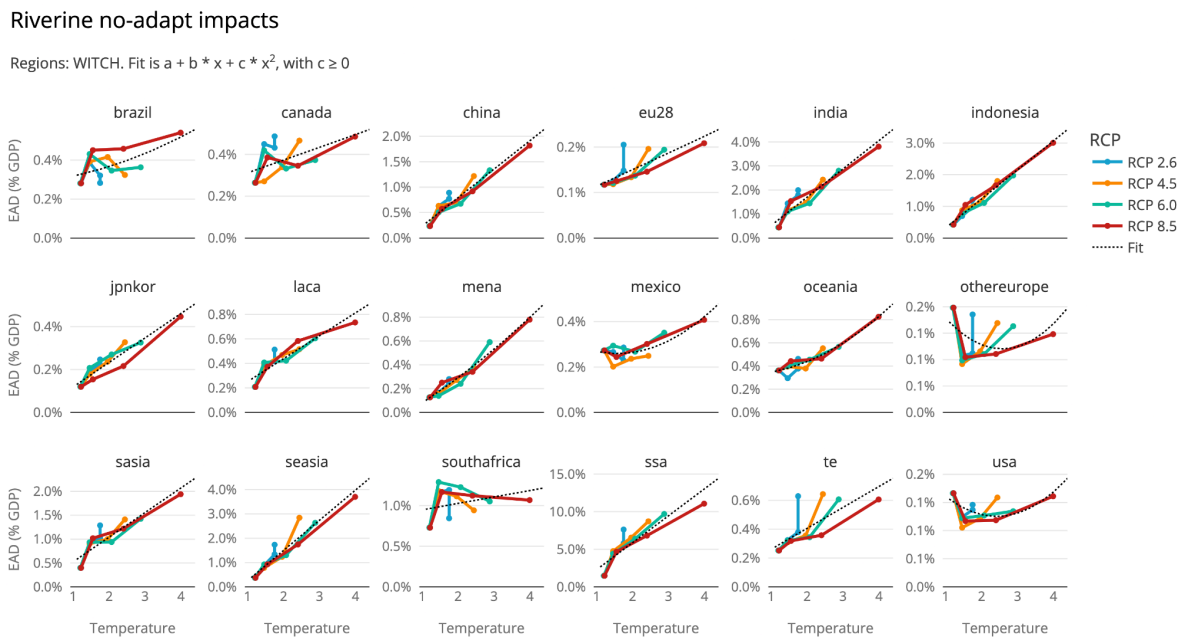

Fig. A-2. WITCH: Gross damages for riverine floodings as a function of GMT (°C above pre-industrial). The coloured lines represent the direct results from GLOFRIS (annualised). The dotted line is the best fit of a quadratic function.

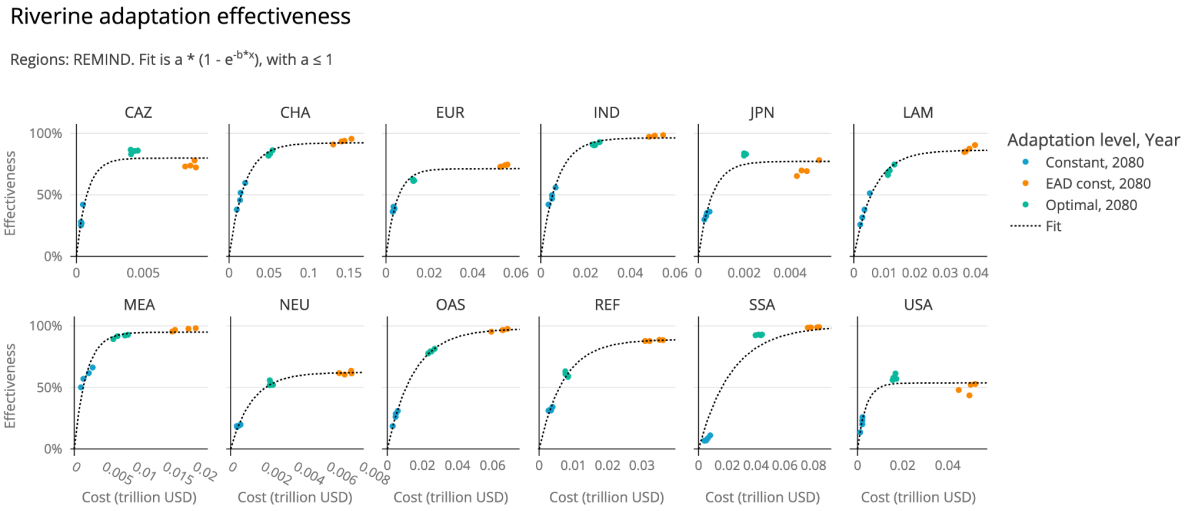

Fig. A-3. REMIND: Adaptation effectiveness (in % of avoided gross damages) for riverine floodings as a function of regional adaptation costs (in trillion US$2017 MER).

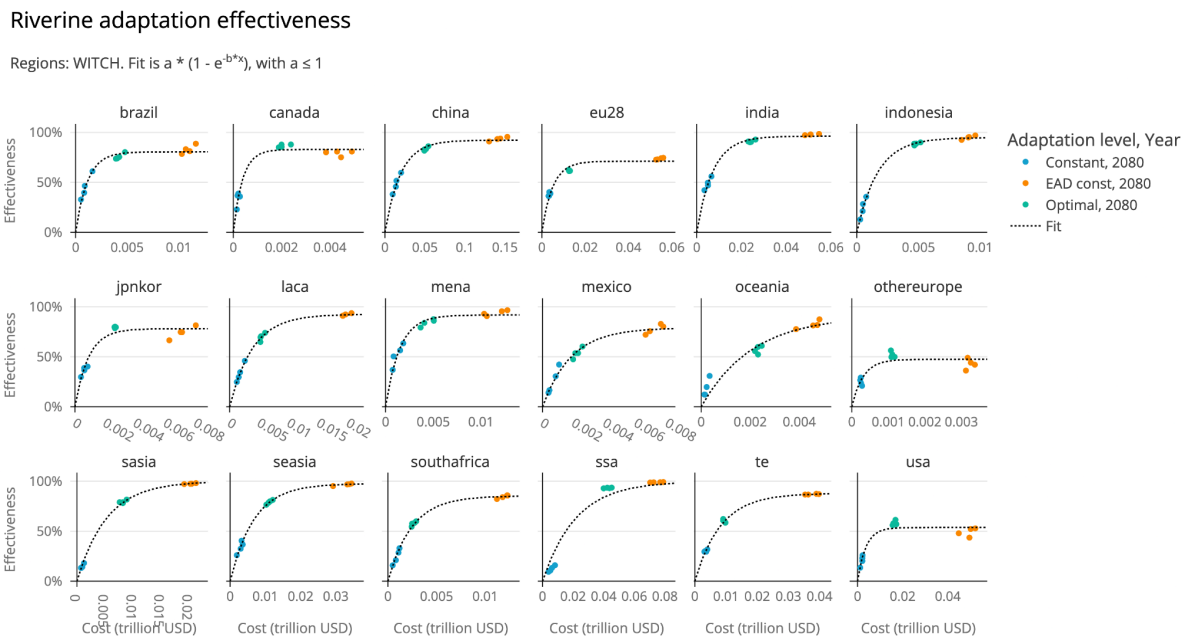

Fig. A-4. WITCH: Adaptation effectiveness (in % of avoided gross damages) for riverine floodings as a function of regional adaptation costs (in trillion US$2017 MER).

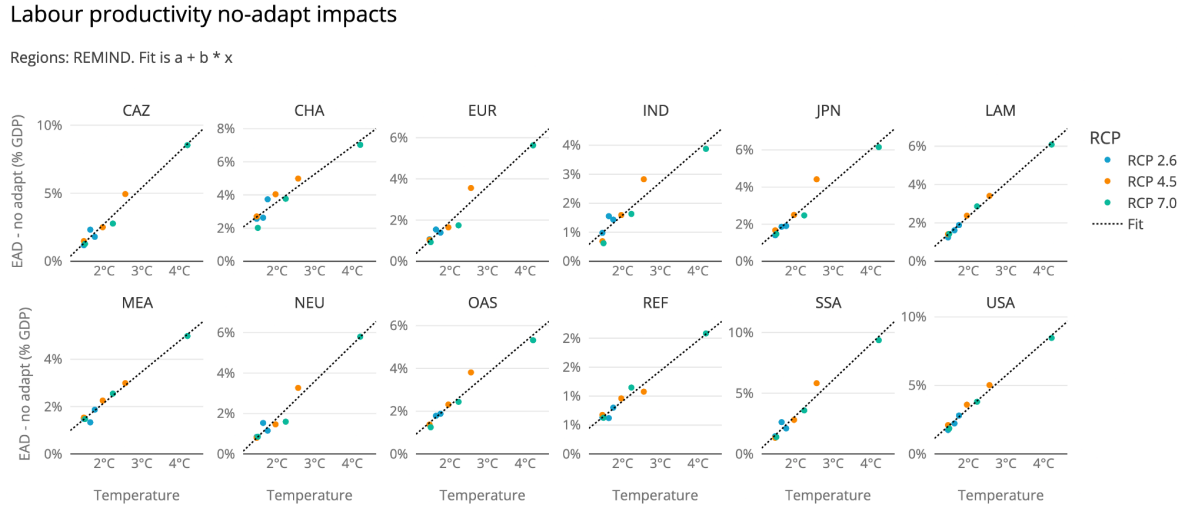

Fig. A-5. REMIND: Gross damages for heat-related labour productivity impacts, as a function of GMT (°C above pre-industrial).

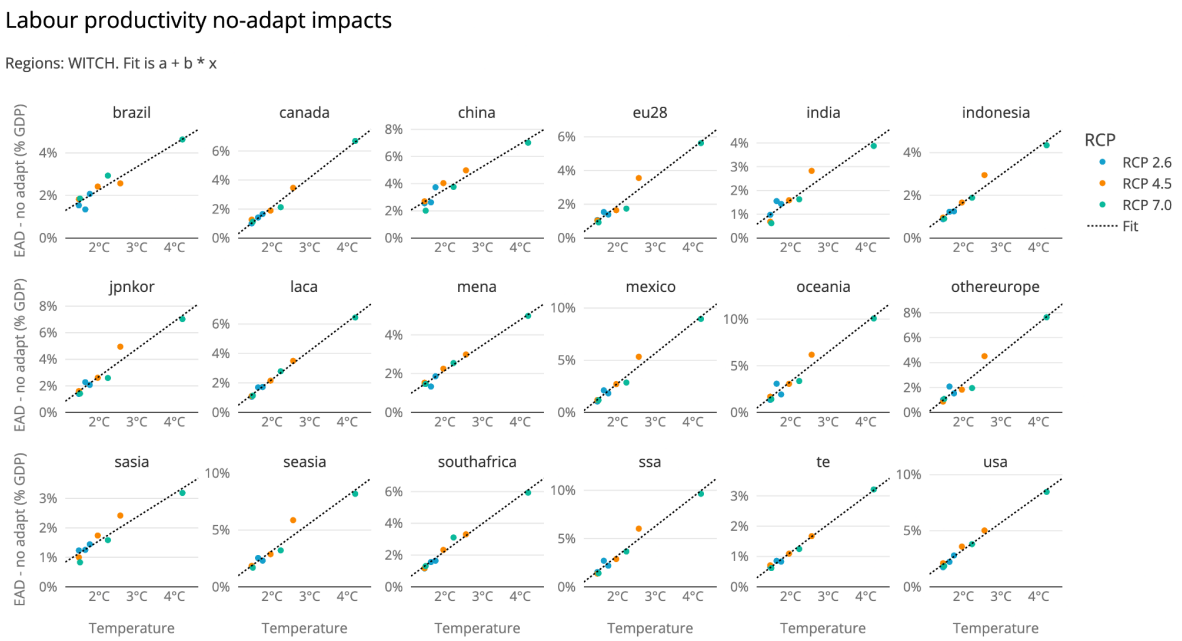

Fig A-6. WITCH: Gross damages for heat-related labour productivity impacts, as a function of GMT (°C above pre-industrial).

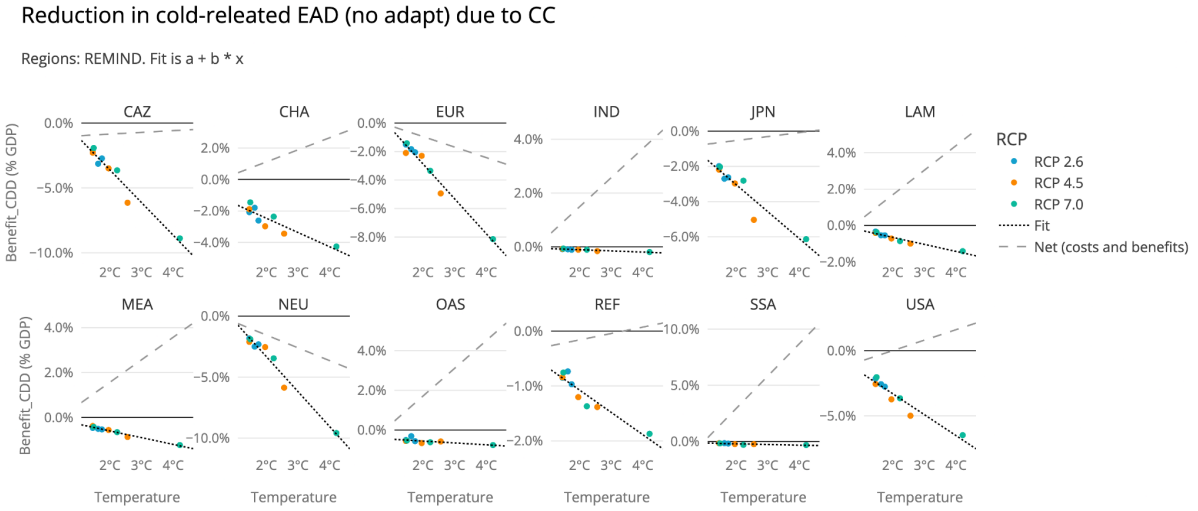

Fig. A-7. REMIND: Cold-related labour productivity benefits (dotted lines), and net costs and benefits (dashed line), as a function of GMT (°C above pre-industrial)

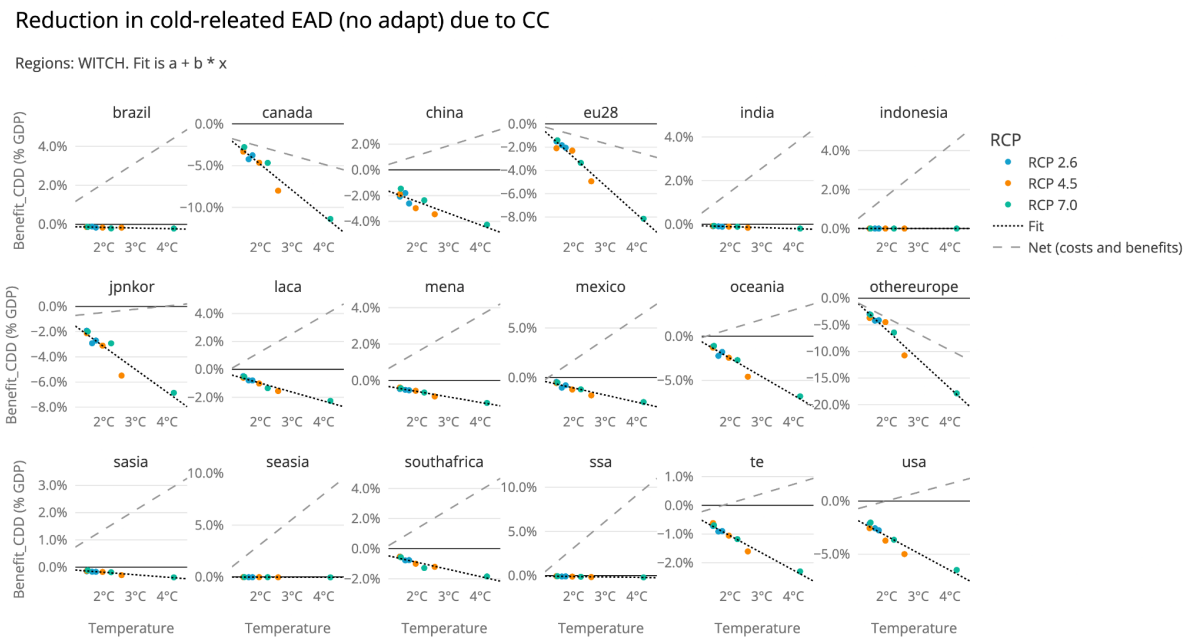

Fig. A-8. WITCH: Cold-related labour productivity benefits (dotted lines), and net costs and benefits (dashed line), as a function of GMT (°C above pre-industrial)

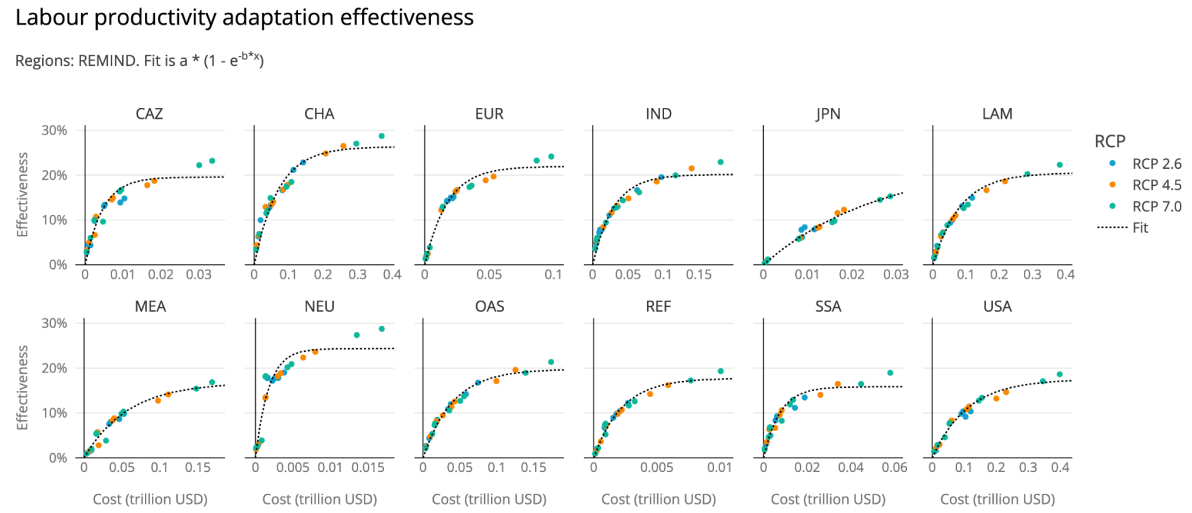

Fig. A-9. REMIND: Adaptation effectiveness (in % of avoided gross damages) for the heat-related labour productivity costs as a function of regional adaptation costs (in trillion US$2017 MER).

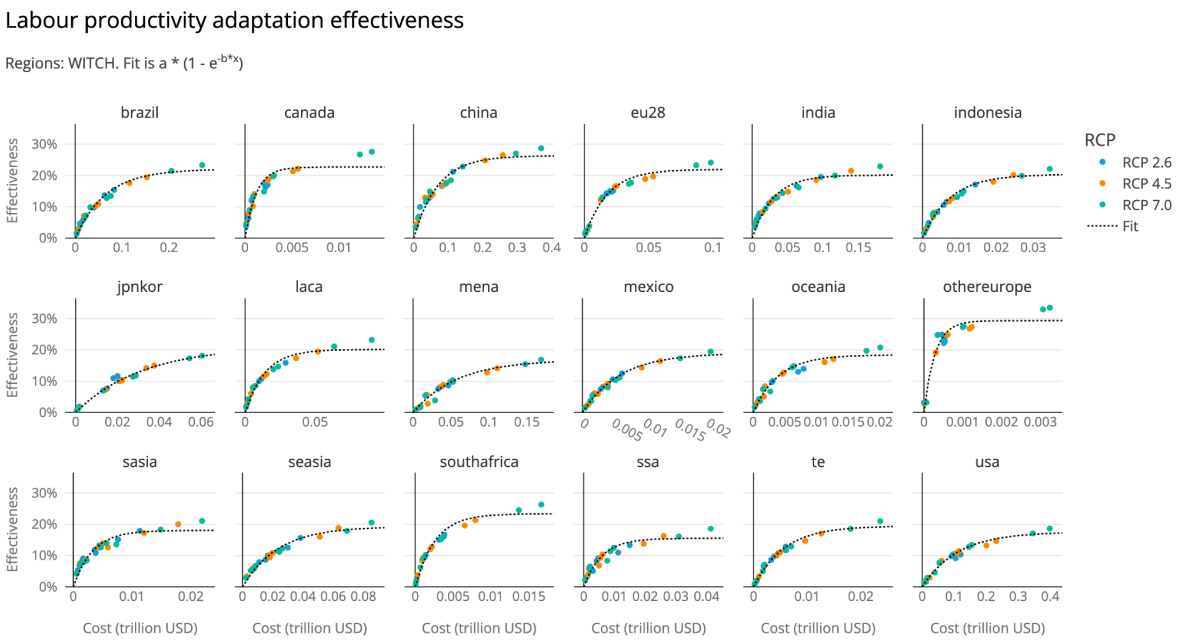

Fig. A-10. WITCH: Adaptation effectiveness (in % of avoided gross damages) for the heat-related labour productivity costs as a function of regional adaptation costs (in trillion US$2017 MER).

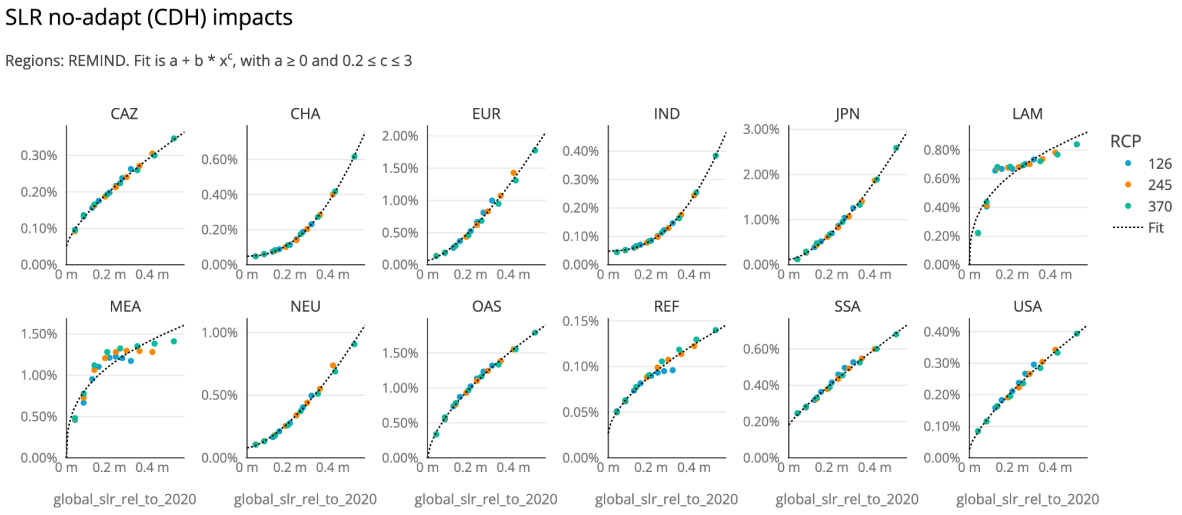

Fig. A-11. REMIND: Gross sea-level rise impacts (constant dike height scenario) as a function of global sea-level rise (in meters, relative to 2020 level).

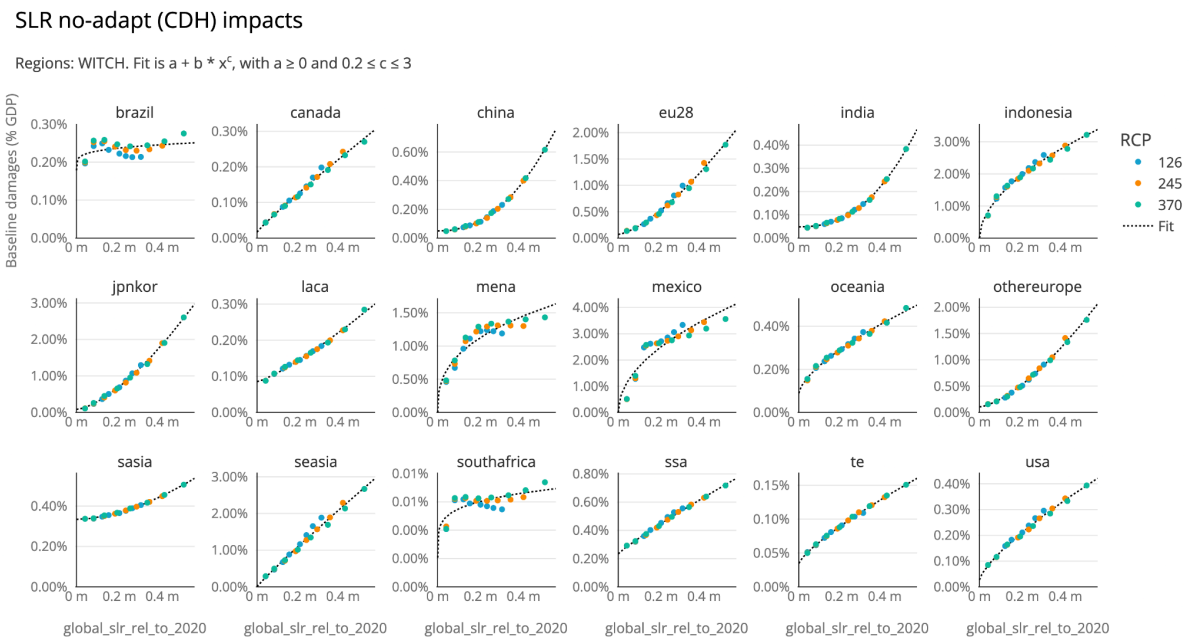

Fig. A-12. WITCH: Gross sea-level rise impacts (constant dike height scenario) as a function of global sea-level rise (in meters, relative to 2020 level).

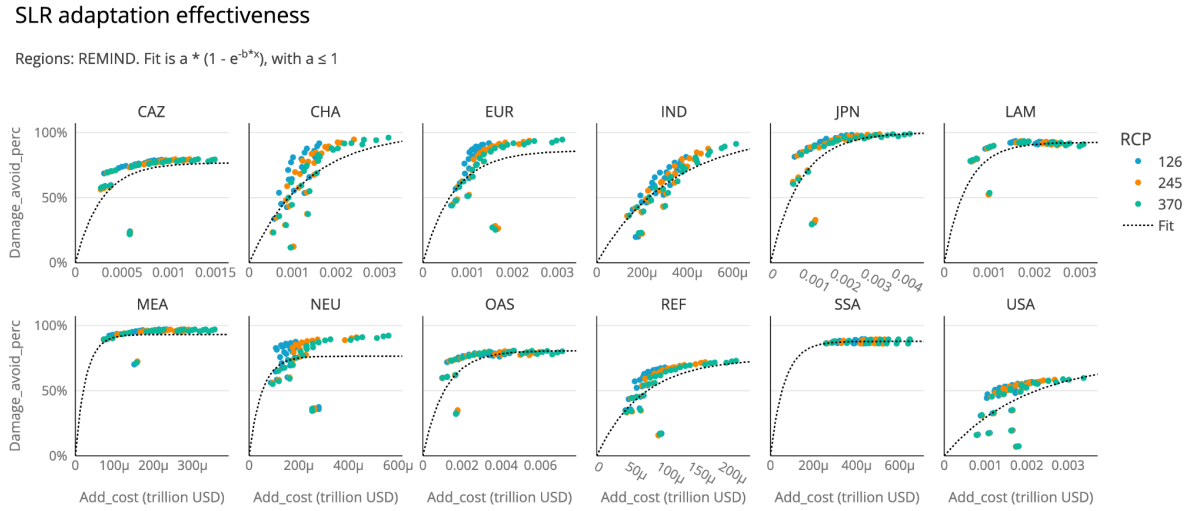

Fig. A-13. REMIND: Adaptation effectiveness (in % of avoided gross damages) for sea-level rise impacts as a function of regional adaptation costs (in trillion US$2017 MER).

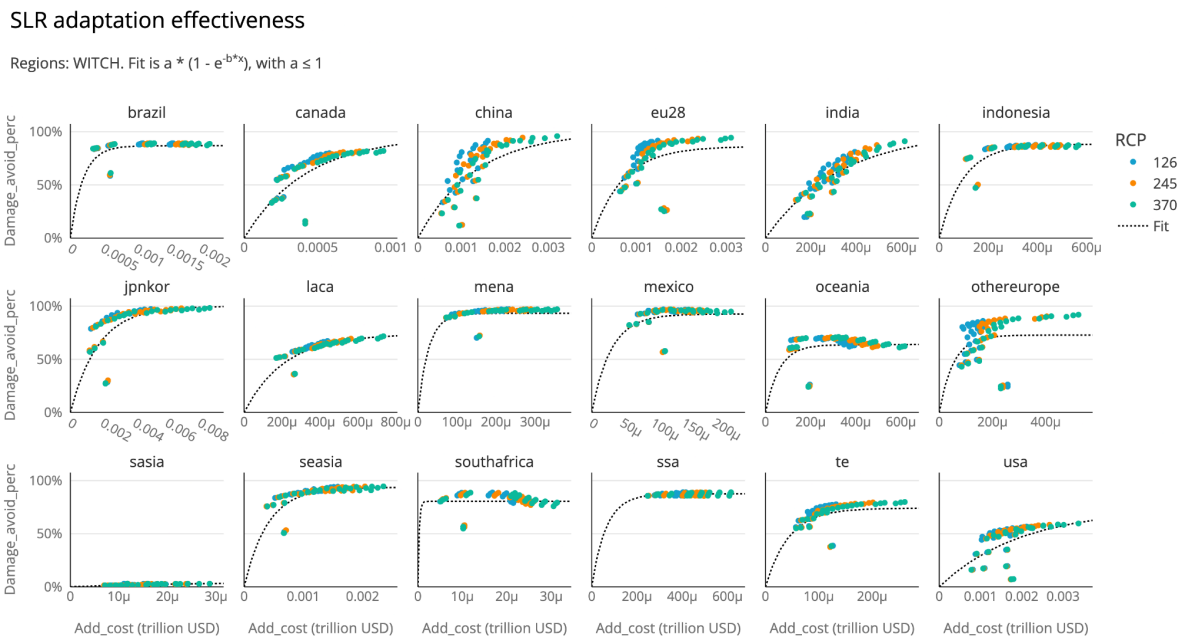

Fig. A-14. WITCH: Adaptation effectiveness (in % of avoided gross damages) for sea-level rise impacts as a function of regional adaptation costs (in trillion US$2017 MER).

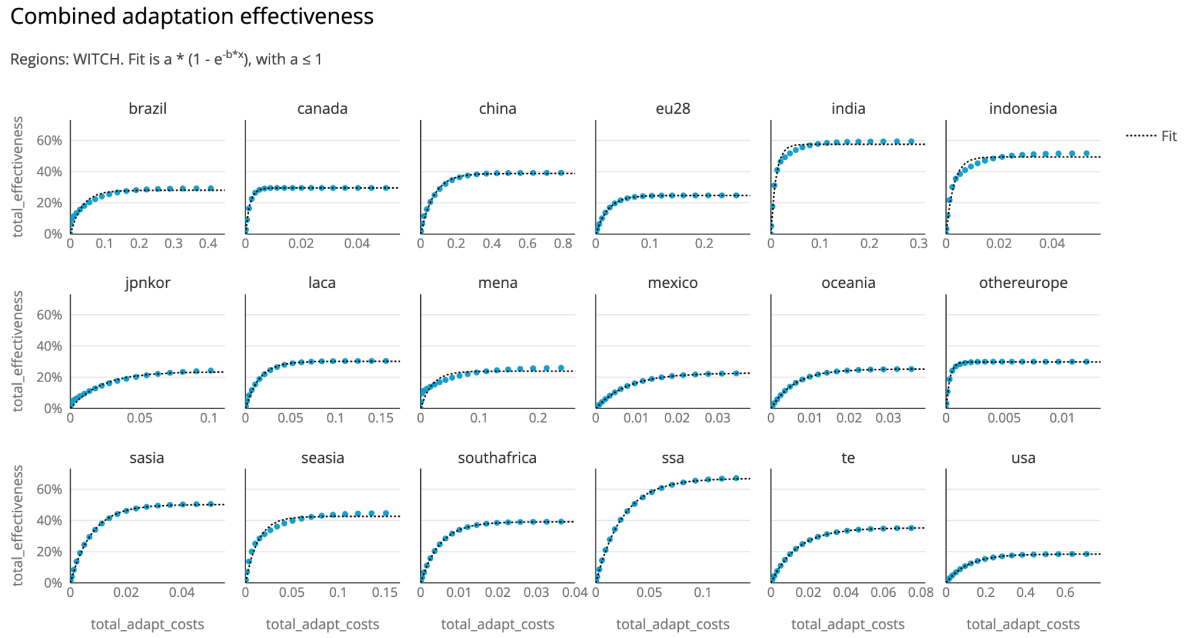

Fig. A-15. REMIND: Combined adaptation effectiveness (in % of avoided gross damages) for riverine and labour productivity impacts combined, as a function of regional adaptation costs (in trillion US$2017 MER). The blue dots are the result of the optimisation routine for 20 values of the total adaptation costs, where the gross damages are calculated with T=2.5°C. The dotted black line is the fit through those points of the negative-exponential saturation curve.

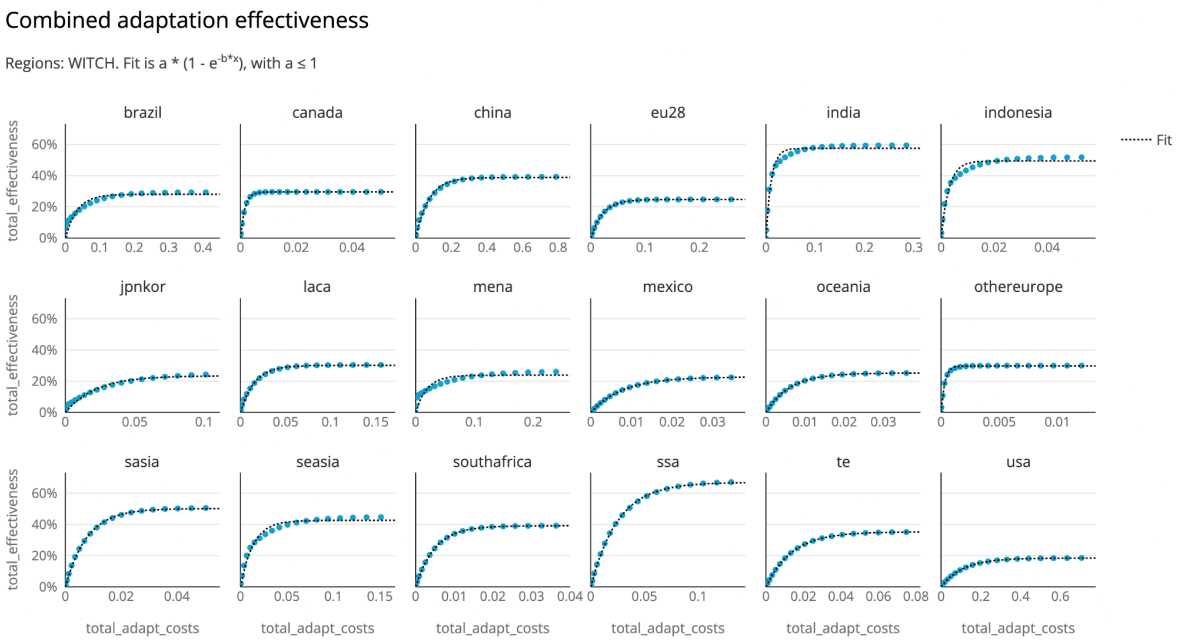

Fig. A-16. WITCH: Combined adaptation effectiveness (in % of avoided gross damages) for riverine and labour productivity impacts combined, as a function of regional adaptation costs (in trillion US$2017 MER). The blue dots are the result of the optimisation routine for 20 values of the total adaptation costs, where the gross damages are calculated with T=2.5°C. The dotted black line is the fit through those points of the negative-exponential saturation curve.

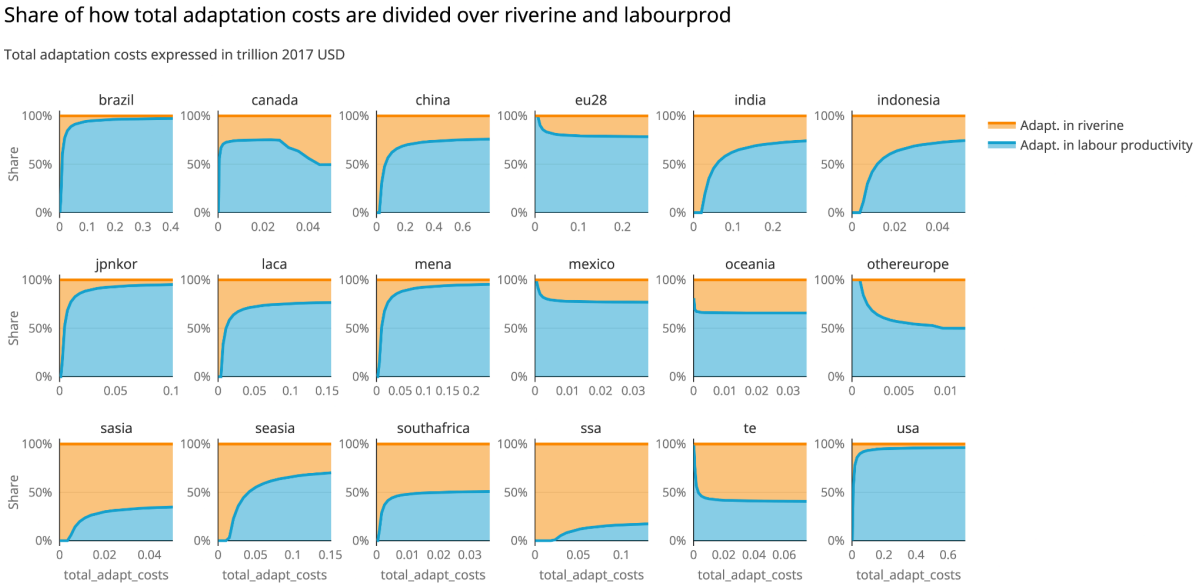

Fig. A-17. REMIND: Share of how the total adaptation costs (x-axis) are split between adaptation in riverine flood protection (yellow) vs in labour productivity adaptation (blue). The x-axis is expressed in trillion US$2017 MER.

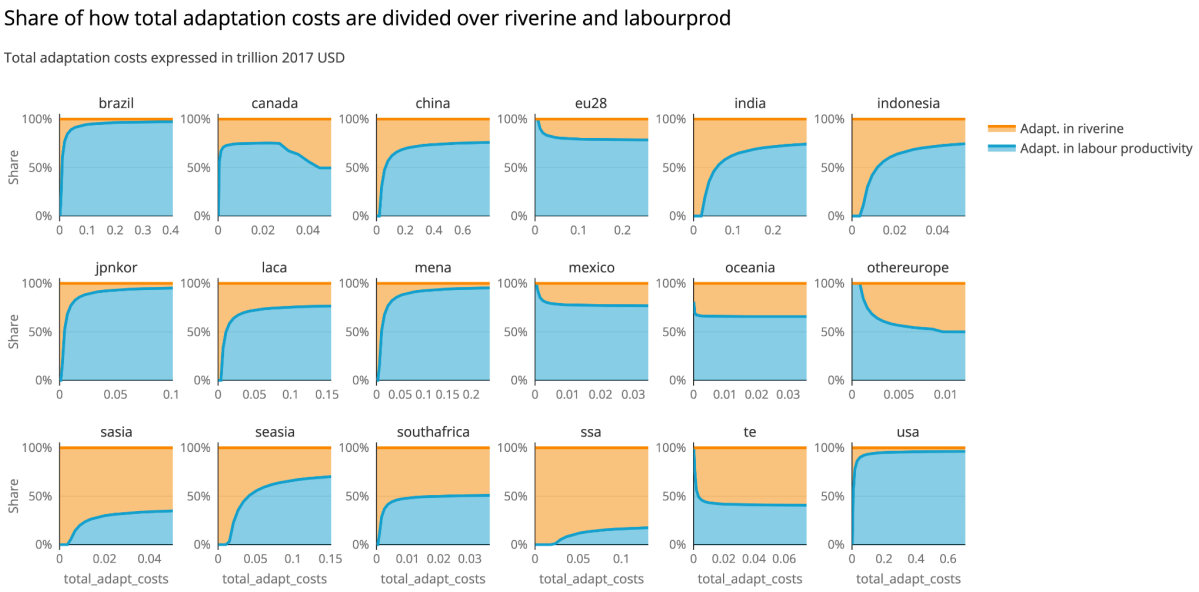

Fig. A-18. WITCH: Share of how the total adaptation costs (x-axis) are split between adaptation in riverine flood protection (yellow) vs in labour productivity adaptation (blue). The x-axis is expressed in trillion US$2017 MER.

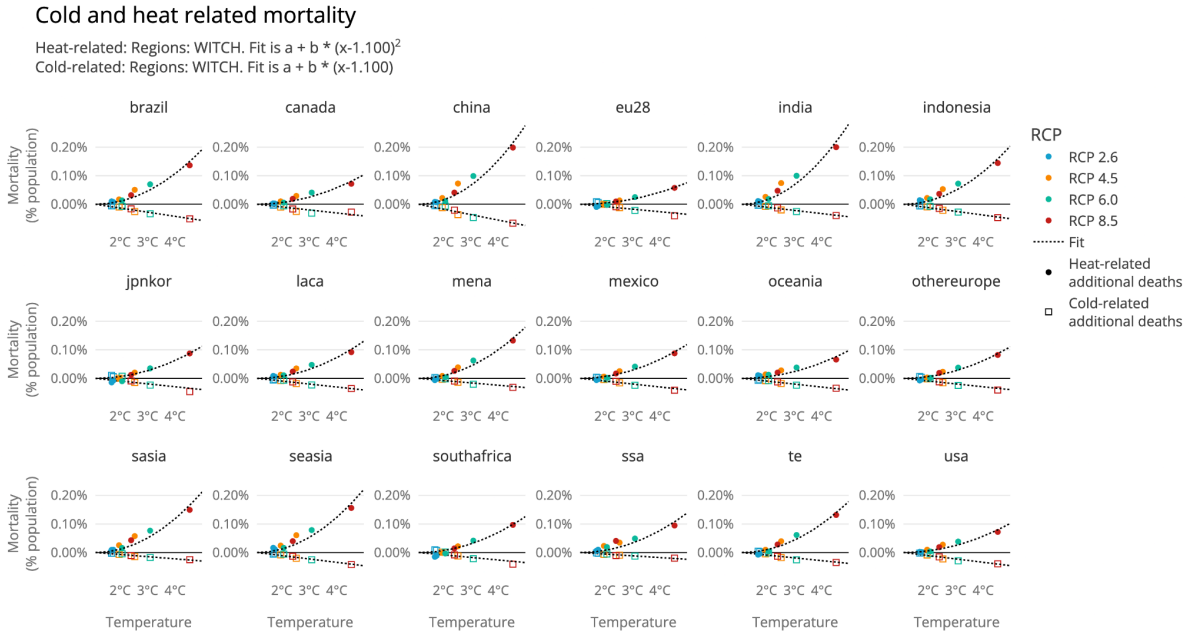

Fig. A-19. REMIND: Mortality damage functions, expressing mortality in % of regional population as a function of global mean temperature. The solid circles represent additional heat-related mortality, while the open squares represent the reduction in cold-related mortality.

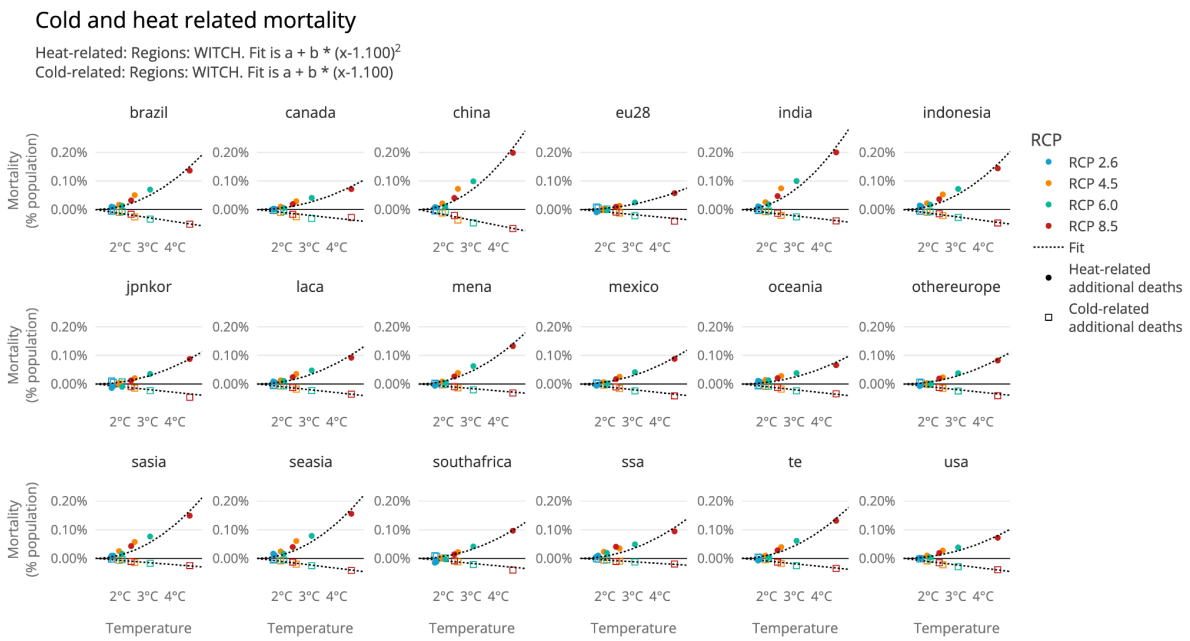

Fig. A-20. WITCH: Mortality damage functions, expressing mortality in % of regional population as a function of global mean temperature. The solid circles represent additional heat-related mortality, while the open squares represent the reduction in cold-related mortality.

7.2. Appendix B: Distribution of damages, adaptation costs and mortality costs.

In this section, we illustrate regional differences in damage costs, adaptation costs and mortality costs for the three models.

7.2.1. REMIND

Gross damages

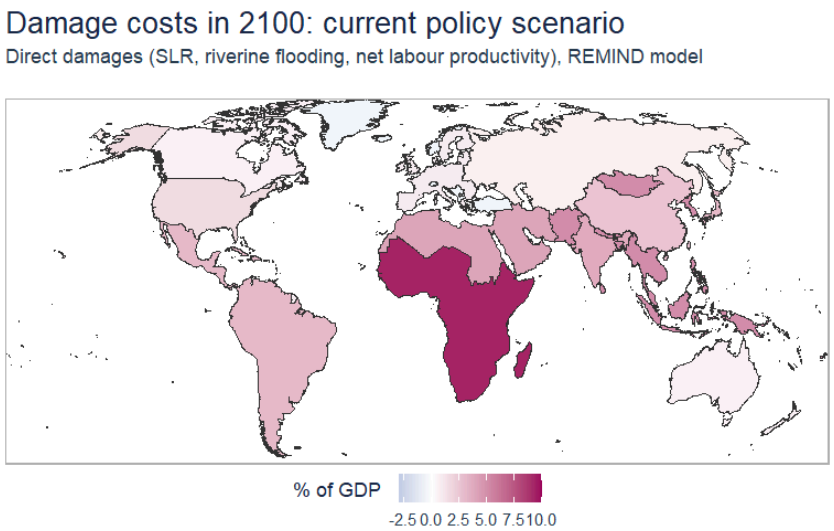

Fig. B-1: Regionally differentiated damage costs in REMIND in 2100 under current policy conditions.

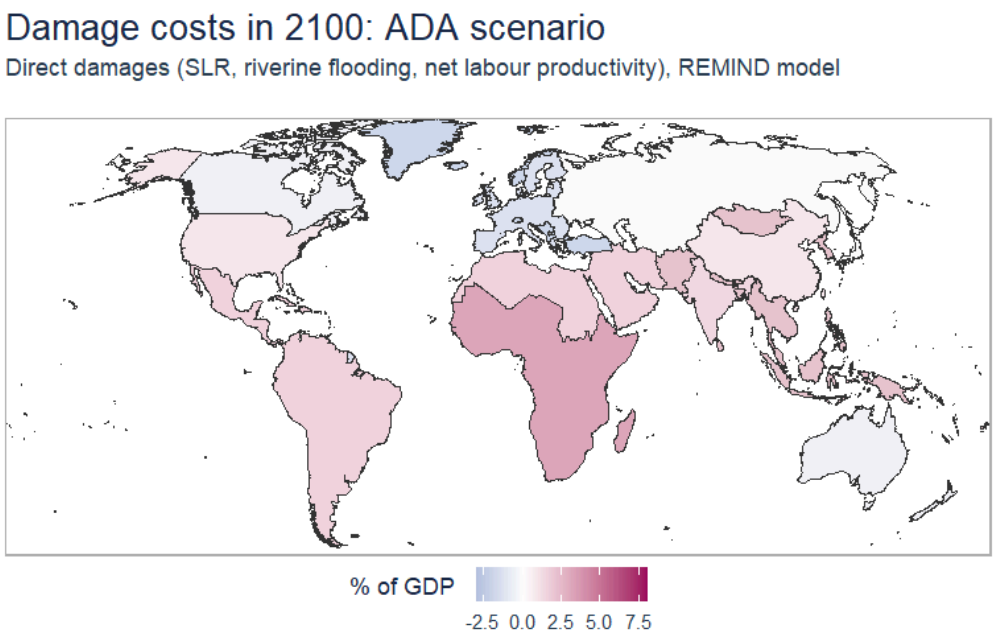

Fig. B-2: Regionally differentiated damage costs in REMIND in 2100 under CBA-optimal policy with adaptation as the sole policy option.

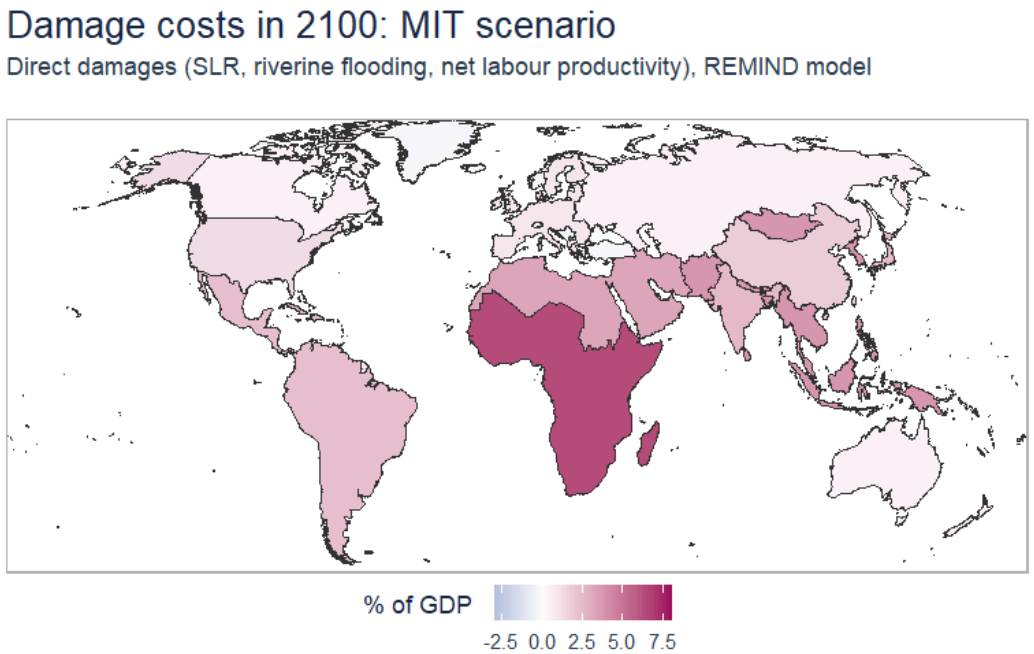

Fig. B-3: Regionally differentiated damage costs in REMIND in 2100 under CBA-optimal policy with mitigation as the sole policy option.

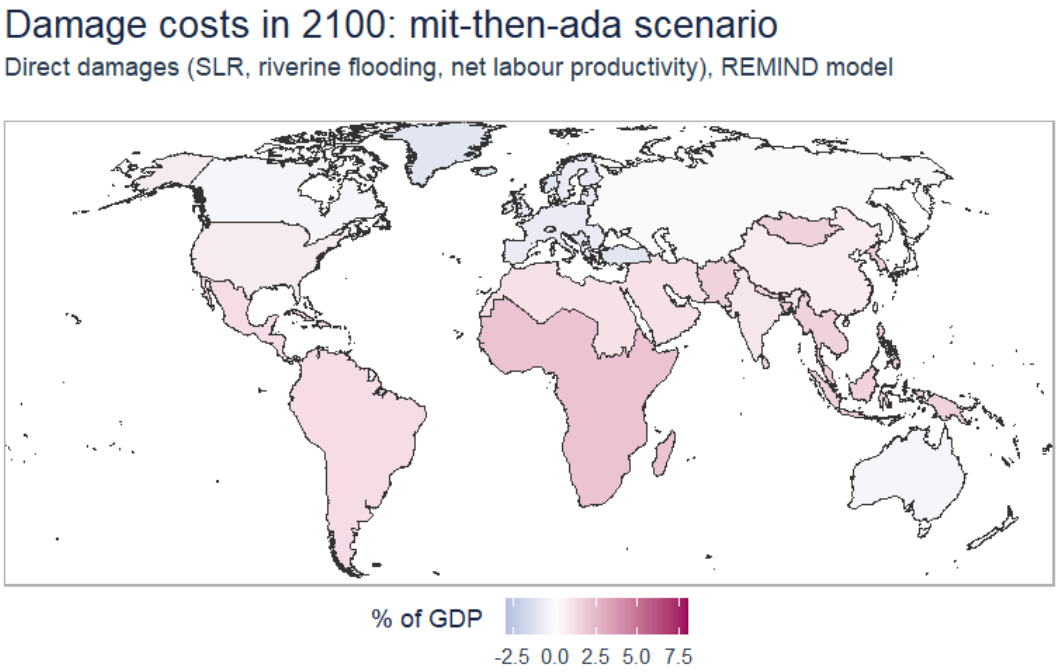

Fig. B-4: Regionally differentiated damage costs in REMIND in 2100 under CBA-optimal policy when mitigation is optimised, followed by optimised adaptation.

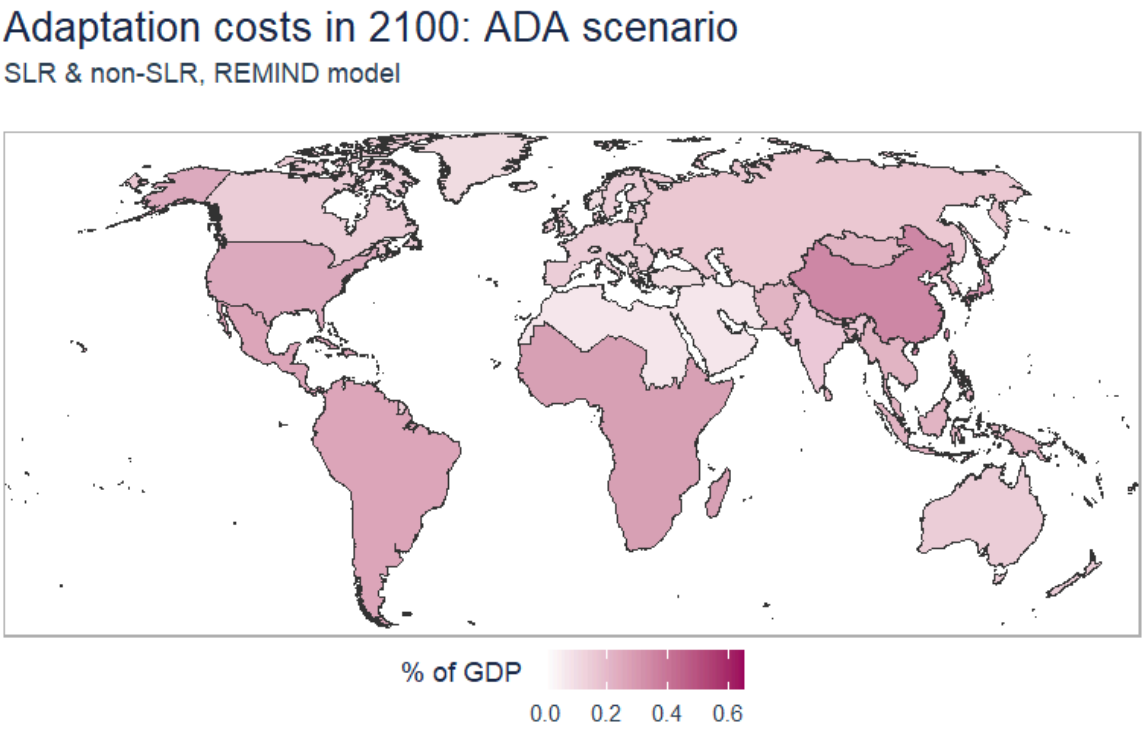

Fig. B-5: Regionally differentiated adaptation costs in REMIND in 2100 under CBA-optimal policy with adaptation as the sole policy option.

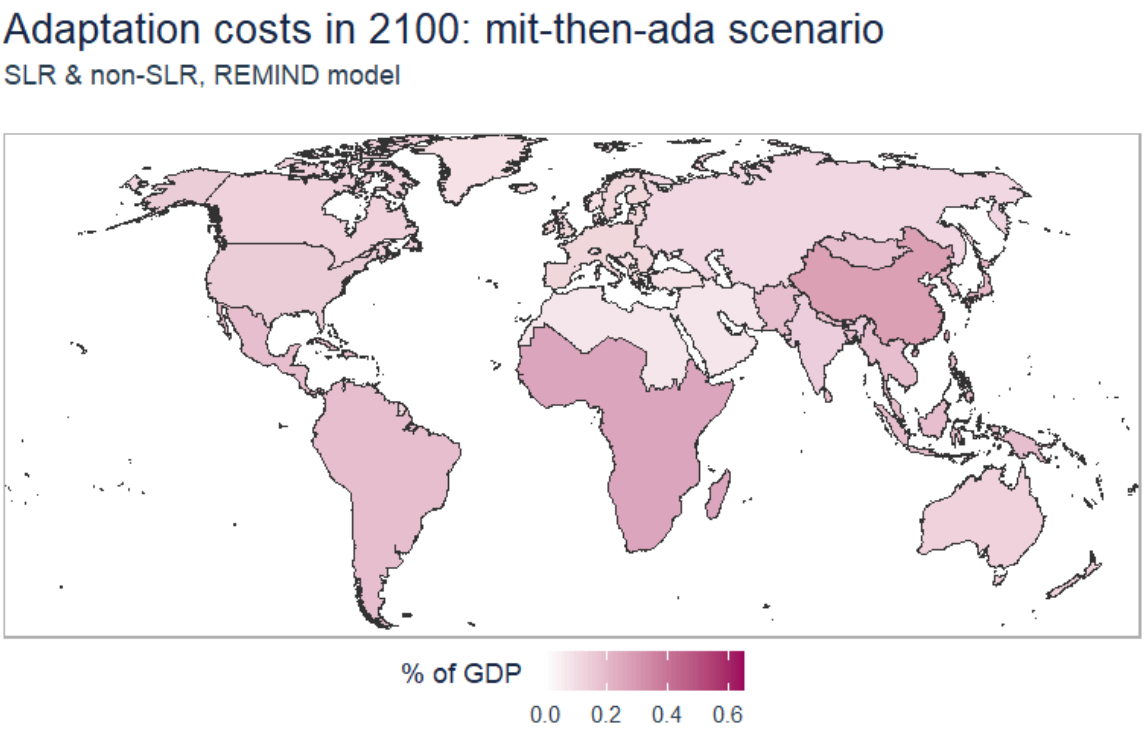

Fig. B-6: Regionally differentiated adaptation costs in REMIND in 2100 under CBA-optimal policy when mitigation is optimised, followed by optimised adaptation.

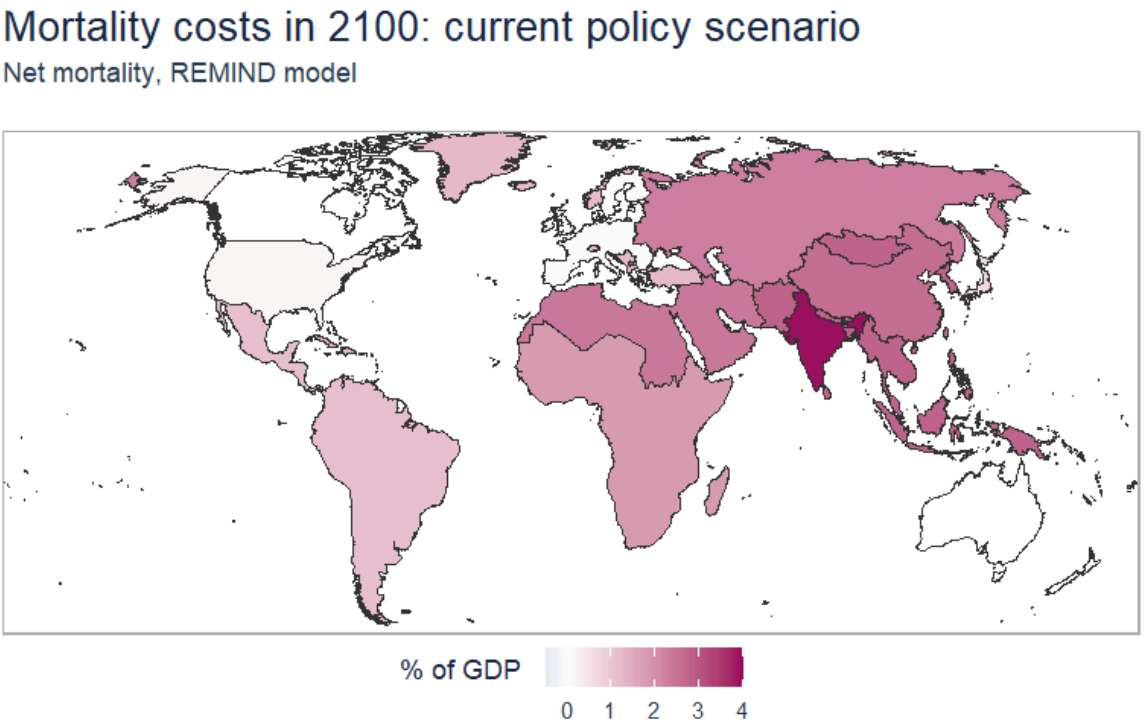

Fig. B-7: Regionally differentiated mortality costs in REMIND in 2100 under current policy conditions.

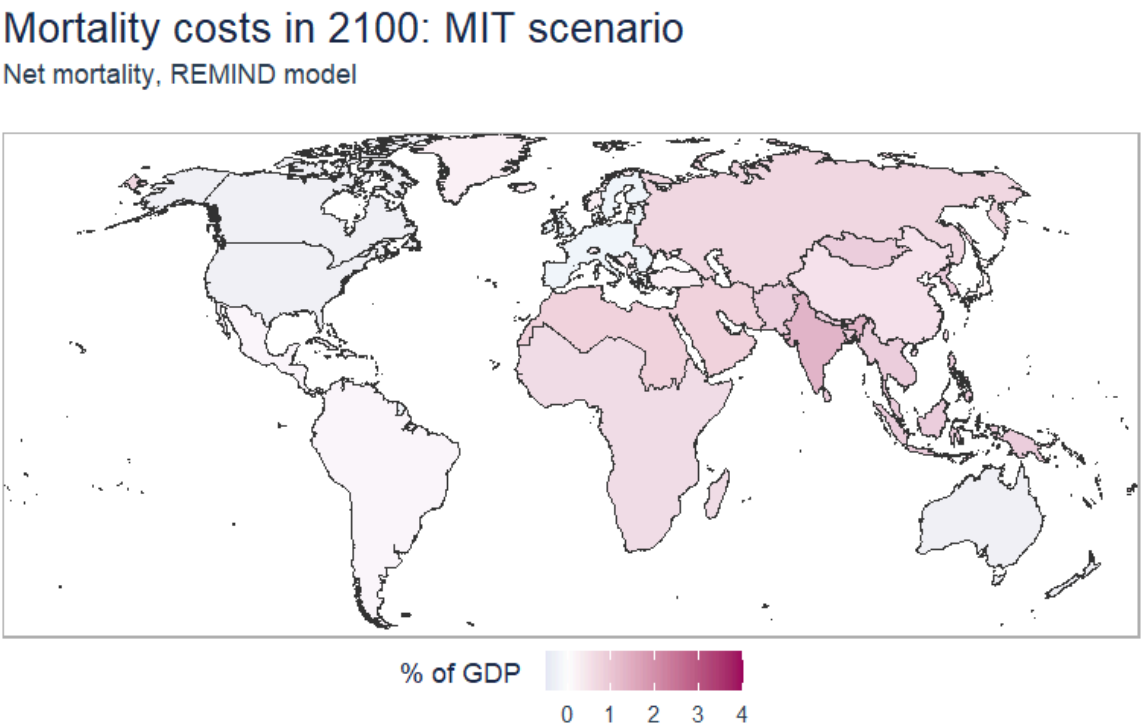

Fig. B-8: Regionally differentiated mortality costs in REMIND in 2100 under CBA-optimal policy when mitigation is the sole policy option.

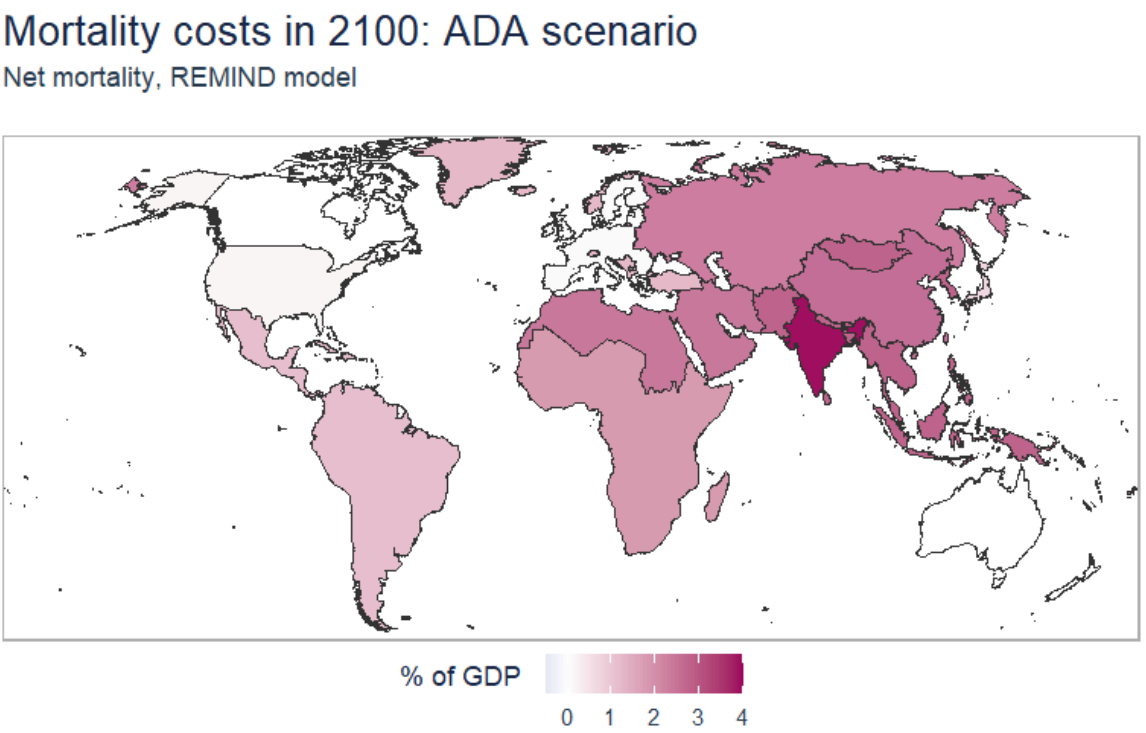

Fig. B-9: Regionally differentiated mortality costs in REMIND in 2100 under CBA-optimal policy when adaptation is the sole policy option.

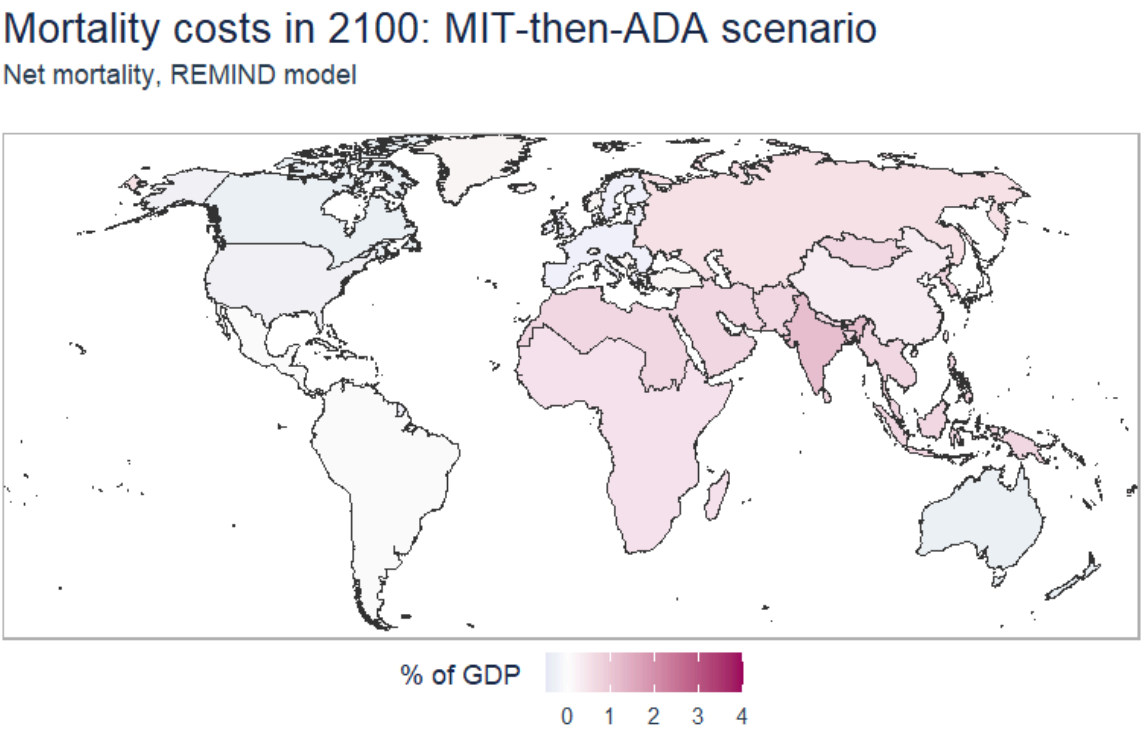

Fig. B-10: Regionally differentiated mortality costs in REMIND in 2100 under CBA-optimal policy when mitigation is optimised, followed by optimised adaptation.

7.2.2. WITCH

Gross damages

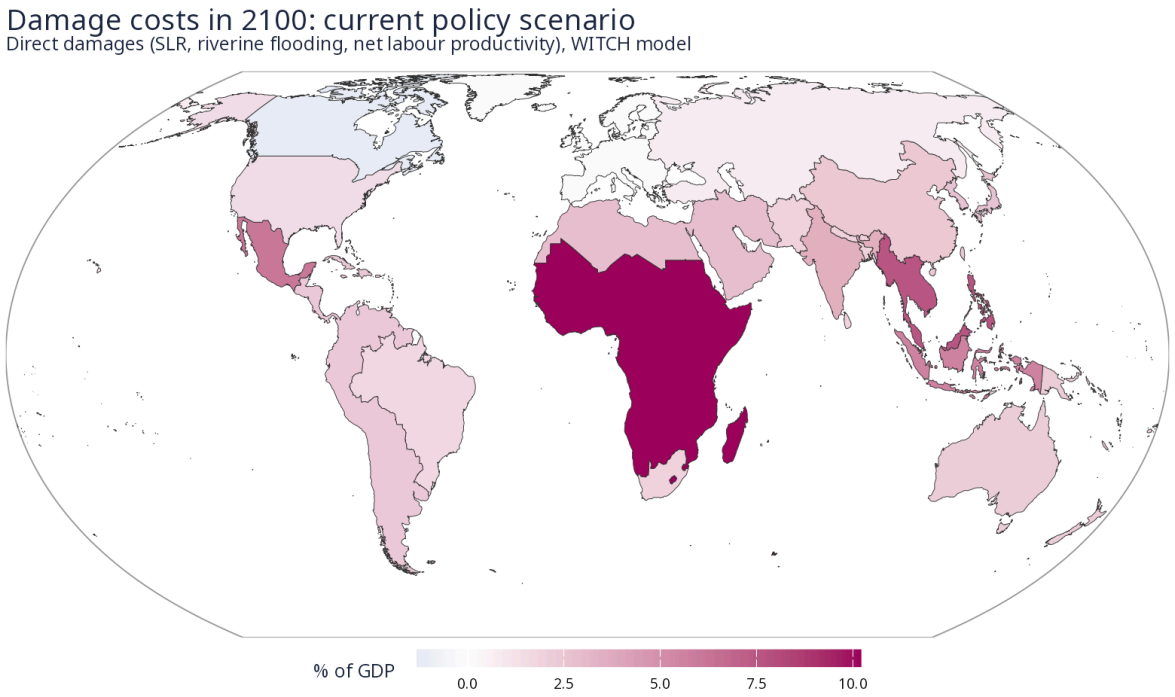

Fig. B-11: Regionally differentiated damage costs in WITCH in 2100 under current policy conditions.

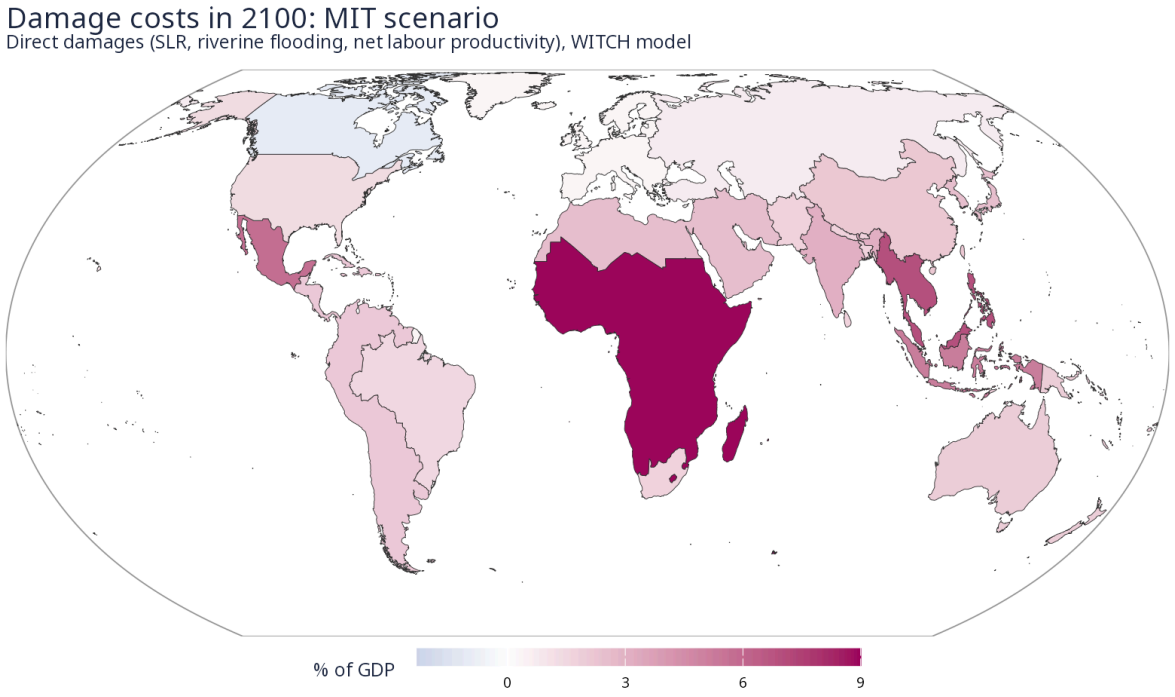

Fig. B-12: Regionally differentiated damage costs in WITCH in 2100 under CBA-optimal policy with mitigation

as the sole policy option.

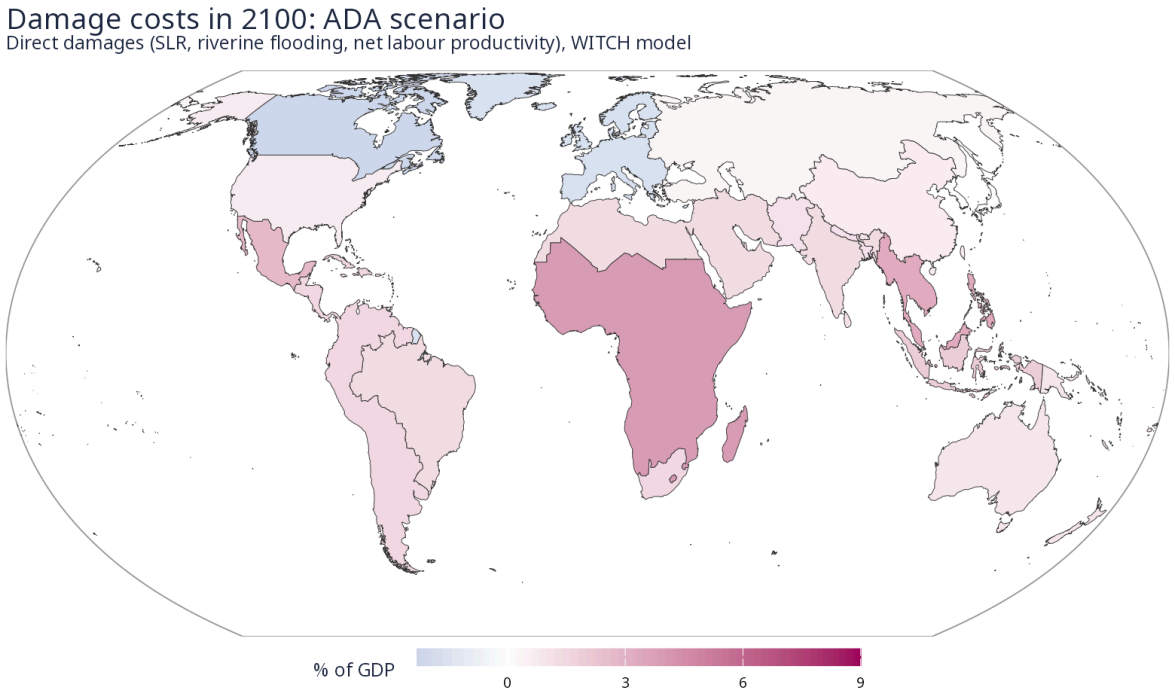

Fig. B-12: Regionally differentiated damage costs in WITCH in 2100 under CBA-optimal policy with adaptation as the sole policy option.

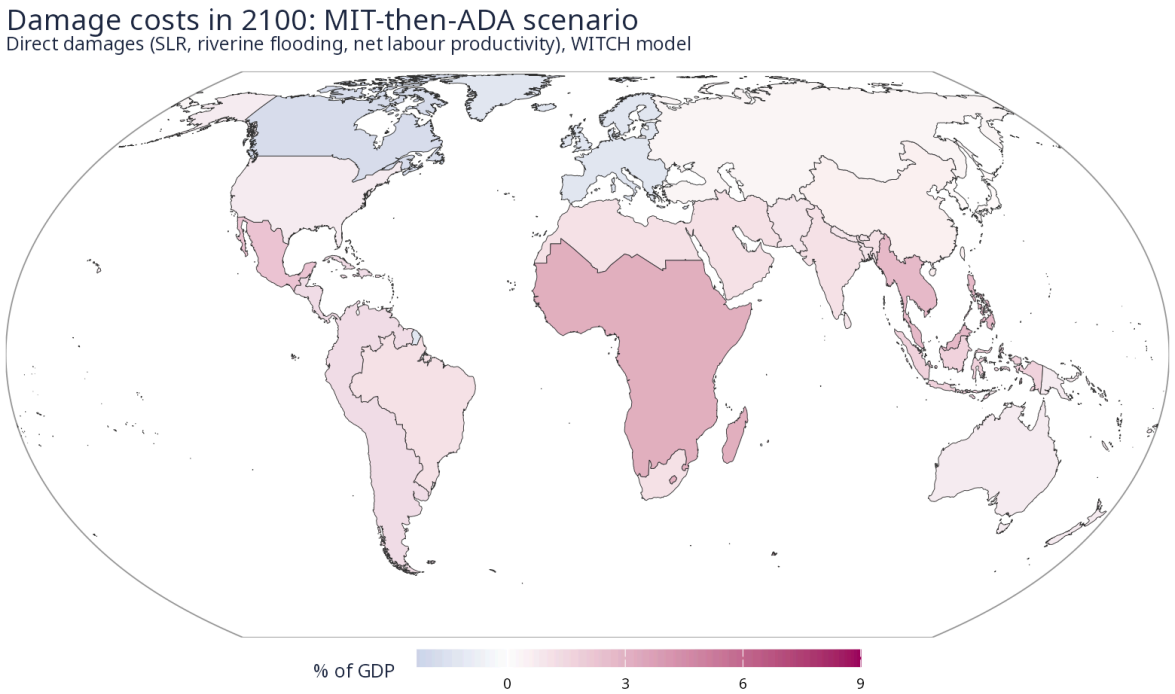

Fig. B-13: Regionally differentiated damage costs in WITCH in 2100 under CBA-optimal policy when mitigation is optimised, followed by optimised adaptation.

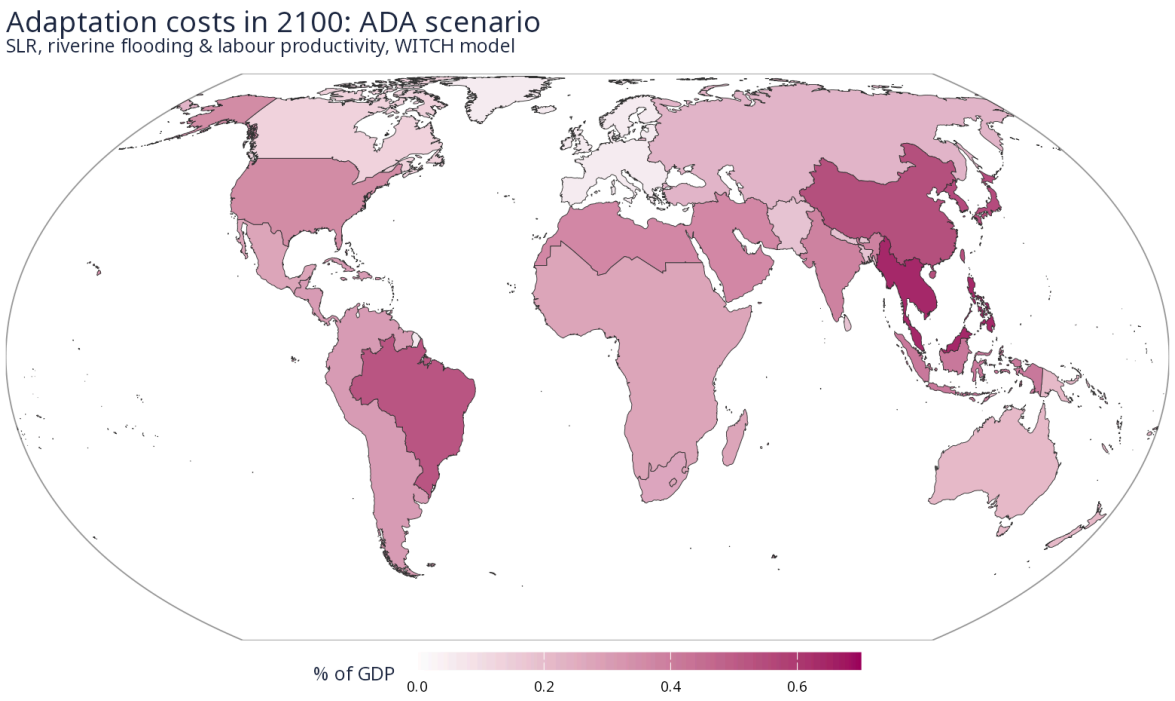

Fig. B-14: Regionally differentiated adaptation costs in WITCH in 2100 under CBA-optimal policy with adaptation as the sole policy option.

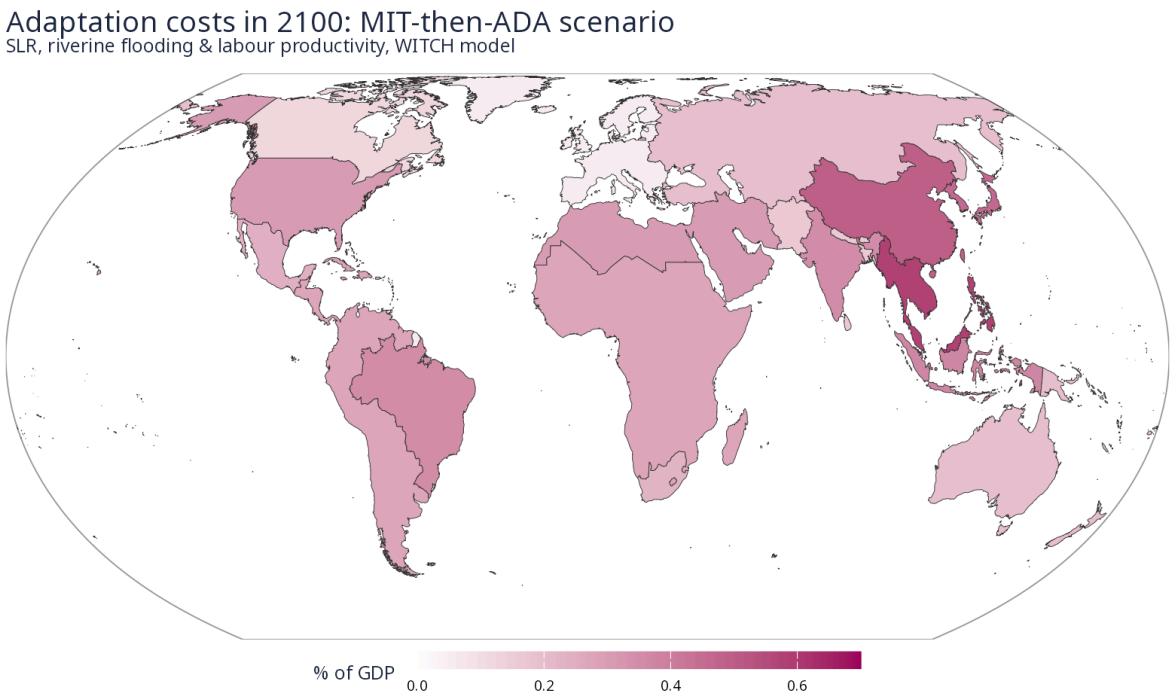

Fig. B-15: Regionally differentiated adaptation costs in WITCH in 2100 under CBA-optimal policy when mitigation is optimised, followed by optimised adaptation.

Mortality costs

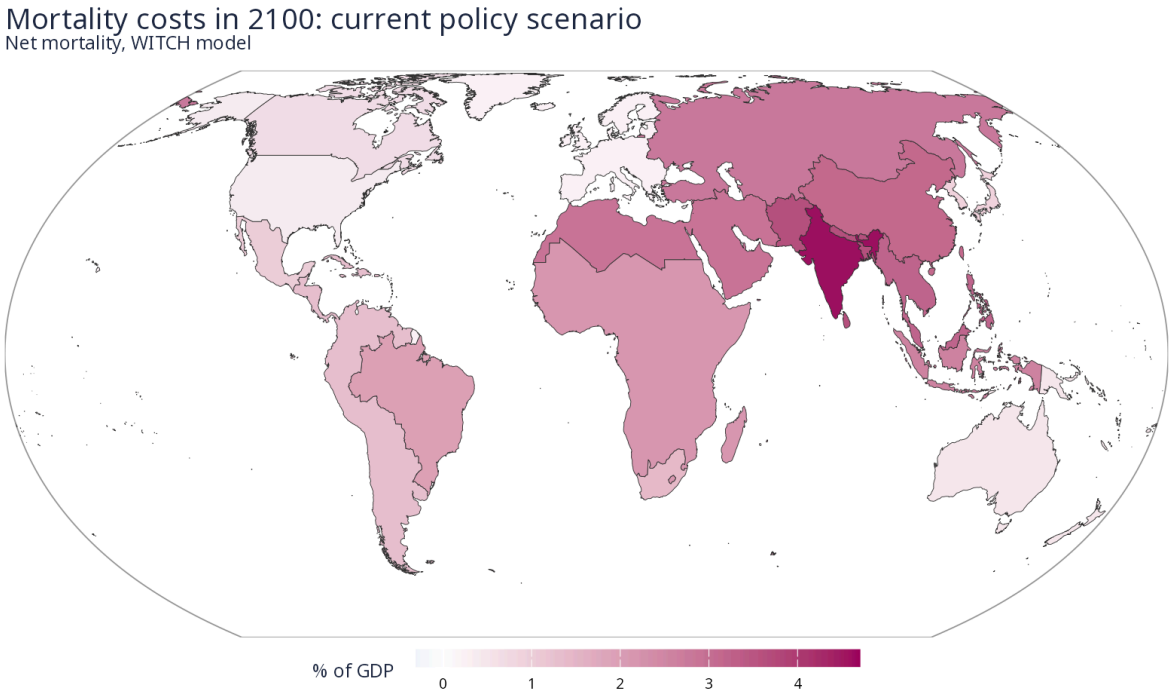

Fig. B-16: Regionally differentiated mortality costs in WITCH in 2100 under current policy conditions.

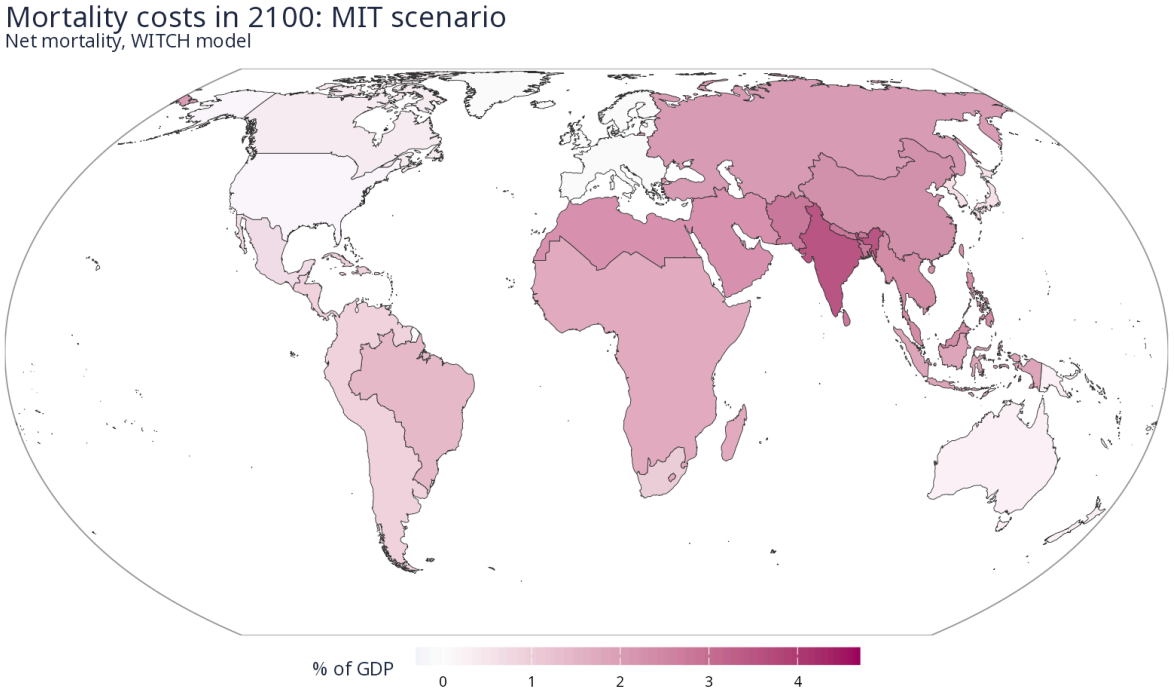

Fig. B-16: Regionally differentiated mortality costs in WITCH in 2100 under CBA-optimal policy when mitigation is the sole policy option.

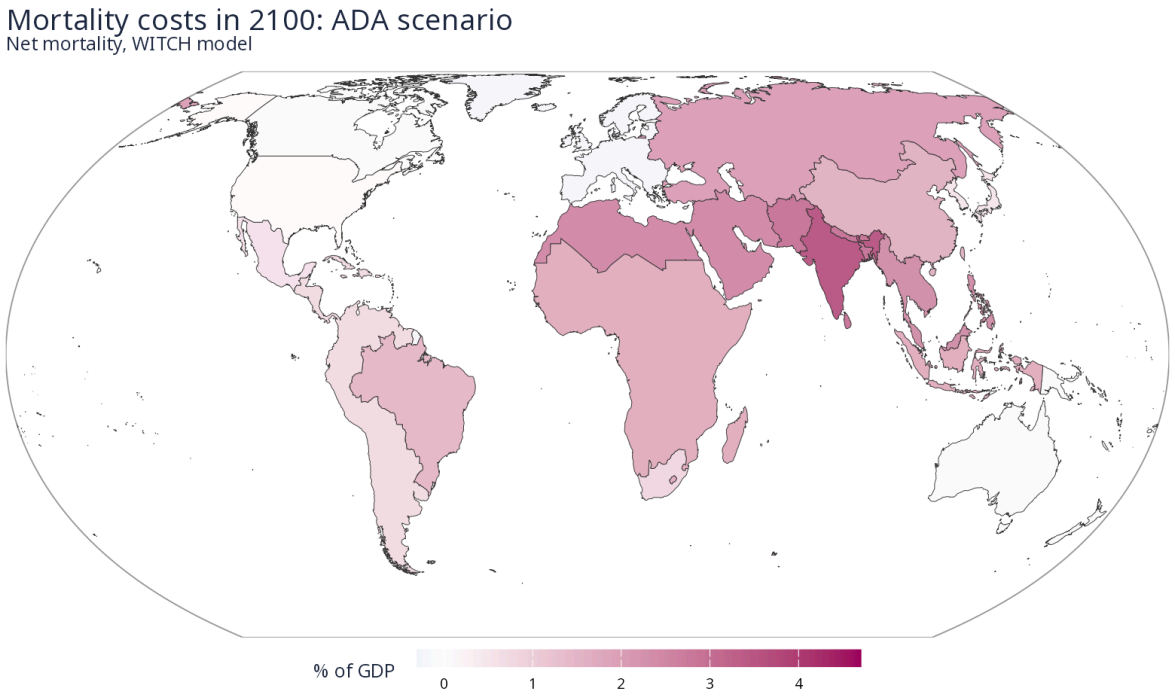

Fig. B-17: Regionally differentiated mortality costs in WITCH in 2100 under CBA-optimal policy when adaptation is the sole policy option.

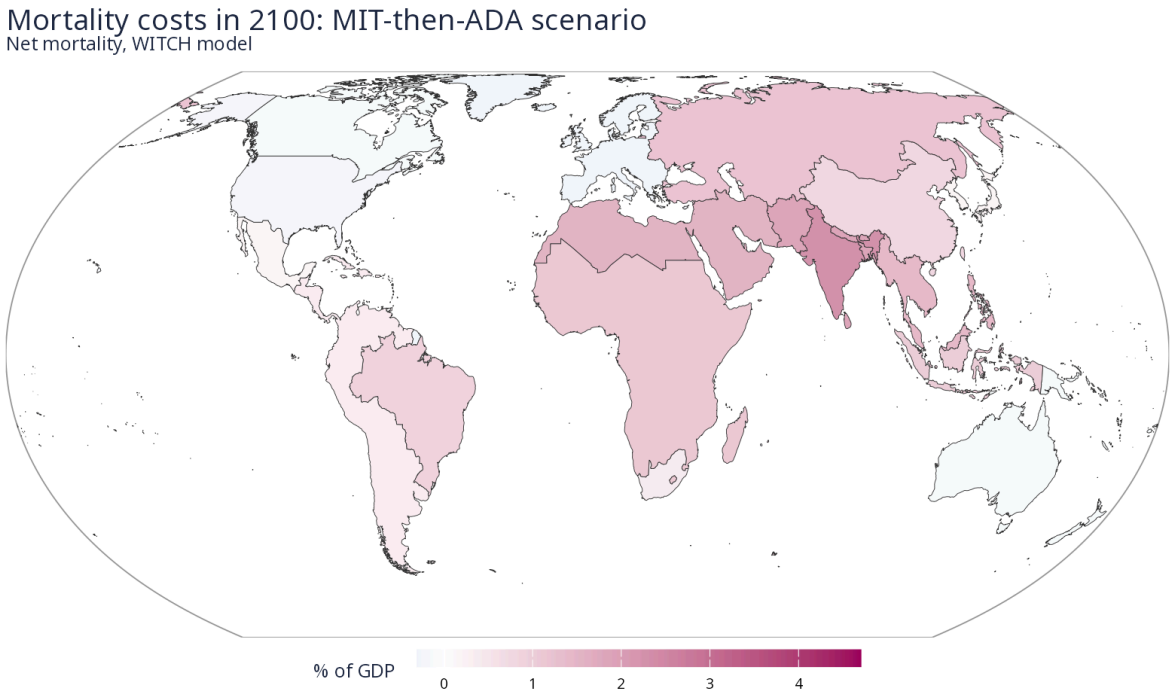

Fig. B-18: Regionally differentiated mortality costs in WITCH in 2100 under CBA-optimal policy when mitigation is optimised, followed by optimised adaptation.

7.2.3. MIMOSA

Damages

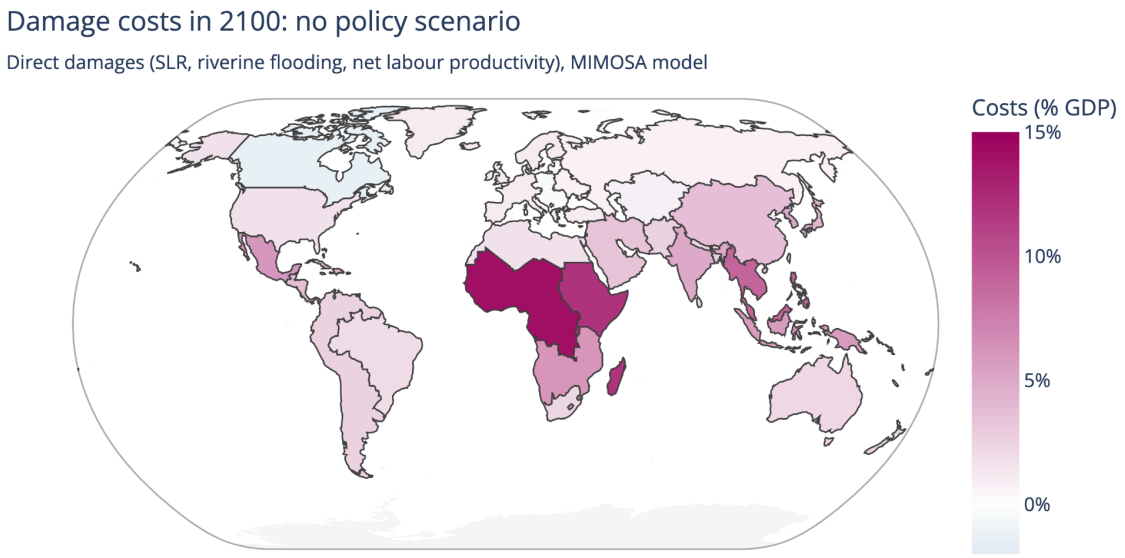

Fig B-19: Regionally differentiated damage costs in MIMOSA in 2100 under current policy conditions.

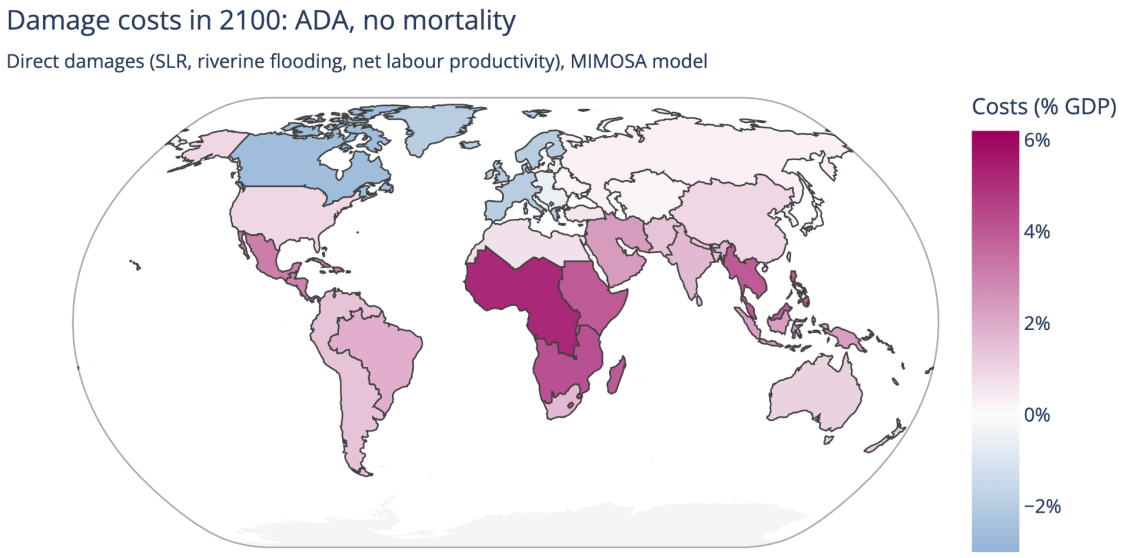

Fig B-20: Regionally differentiated damage costs in MIMOSA in 2100 2100 under CBA-optimal policy with adaptation as the sole policy option.

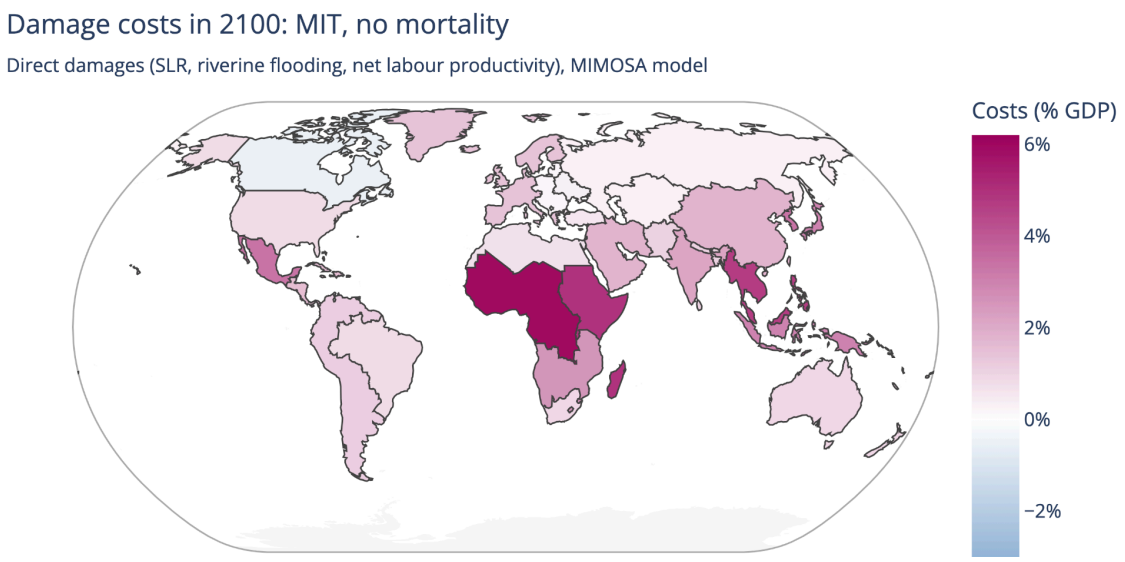

Fig. B-21: Regionally differentiated damage costs in MIMOSA in 2100 under CBA-optimal policy with mitigation as the sole policy option.

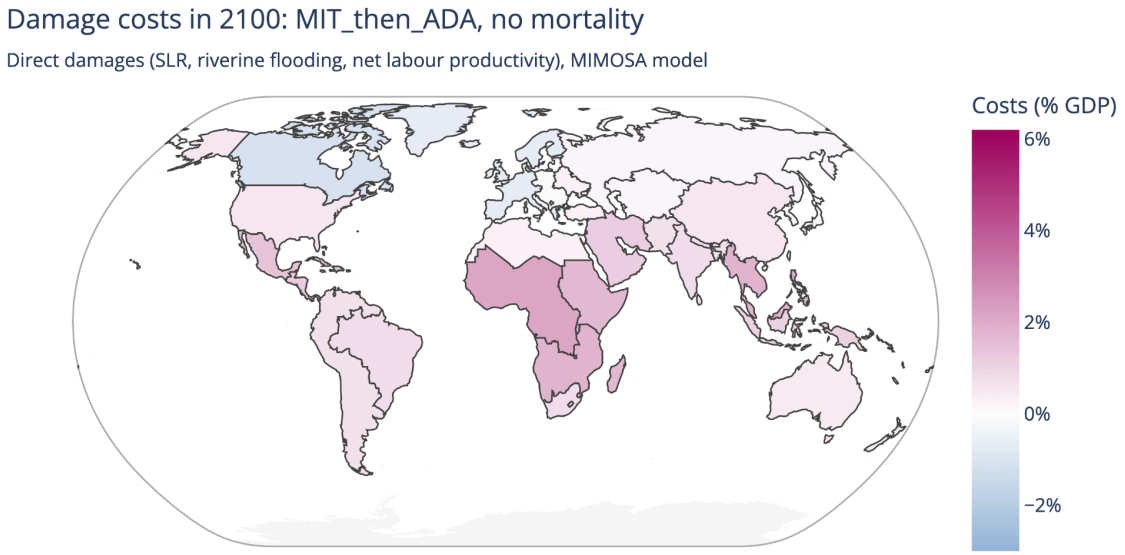

Fig. B-22: Regionally differentiated damage costs in MIMOSA in 2100 under CBA-optimal policy when mitigation is optimised, followed by optimised adaptation.

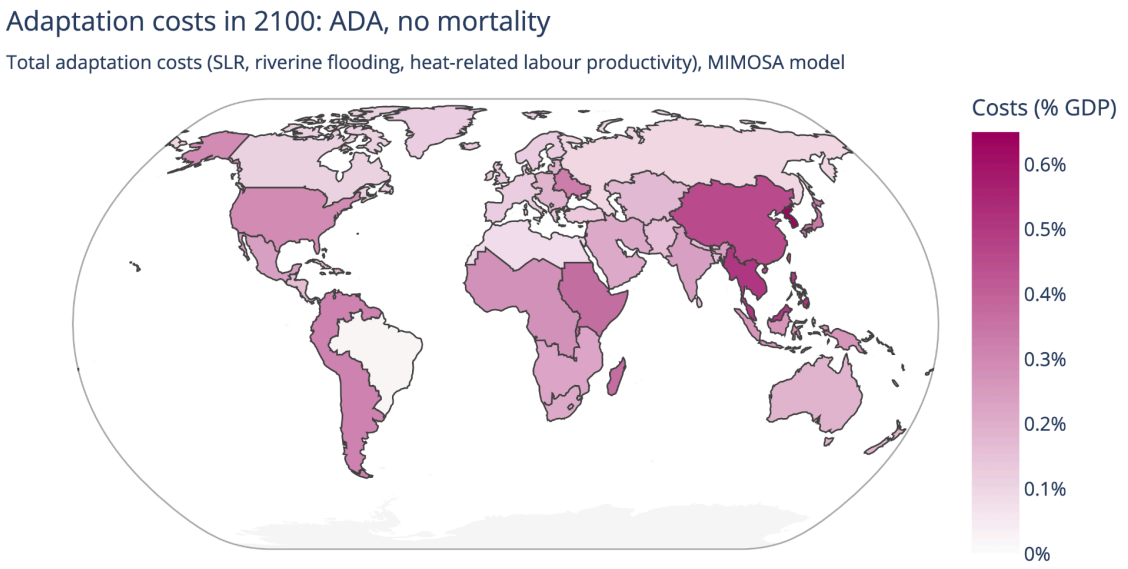

Fig. B-23: Regionally differentiated adaptation costs in MIMOSA in 2100 under CBA-optimal policy with adaptation as the sole policy option.

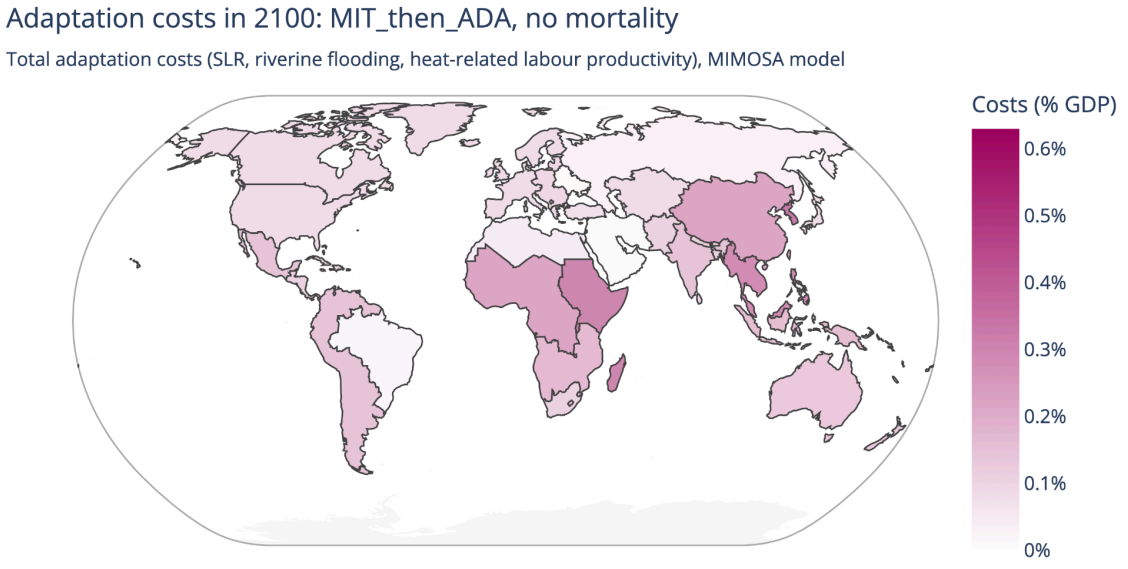

Fig. B-24: Regionally differentiated adaptation costs in MIMOSA in 2100 under CBA-optimal policy when mitigation is optimised, followed by optimised adaptation.

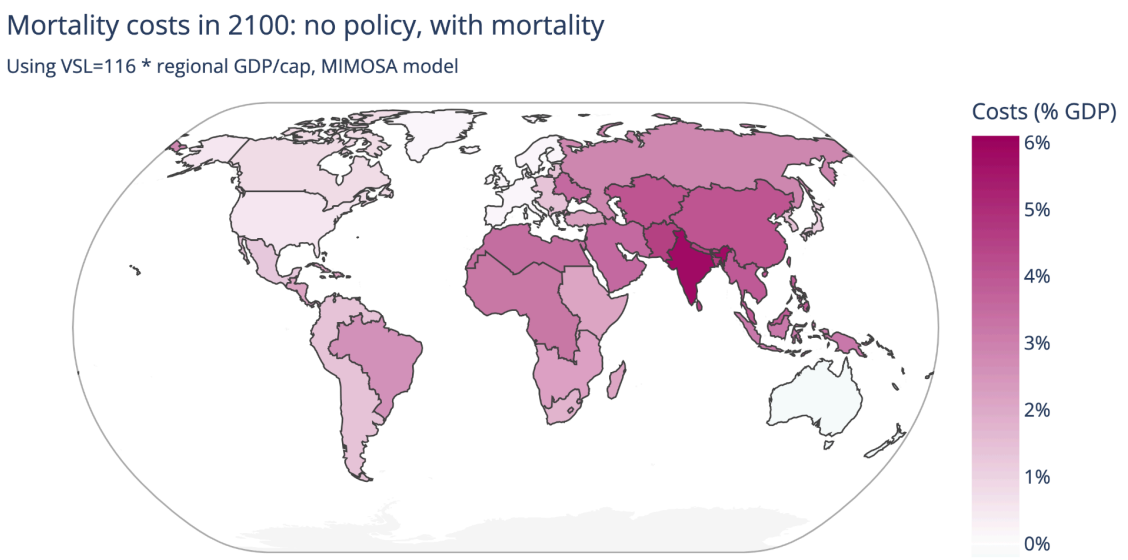

Fig. B-25: Regionally differentiated mortality costs in MIMOSA in 2100 under current policy conditions.

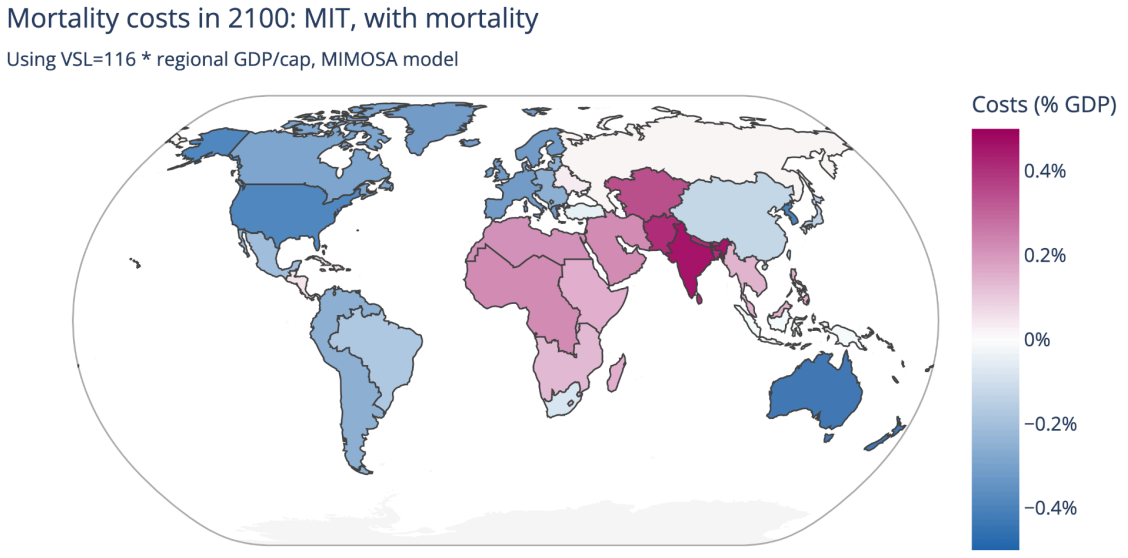

Fig. B-26: Regionally differentiated mortality costs in MIMOSA in 2100 under current policy conditions

7.3. Appendix C: Adaptation protection level under successful adaptation (ADA) vs. an implementation gap (ADA_impl_gap)

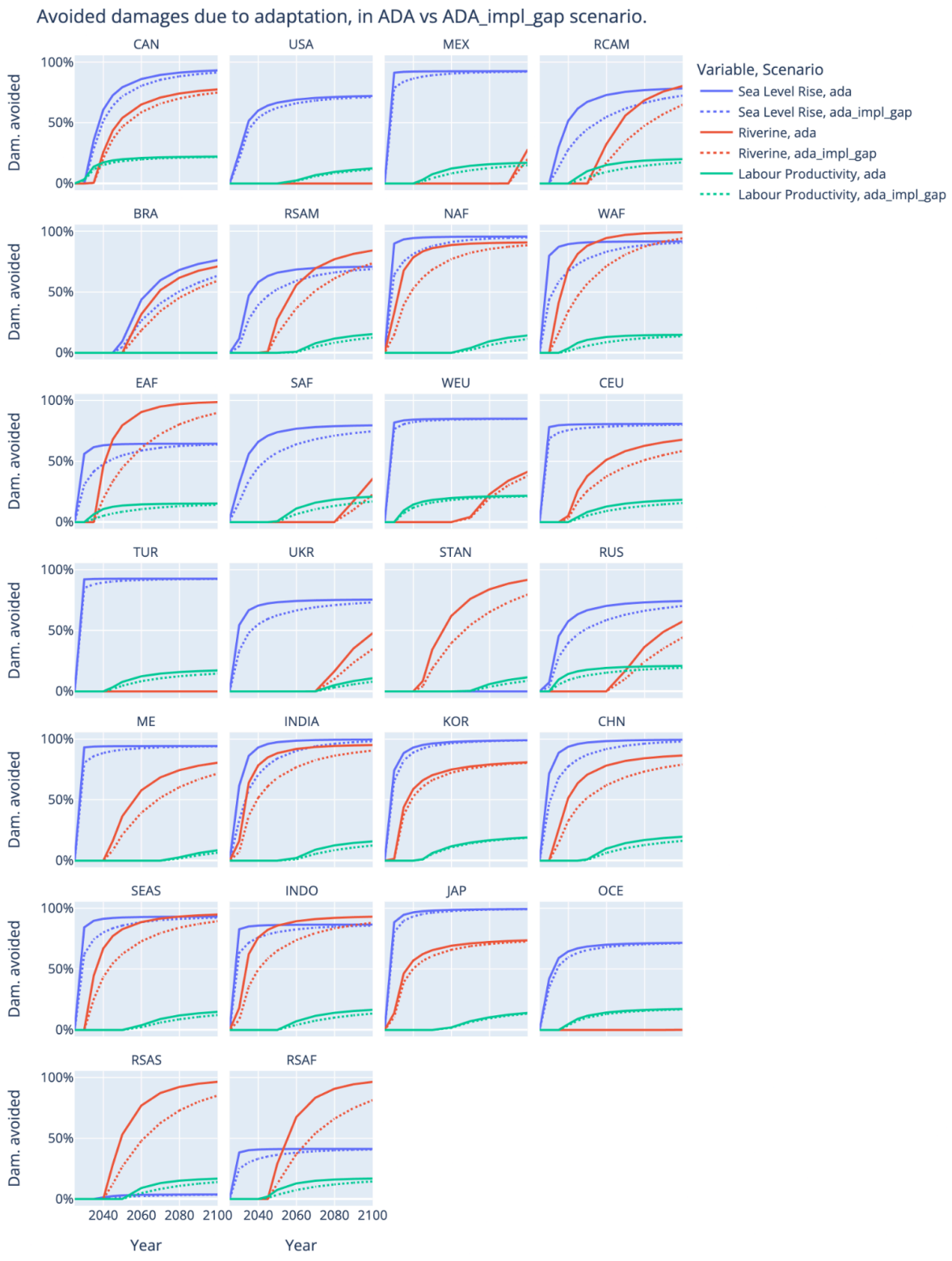

Fig. C-1. Avoided damages from adaptation (in % of gross damages) for the MIMOSA scenarios ADA (solid lines) and ADA_impl_gap (dotted lines).

7.4. Appendix D:

Reduced-form climate change damage functions. A robustness test with ACCREU insights.

Francesco Bosello, Ramiro Parrado, Ramon Key, Gabriele Standardi

1. Introduction

Reduced-form climate change damage functions (RFCCDFs) can be defined as relationships linking one or a few aggregate climate indicators (typically global or regional mean temperature increase, sometimes sea-level rise) to the change in a macroeconomic variable (typically the percentage deviation of GDP, consumption or welfare) from a no-climate-change baseline (Bosello 2014; Bosello and Parrado, 2020).

The term “reduced form” refers to the fact that the complex causal chain of responses triggered by temperature increases (or other climate stressor) on climatic hazards, from these on environmental impacts and from these on social and economic impacts, are condensed in few parameters shaping the relation.

In other words, RFCCDFs do not offer an explicit and “structural” description of the causal chain linking climate change to economic performances but estimate or “emulate” this relationship by regressions, data interpolations or, sometimes, semi-qualitative techniques based upon “experts’ opinions”.

This has led to many criticisms against their use and, by extension, to the models applying them. The two major objections from the literature are the following:

- RFCCDFs are just descriptive and not explanatory tools. They are a particular kind of “black boxes” or “aggregators” that can provide, accordingly, very limited support to policy action.
- They heavily depend upon the underlying data set, the quality of information used for their estimation, and the functional form chosen for the damage function itself. This, in its turn, has many consequences. RFCCDFs may lack robustness while at the same time overlooking important impact and cost drivers, especially those linked to non-marketable dimensions (Rising et al., 2022). In a nutshell, they may convey misleading or close to useless information on damages when, and as some authors add, typically, they lack sufficient empirical foundation (Pindyck, 2017). These weaknesses increase when RFCCDF are used for long-term scenario analyses. This last shortcoming is worsened by the fact that damage-relations are estimated or calibrated to limited ranges of temperature increase, say +1° to +3°C with respect to the pre-industrial level, and that, for tractability inside the Integrated Assessment Models (IAMs) where they are applied, they are continuous. Therefore, it is also unlikely that losses associated with catastrophic outcomes or irreversibility are properly factored in (Dietz et al. 2021, Keen et al. 2022).

All this said, RFCCDFs are being amply used by cost-benefit IAMs. In fact, they are one of IAMs distinctive features (Bosello and Parrado 2020). On the one hand, given their tractability they can be easily included in complex dynamic policy optimization or policy evaluation assessments which are at the core of IAMs use. On the other hand, they are flexible enough to include to a certain

extent those complexities, like, for instance, catastrophic uncertainty, or discontinuity, which they originally lack.

In this vein, some exercises extrapolated RFCCDFs from the output of computable general equilibrium models (CGEMs) (Ignjačević er al., 2026; Boitier et al., 2025; Van der Wijst et al, 2023; Bosello and Parrado, 2021).

One of the purposes of these assessments is to embed, and disentangle, in the reduced form functions the role of market adjustments (or differently said the endogenous resource allocation mechanism driven by price signals) which are explicitly represented in CGEMs.

In particular, Van der Wijst et al. (2023), report the RFCCDFs obtained for 17 world macro-regions and for the whole world extrapolated from the output of the ICES CGE model within the context of the COACCH project (www.coacch.eu).

The COACCH project is the precursor of ACCREU which uses similar methodologies and model categories for the economic assessment of climate change damages. ACCREU still uses an improved version of the ICES CGE model (ICES-REG by Standardi et al (2023)), to quantify the macroeconomic cost of climate change impacts on the EU regional and global economic systems (see ACCREU deliverable D4.1). Although virtually identical conceptually (see ACCREU D4.1), the COACCH and ACCREU assessments differ under many substantive respects. These relate to the scenarios used, the climate change impact categories examined, some features of the economic transmission mechanisms, notably investment mobility (see table 1), and, of course, the new data set for the climate change impacts implemented into the CGE model that benefits from the advancement of climate and impact science and modelling methods since the conclusion of COACCH[3]. Therefore, comparing ACCREU and COACCH RFCCDFs would be a perfect test to check the robustness of these tools.

Table 1: Main differences in the ACCREU and COACCH exercises leading to the estimation of RFCCDFs

ACCREU	COACCH
Scenarios (3): SSP2-RCP2.6; SSP2-RCP4.5; SSP2-RCP7.0 All impacts within each scenario combination have been specified for a “low – medium-high” range determined by the variability in output from the climate and the impact models used	**Scenarios (9):** SSP2-RCP2.6; SSP2-RCP4.5; SSP2-RCP6.0; SSP1-RCP2.6; SSP1-RCP4.5; SSP3-RCP2.6; SSP3-RCP4.5; SSP5-RCP4.5; SSP5-RCP8.5 All impacts within each scenario combination have been specified for a “low – medium - high” range determined by the variability in output from the climate and the impact models used.
Impact categories (7): Agriculture, energy demand, labour productivity, labour supply, sea-level rise, riverine floods, forest fires.	**Impact categories (9):** Agriculture, forestry, fishery, energy supply, energy demand, labour productivity, sea-level rise, riverine floods, transport.
Economic mechanisms: ● *High investment mobility:* The model default setting is considered: it assumes almost perfect mobility across macro-regions, countries and EU NUTS2	**Economic mechanisms:** ● *High investment mobility* and ● *Low investment mobility:* The latter introduces a lower investment mobility across EU NUTS2 regions. Regional losses

[3] For a full description of the direct impact assessment exercises developed in the ACCREU project refer to ACCREU D2.2, D2.3, D2.4, D2.5, D2.6, for the full description of the methodology translating direct impacts into GDP effects, to ACCREU D4.1.

areas. That implies easier interregional spreading of potential losses on capital stock.	on capital stock spread less easily outside the impacted regions. Country level economic losses in the EU tend to be lower than with “high” investment mobility.
Sectoral detail of the CGE model: **23 sectors:** Crops, Livestock, Forestry, Fishery, Coal, Oil, Gas, Heavy Industry, Food Industry, Other Industries, Oil Products, Transmission & Distribution, Power generation (Nuclear, Fossil, Renewables), Construction, Road Transport, Water Transport, Air Transport, Services, Public Services, Health, Dwellings;	**Sectoral detail of the CGE model:** **24 sectors:** Vegetables and Fruits, Other Crops, Livestock, Timber, Fishery, Coal, Oil, Gas, Oil Products, Transmission & Distribution, Power generation (Nuclear, Fossil, Wind, Hydropower, Solar, Other Renewables), Heavy industry, Construction, Light industry, Road Transport, Water Transport, Air Transport, Services, Public Services
Number of EU subnational regions: 135	**Number of EU subnational regions: 138**

2. Estimating and comparing RFCCDF

The geographical detail of the ICES CGE model is higher than that of the IAMs used in ACCREU. The EU and the UK, in particular, are disentangled into 135 single sub-national regions. In the COACCH and ACCREU projects macroeconomic loss data have been thus aggregated to match the resolution of the WITCH, REMIND and MIMOSA IAMs. For compactness’s sake here we report and then compare the damage functions estimated for the MIMOSA IAM. Anyway, the geographical resolution of the three different IAMs is roughly comparable.

To fully match the COACCH exercise we report separate damage functions referring to sea-level rise damages, expressed in relation to centimeters (cm) of mean sea level increase and non-sea-level rise damages expressed in relation to temperature increase. In the case of sea-level rise, we pick COACCH simulations **without additional adaptation** (assuming constant protection at 1995 levels**)** that we compare with ACCREU simulations **assuming LOW adaptation**. The fitting system used is a quantile regression method and linear or quadratic specification depending on the region. In the case of non-sea-level rise damages, the fit is a quantile regression and a quadratic specification.

More specifically the functional forms used are as follows:

$$D = \hat{\beta}_1 x \quad (1)$$

$$D = \hat{\beta}_1 x + \hat{\beta}_2 x^2 \quad (2)$$

Where D = GDP loss as a percentage of the baseline level

x = climatic variable (sea-level rise or change in temperature)

$\hat{\beta}$ = estimated coefficient

Figure 1 reports the visual comparison of damage functions, while tables 2 to 5 in the appendix report the coefficients.

Figure 1: Reduced-form climate-change damage functions from ACCREU and COACCH projects(*).

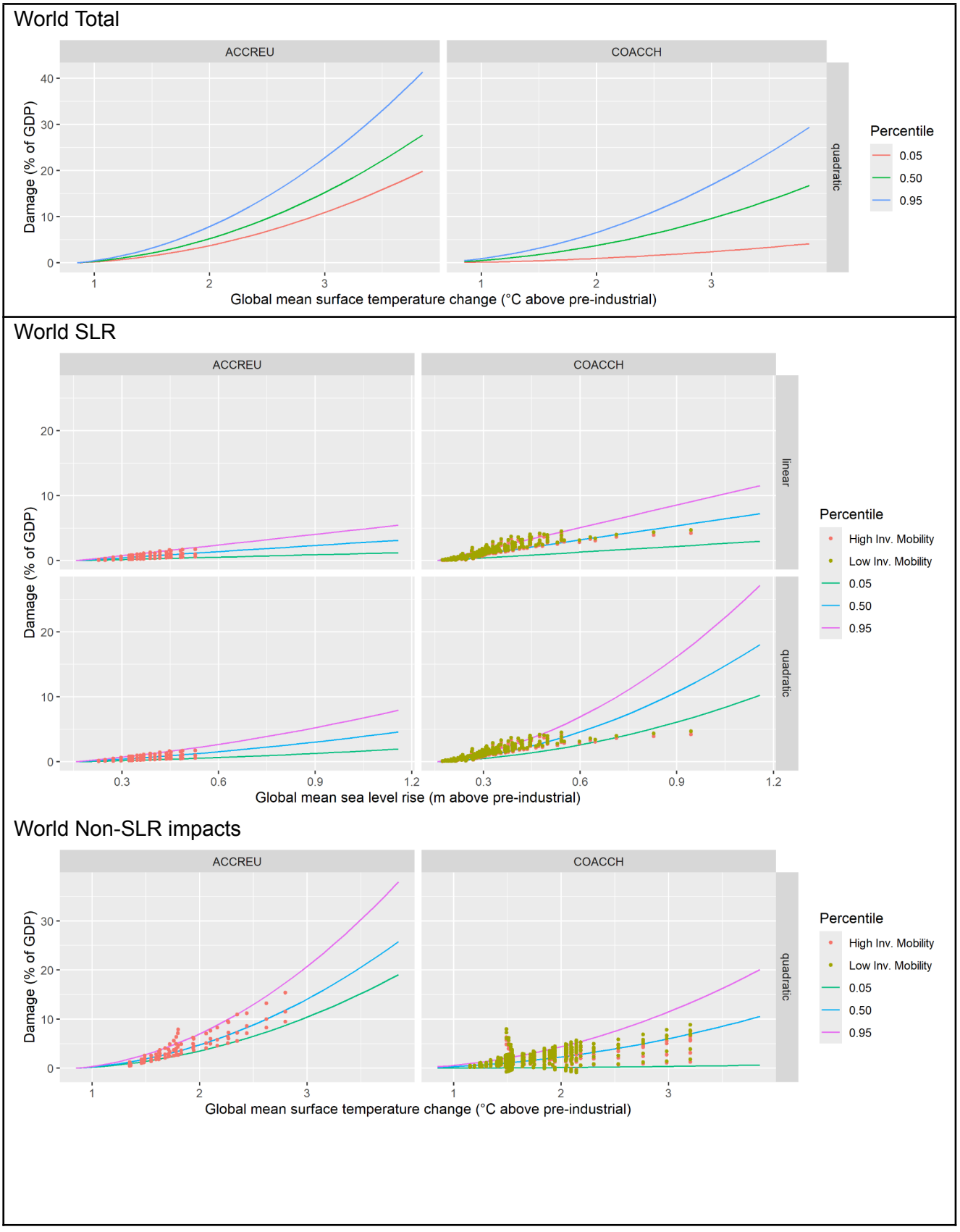

Canada SLR

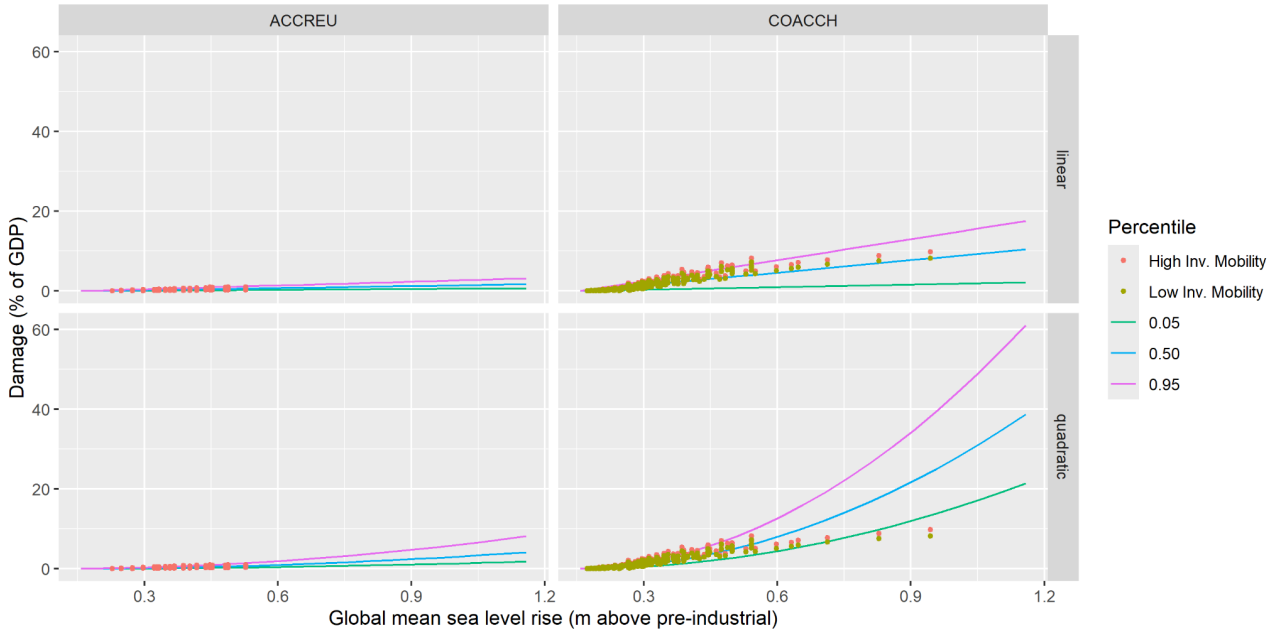

Canada Non-SLR impacts

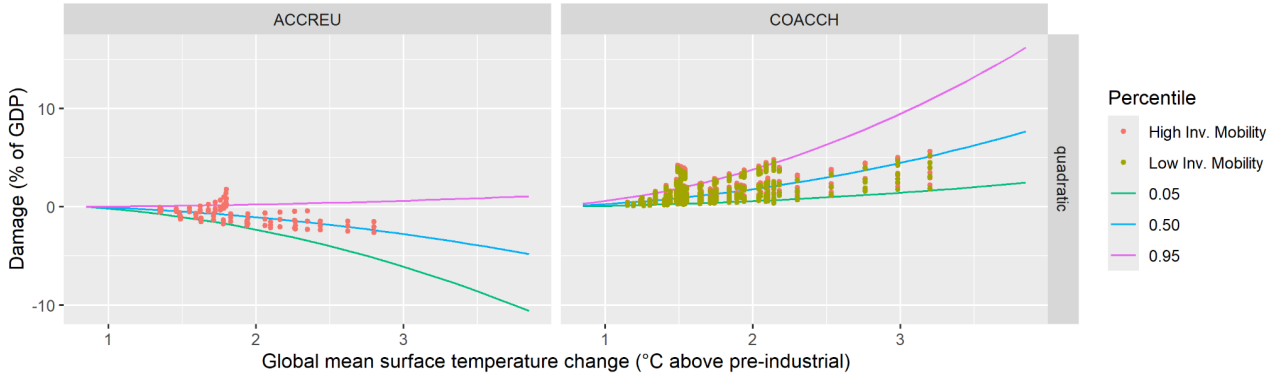

USA SLR

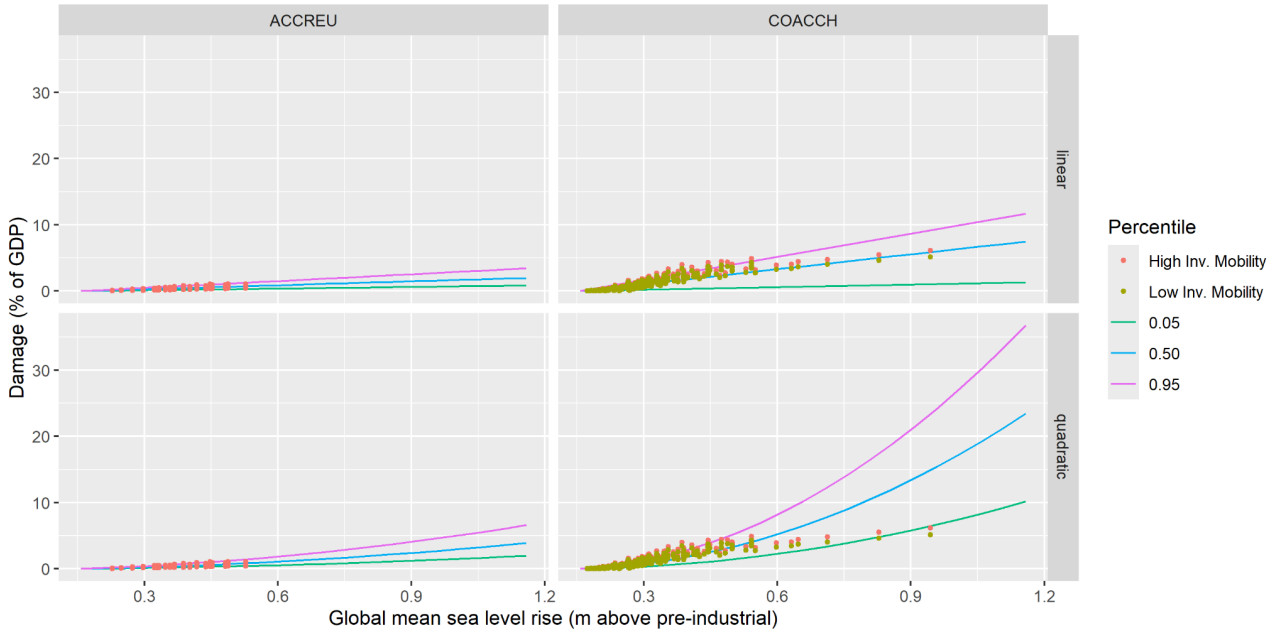

USA Non-SLR impacts

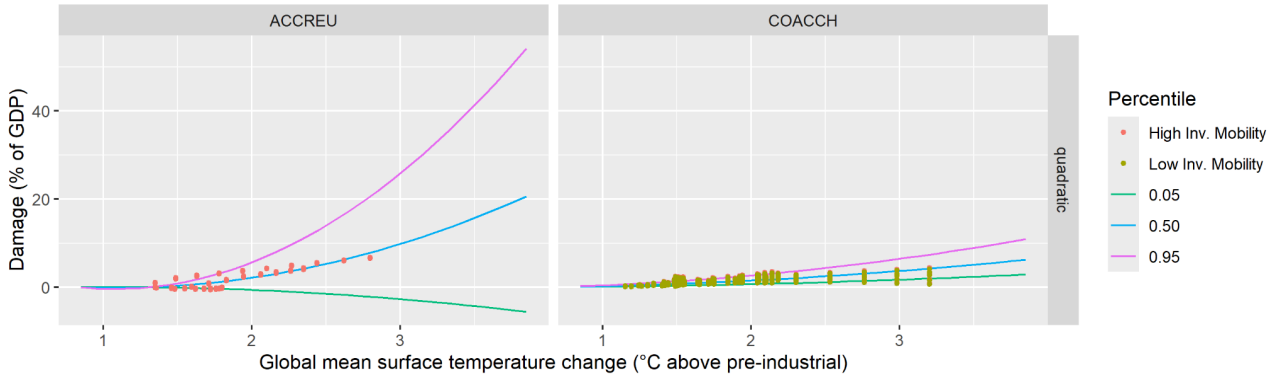

Rest of South-America SLR

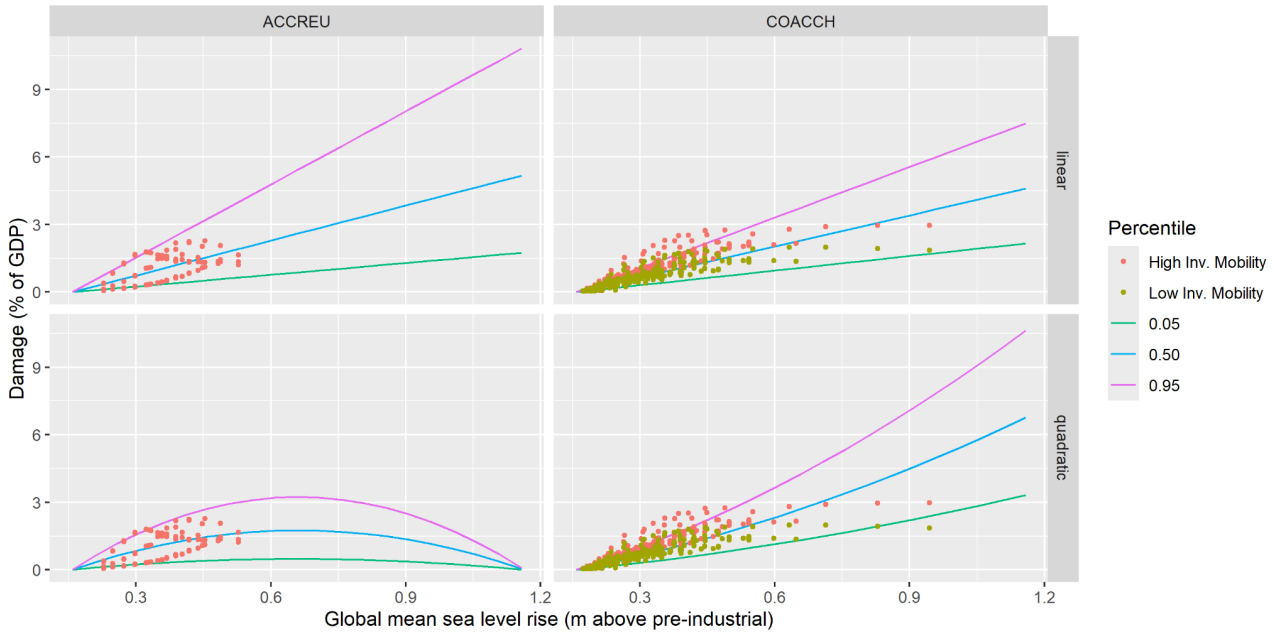

Rest of South America Non-SLR impacts

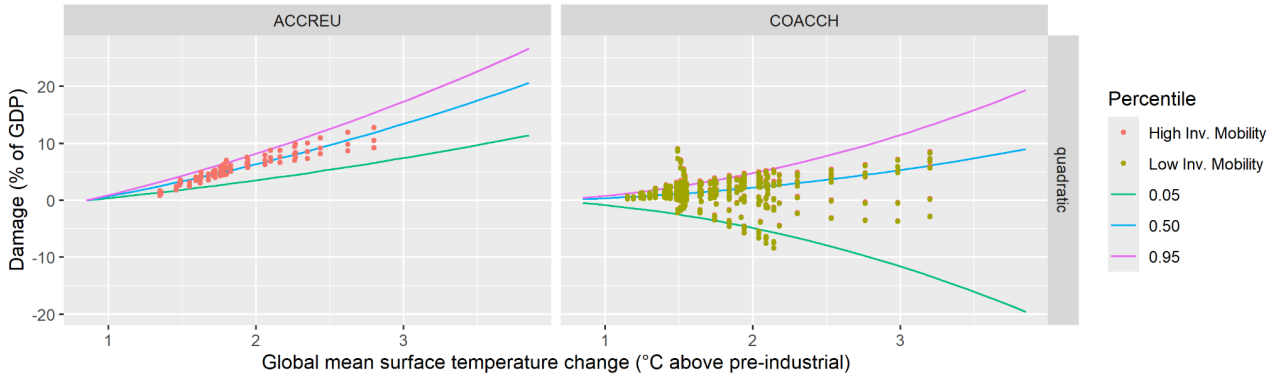

Central Eastern EU SLR

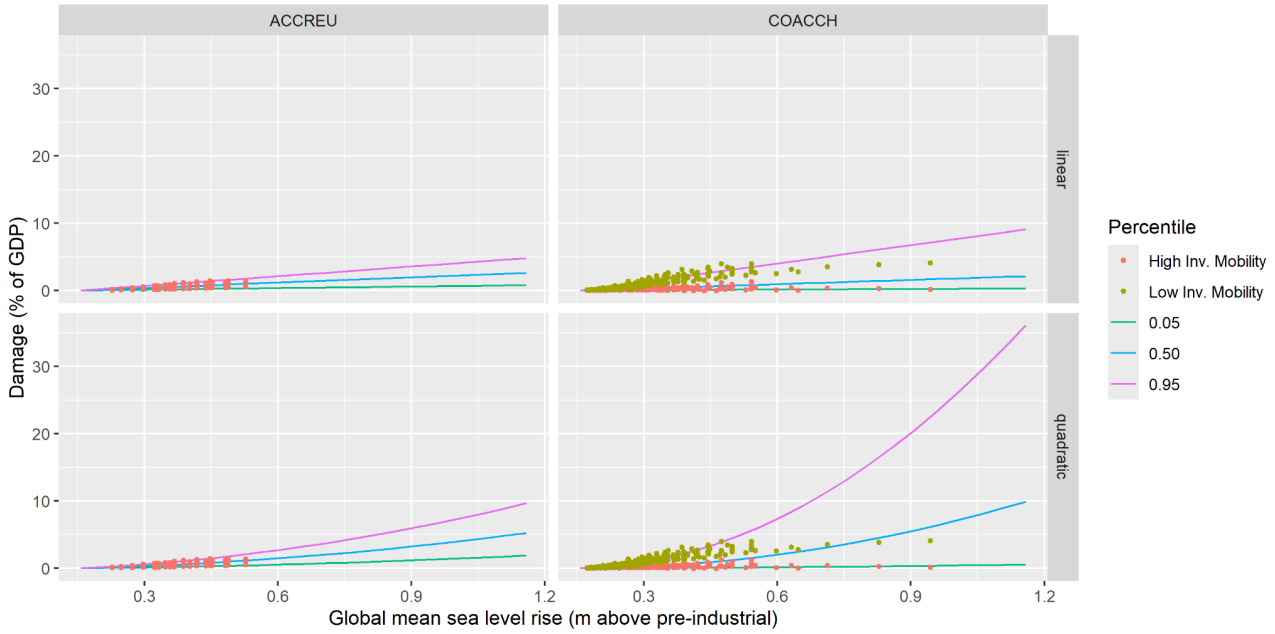

Central Eastern EU Non-SLR impacts

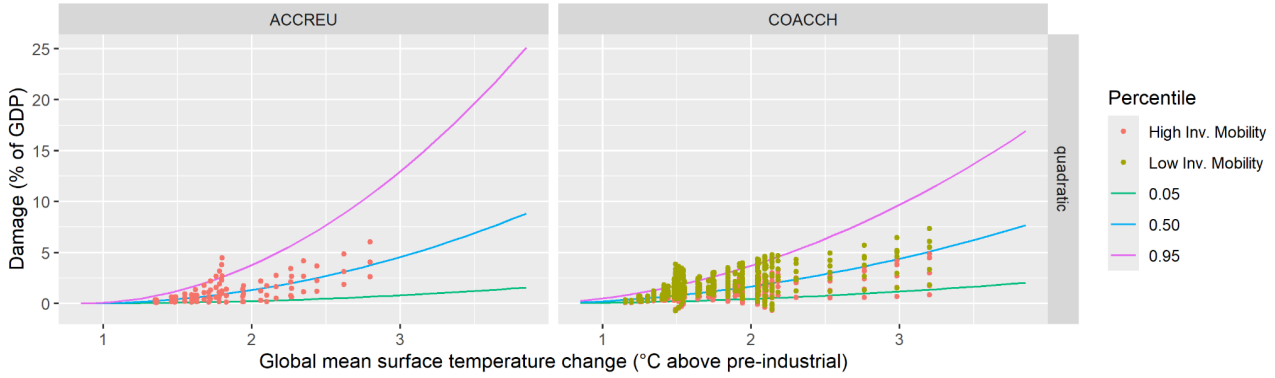

Western EU SLR

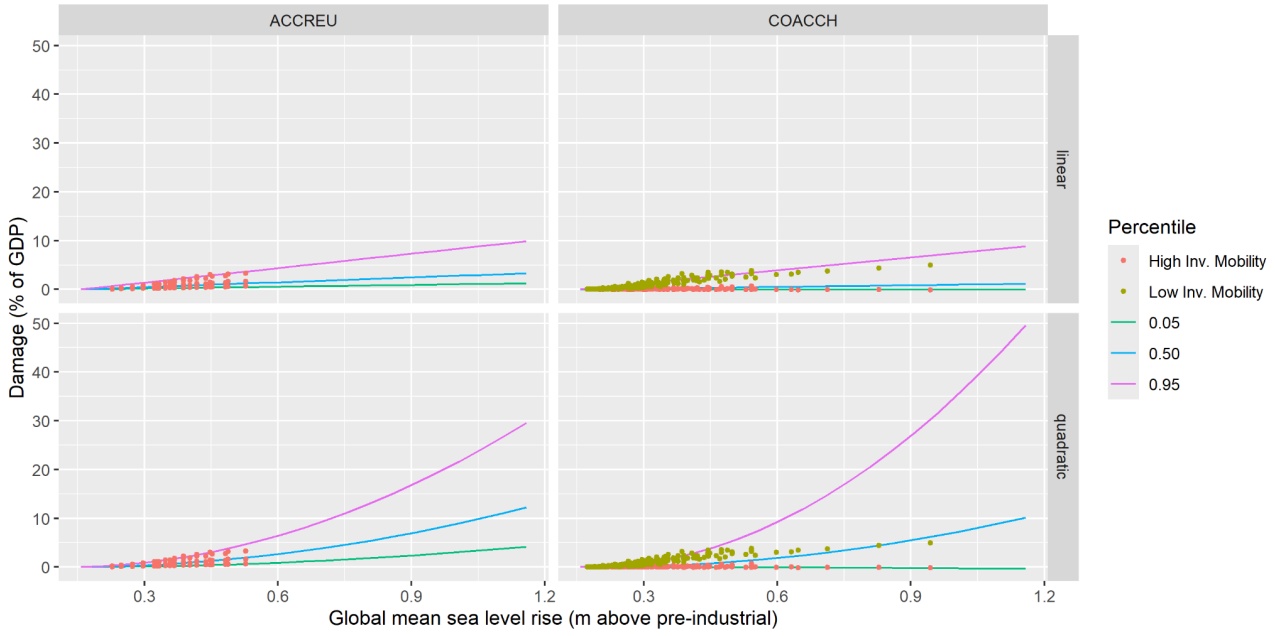

Western EU Non-SLR impacts

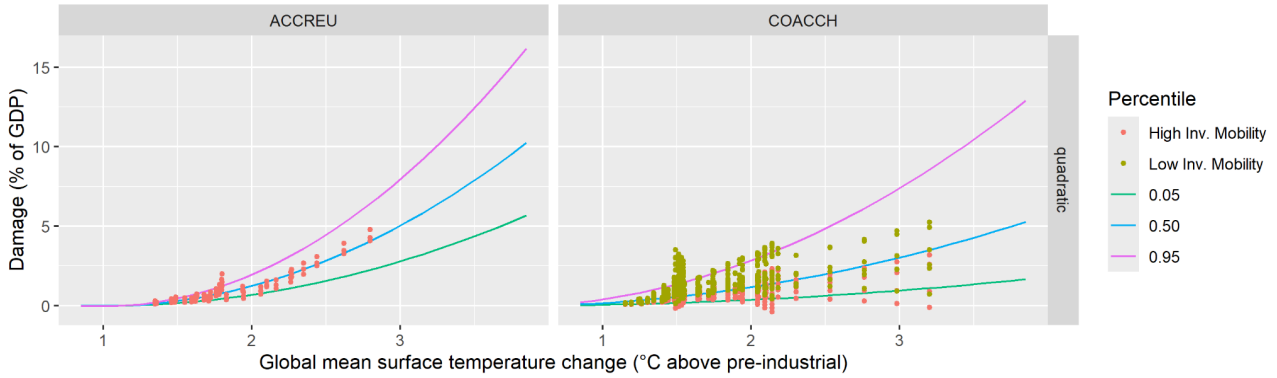

China SLR

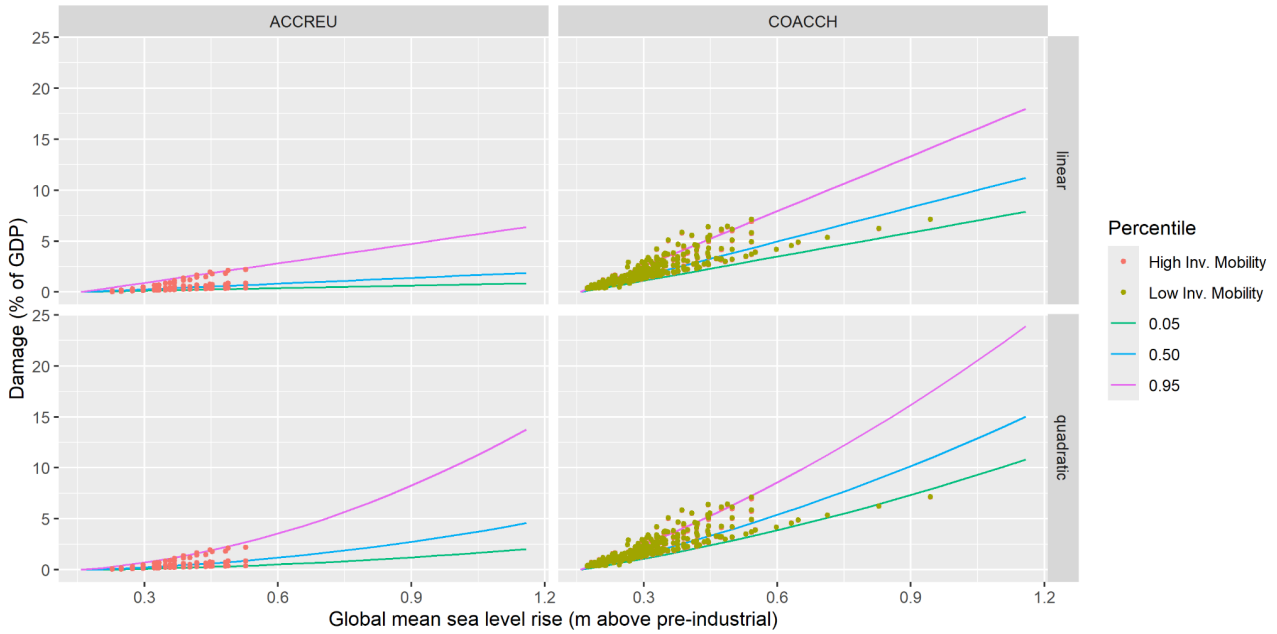

China Non-SLR impacts

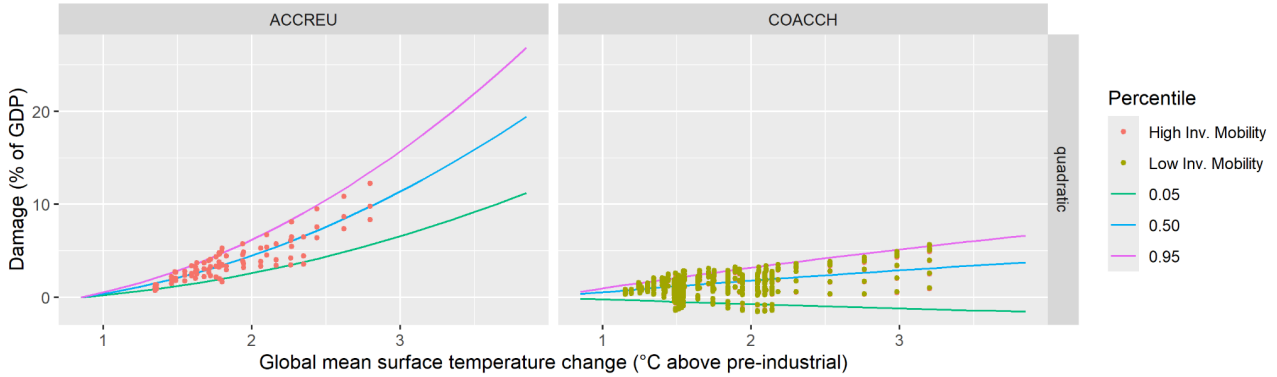

India SLR

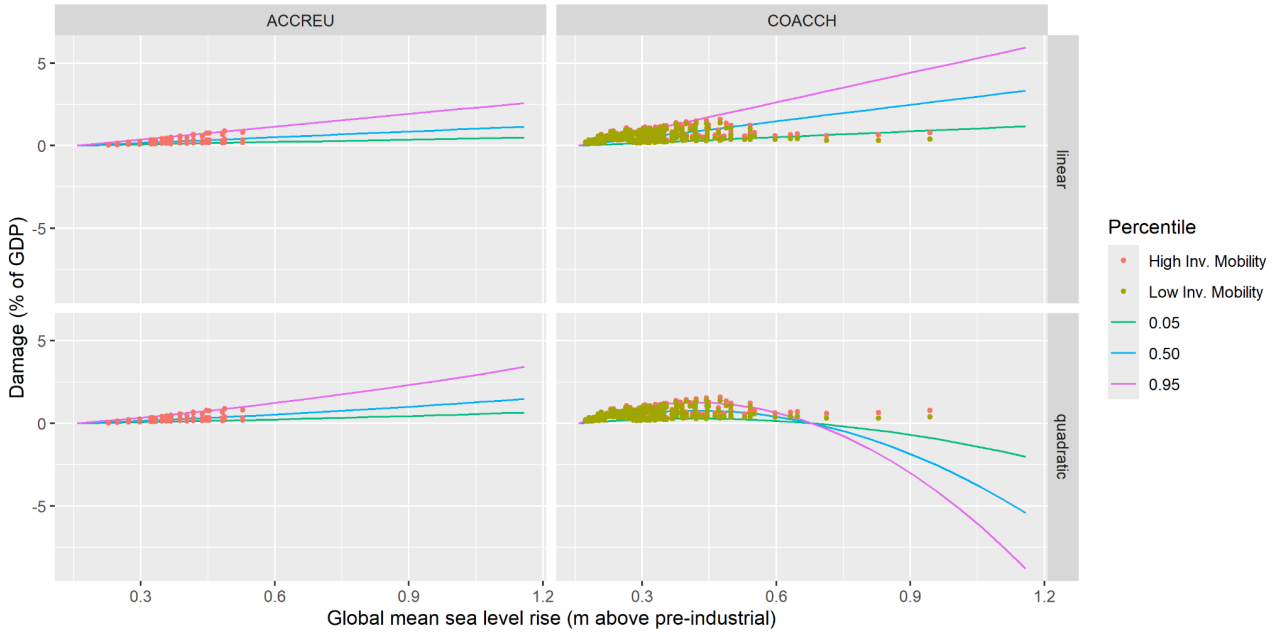

India Non-SLR impacts

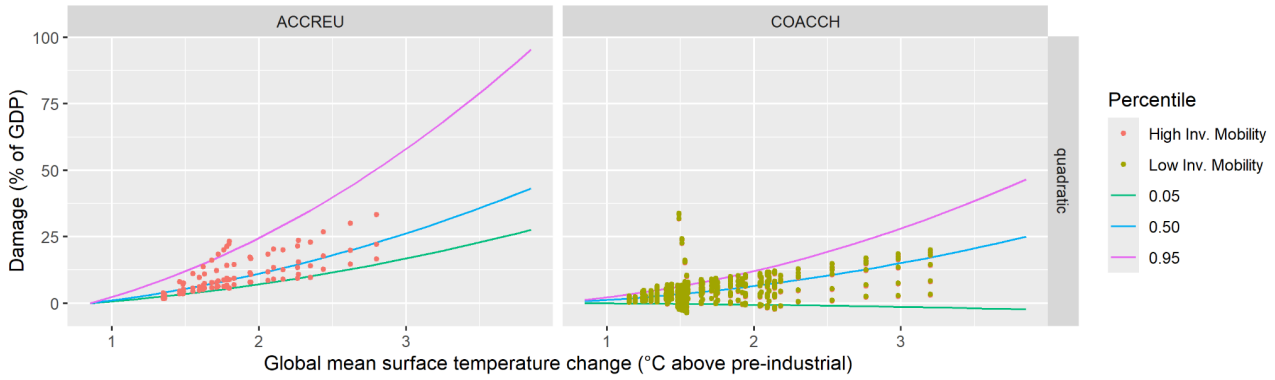

Japan SLR

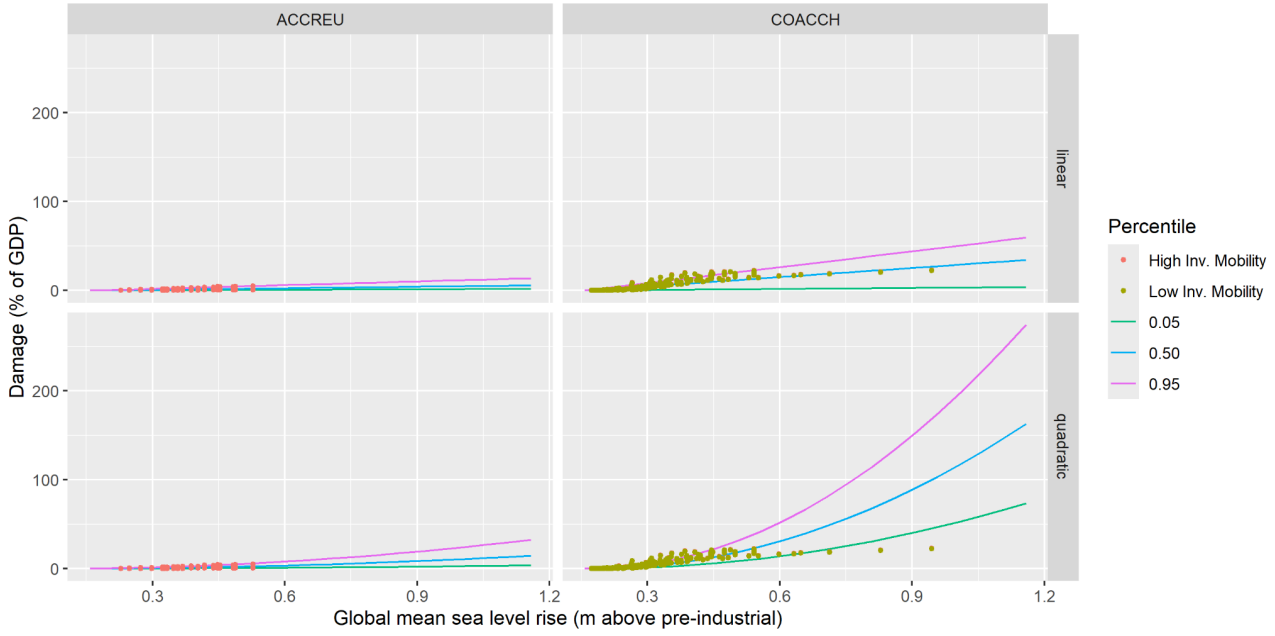

Japan Non-SLR impacts

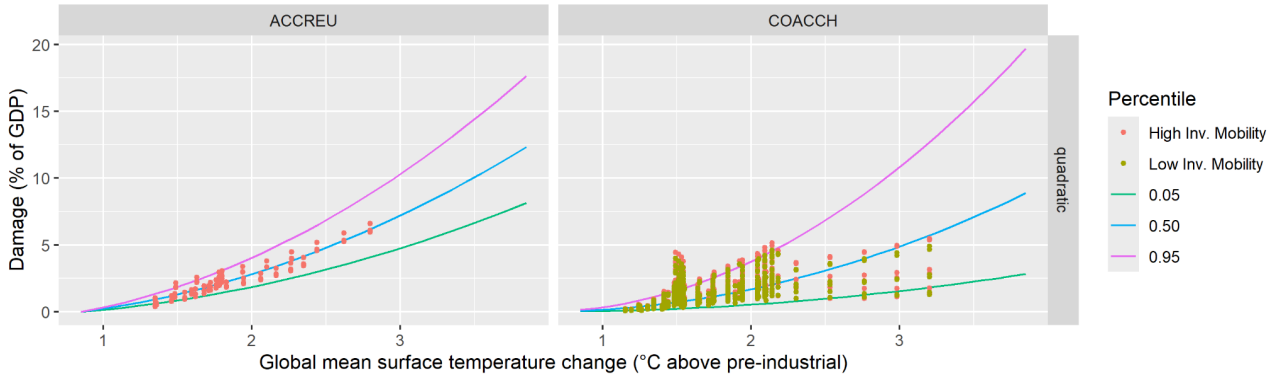

South East Asia SLR

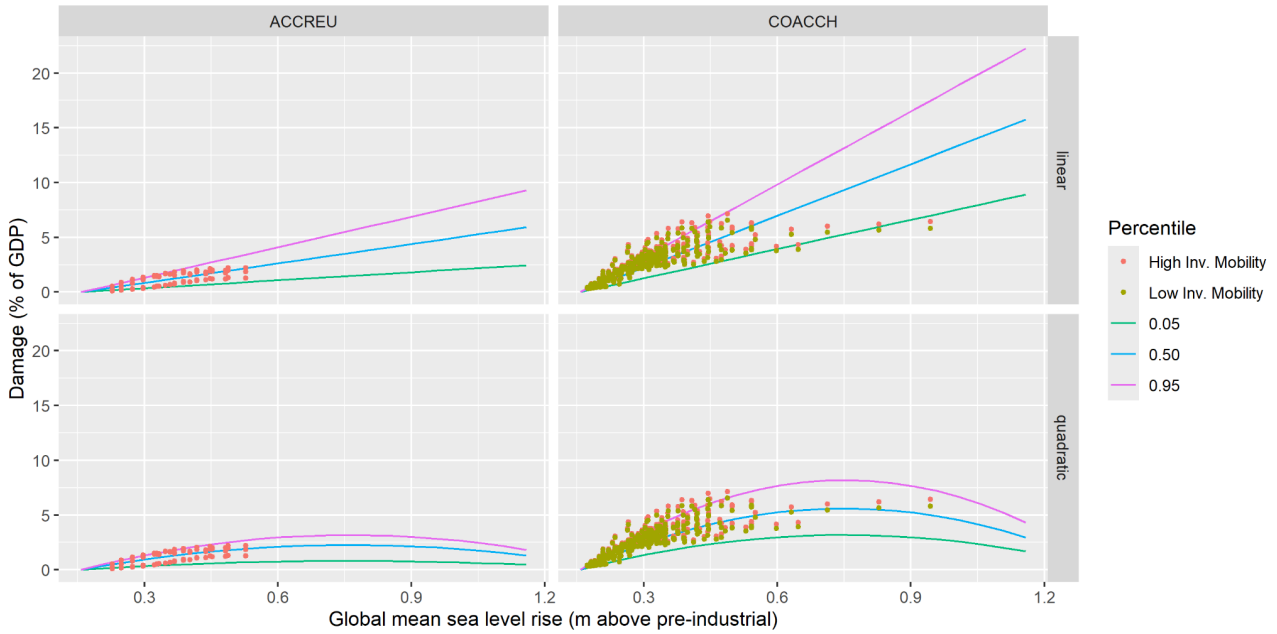

South East Asia Non-SLR impacts

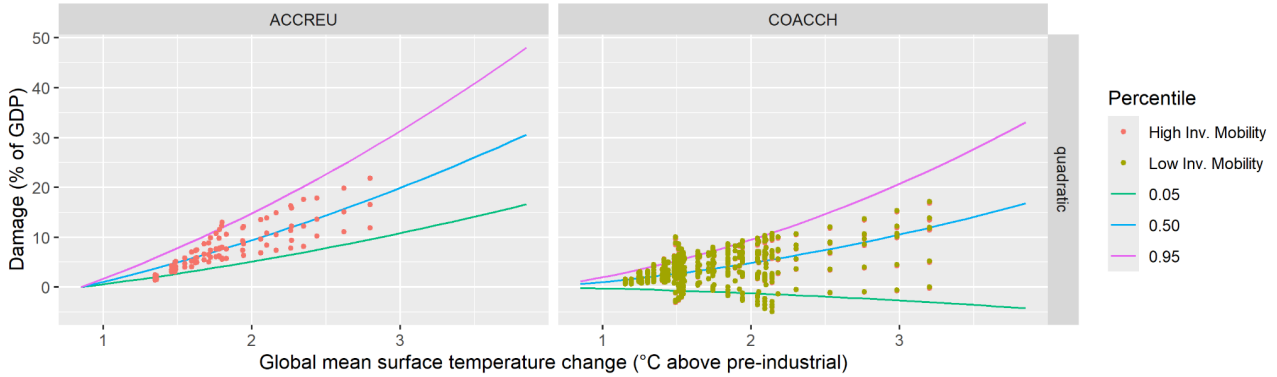

Rest of South Asia SLR

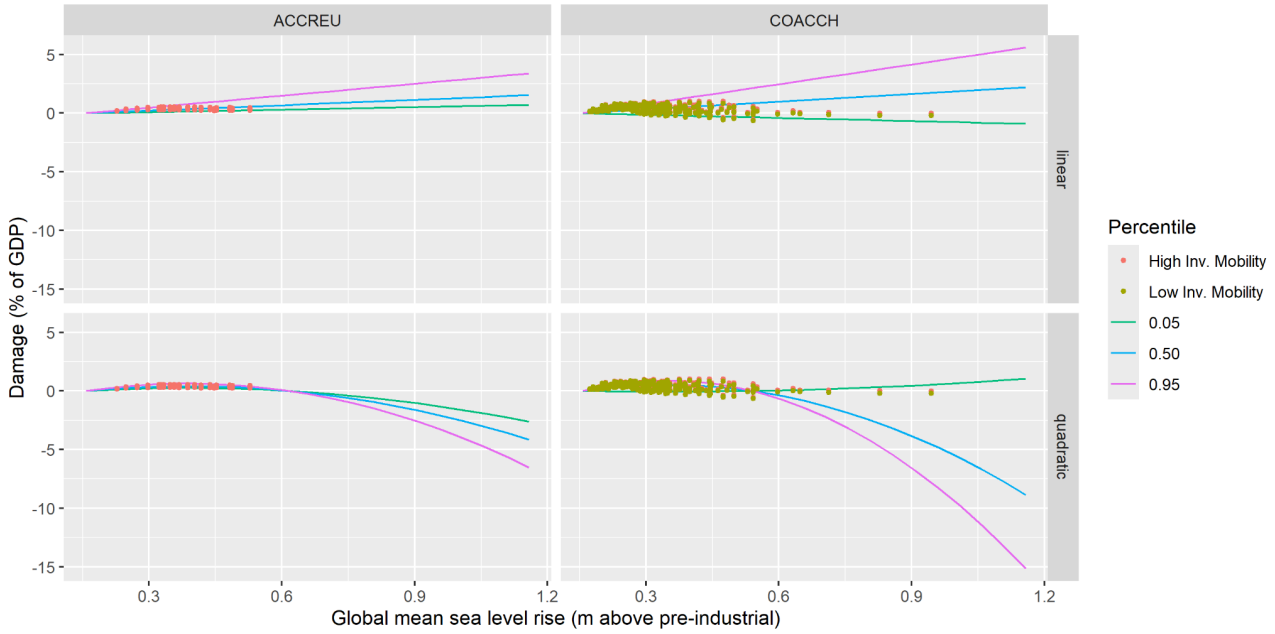

Rest of South Asia Non-SLR impacts

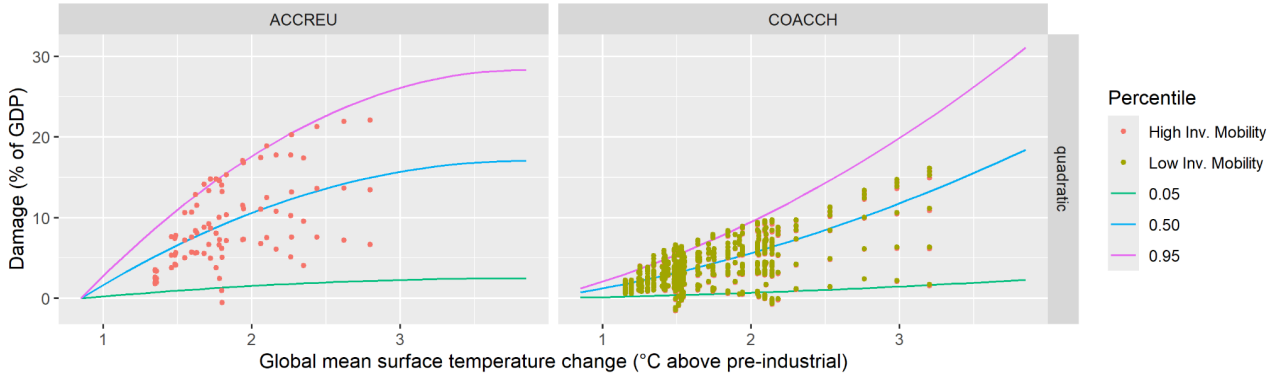

Middle East SLR

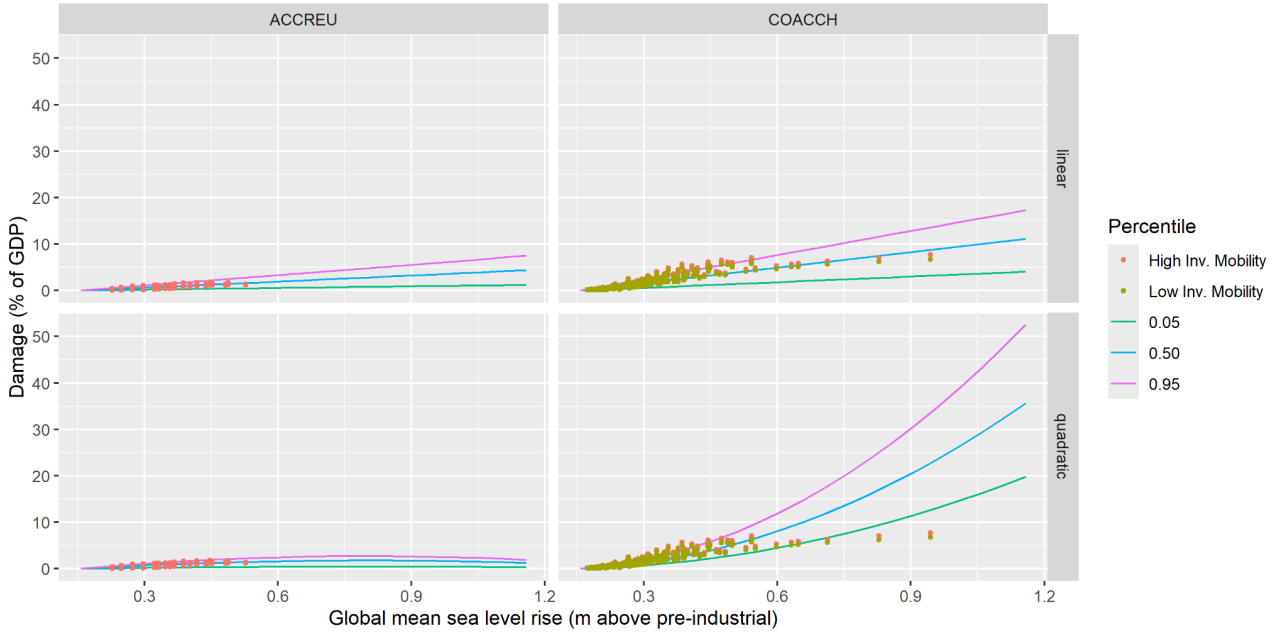

Middle East Non-SLR impacts

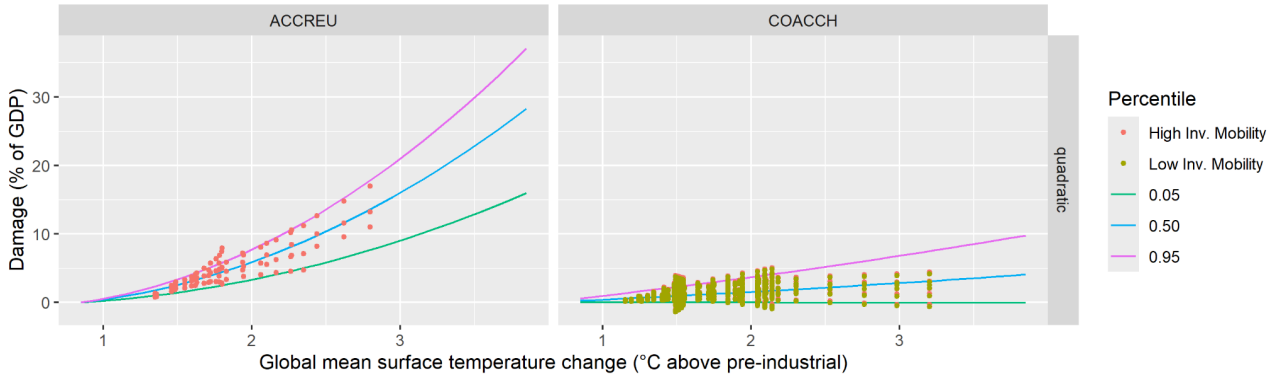

Oceania SLR

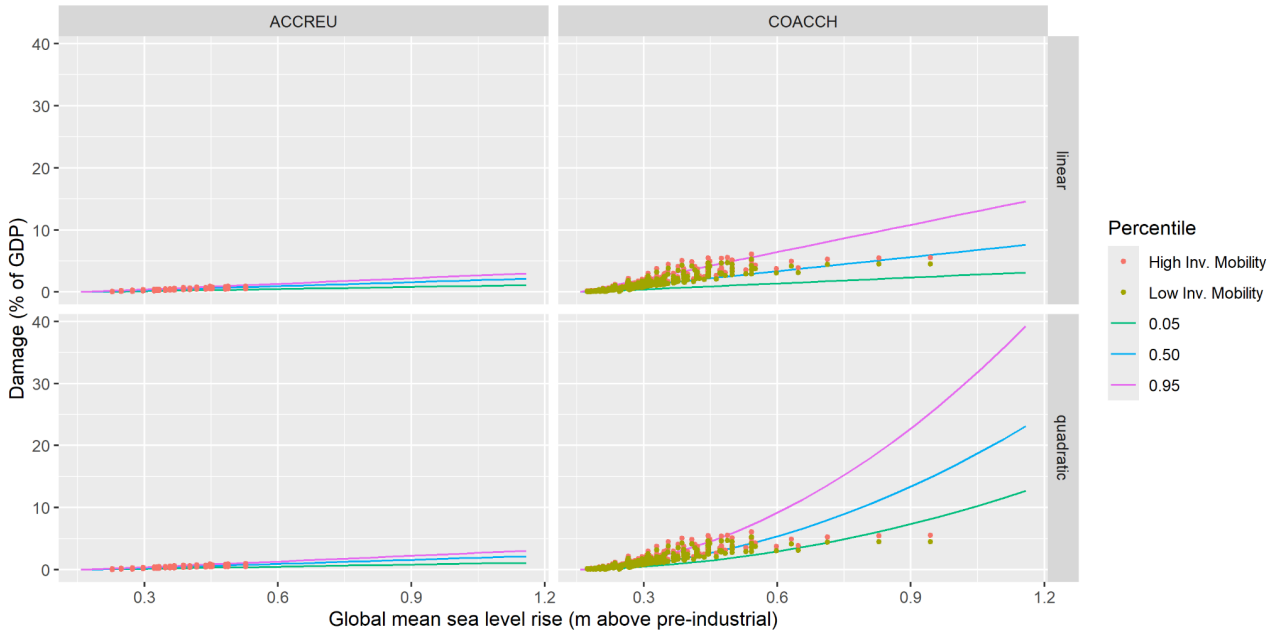

Oceania Non-SLR impacts

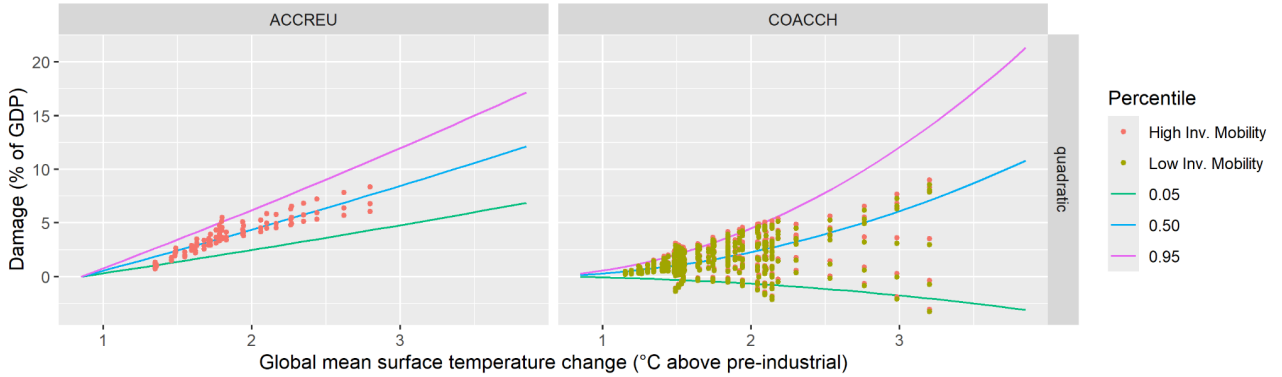

South Africa SLR

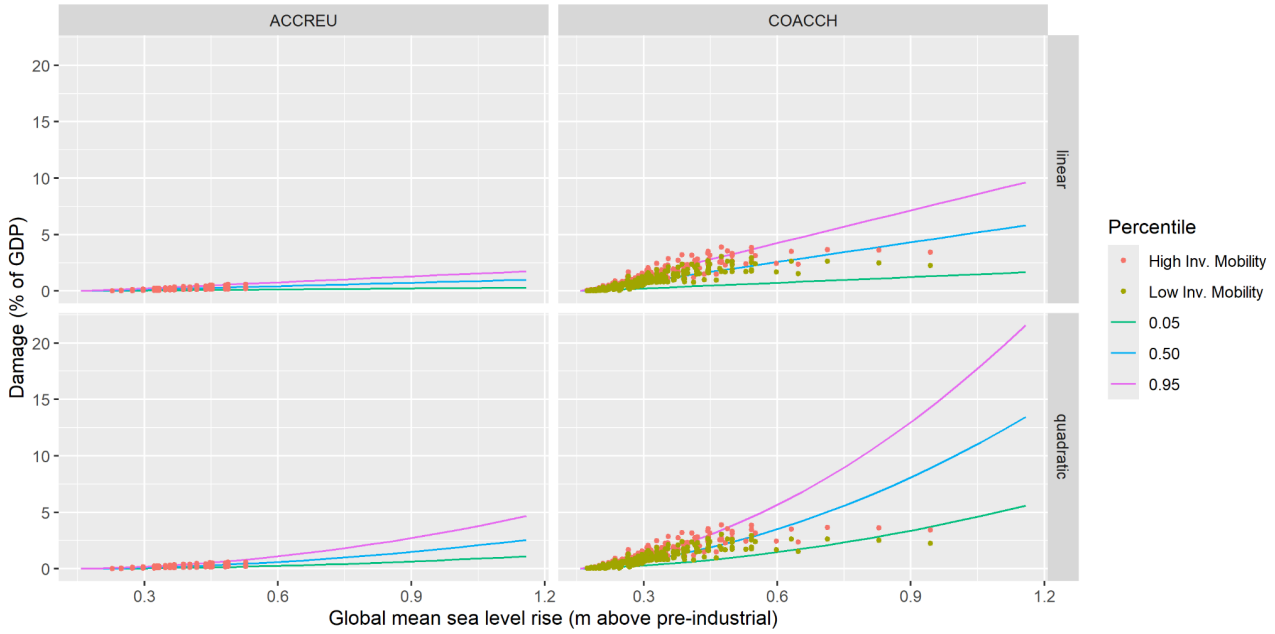

South Africa Non-SLR impacts

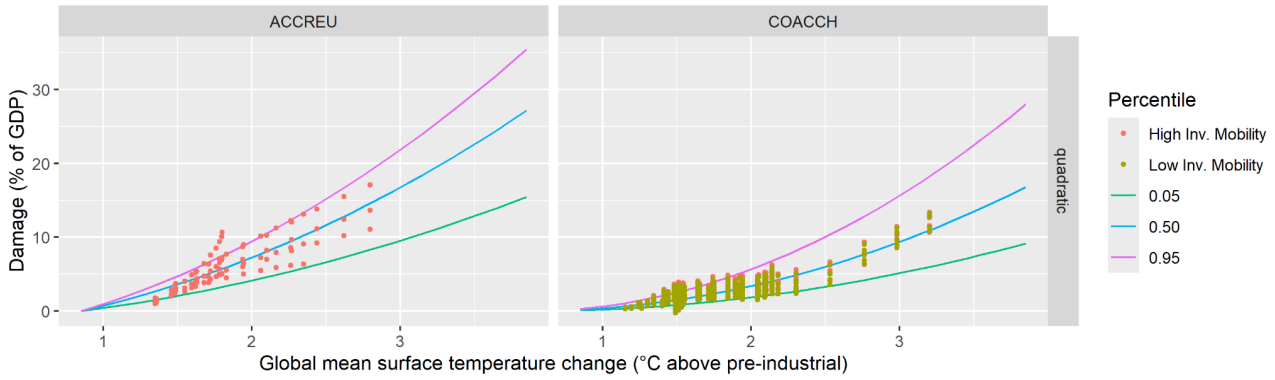

East Africa SLR

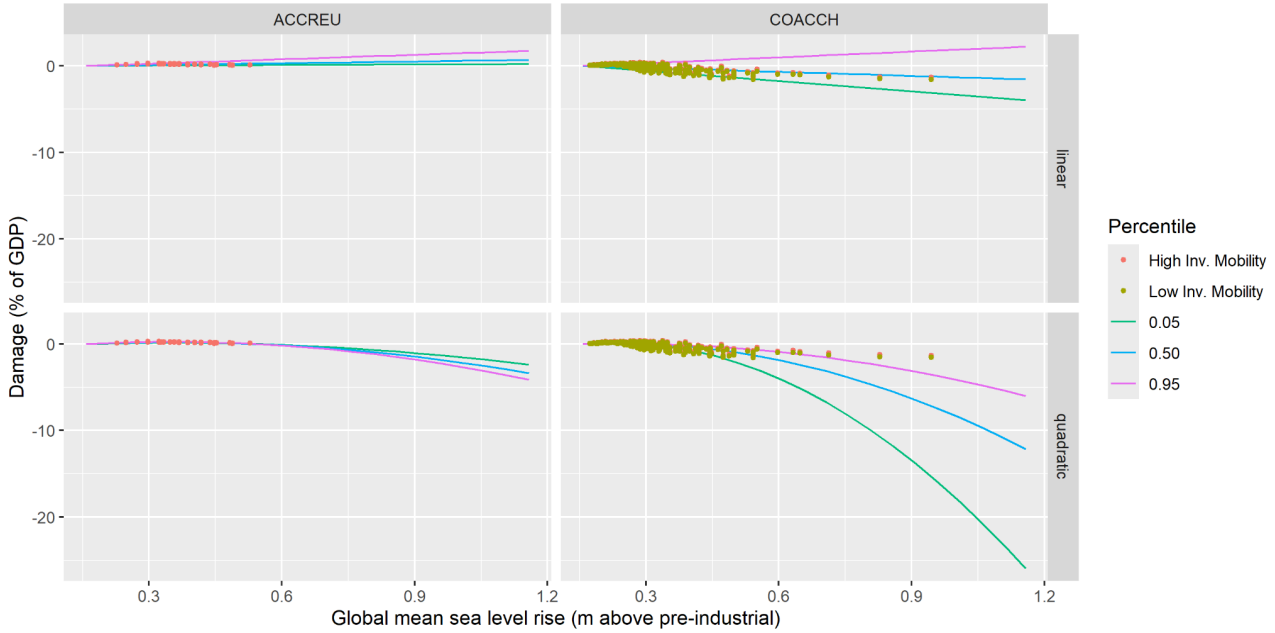

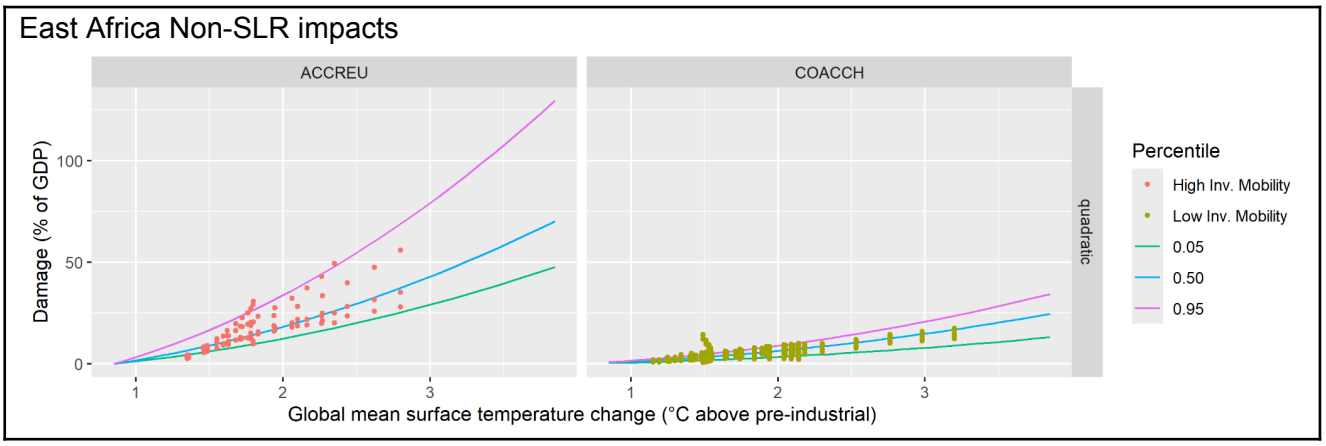

(*) Dots in figures refer to the outputs from the CGE model assessments (GDP macro-regional impacts expressed as % change with respect to the baseline) in the different scenarios.

As can be noted, at the global level, all impacts jointly imposed, the RFCCDfs from the two projects are reasonably similar.

Disentangling impacts categories, however, it emerges that SLR-related GDP losses are lower in ACCREU than in COACCH (featuring a global GDP loss of the in the former 1.5% vs the 4% in the latter for a + 53.3 cm SLR with respect to pre-industrial levels), while the non-SLR related GDP losses increase (featuring a global GDP loss of the 12% in the former vs the 5% in the latter for a + 2.8°C temperature increase scenario with respect to pre-industrial levels). The first outcome depends upon updated DIVA model runs featuring a recalibration of the dike protection levels in the initial year of the simulation. The non-SLR component is influenced mostly by the introduction of the additional impact channel represented by labour supply (COACCH only considered impacts on labour productivity) that turns out to play a major role on GDP performances whether positive or negative. This is evident in Canada, which is the country that also shows the strongest difference in results across ACCREU and COACCH. In ACCREU, on aggregate, Canada is projected to gain from climate change. This occurs as the effects of warmer temperatures that increase labour supply overcompensate the negative effects from the other impacts on GDP production.

This pattern is replicated in macro regions. Taking as reference the 2.8°C temperature and the 53.3 cm SLR thresholds which are the upper bounds used in ACCREU for the estimation of the damage functions, it can be noted that Non SLR impact-related GDP losses roughly double, while SLR economic losses are lower by around 60% in ACCREU with respect to COACCH.

In this picture, China and the Middle East are outliers demonstrating respectively a 3 and 4-fold increase in non-SLR-driven GDP losses compared with COACCH (reaching 10% in China and 14% in MDE for a 2.8°C increase) according to the ACCREU estimates. In these same regions, SLR GDP costs are smaller though. Macroeconomic impact assessments are more stable across the two projects for the EU. Moving from COACCH to ACCREU results, Non-SLR impact driven GDP losses increase from 2.6% to 4% in Western EU and remain almost stable at 4% in Central EU.

3. Conclusions

From these findings we can derive both positive and more problematic conclusions in relation to RFCCDFs and their use.

On the positive side:

Considering the huge differences across the ACCREU and COACCH exercises, the reasonable comparability of the GDP outcomes is comforting. There are no changes in the orders of

magnitude, (although we must admit that one country Canada shows opposite results), moreover differences in the macroeconomic assessments of the single impacts tend to compensate over the large geographical aggregates considered.

The use of RFCCDFs is informative. Firstly, it hints quantitatively and qualitatively, which impact categories are more likely to influence the macroeconomic performance of countries. Most of the emerging ACCREU-COACCH differences can be tracked back to the addition of new knowledge on one impact - in this case updated inputs from the SLR analysis - and the addition of a new impact category - in this case climate change effects on labour supply. Both impacts have a cross-sectoral and pervasive influence on the production capacity of countries through the effect on capital and labour that are key factors of production. Secondly, it also suggests in which areas research efforts should focus to reduce the uncertainty of impact assessments.

This said, criticalities do not vanish:

Even though major impact categories have been already included, it is not possible to anticipate how results would change with the introduction of further categories with potentially pervasive economic effects. Topical examples are, for instance, massive biodiversity or ecosystem losses impacting provisioning and regulating ecosystem services.

Despite ACCREU RFCCDFs relying on a smaller set of seven impact categories producing higher damages compared to COACCH's nine impact categories, the number of scenarios simulated produced only a fraction of datapoints compared to COACCH's. This highlights the need for extending the available information for the estimation of damage functions by increasing the impact categories, using new direct impact estimates as well as considering higher climate change signals that translate into wider ranges of temperature and sea-level rise increase.

RFCCDFs in general, and those estimated by the ACCREU and COACCH projects in particular, quantify impacts only if they exert a detectable and measurable influence on economic performance. This do not consider non-market effects and welfare effects associated with important factors like worsening health conditions or increasing inequality which are hardly monetizable.

Similarly, the assessment performed, and, accordingly, the resulting RFCCDFs, do not consider all those elements that act as impact and cost amplifiers. These are frictions in economic adjustments, lack of institutional capacity, policy inertias, cultural and behavioral barriers that slow the deployment of coping strategies and solutions.

Divergences across the estimated macroeconomic impacts amplify with the extension of the simulation horizon. This is inherent to the extrapolation procedure based on a limited number of observations (or on a large number of observations but concentrated in narrow temperature intervals) and to the quadratic functional form chosen. This means that the function can be sensitive to a relatively minor change in the data support. In our exercise, extrapolated mean GDP losses at 3°C are still broadly comparable across ACCREU and COACCH in most cases (although China, the Middle East and the USA show quite different projections). For higher temperature increases the two functions are not comparable anymore.

This leads to the following considerations:

- Consider the economic impacts produced by RFCCDFs as lower bounds of the true cost of climate change.
- Consider extrapolated losses beyond 3-4°C of temperature increase highly speculative. In fact, we would suggest not using RFCCDFs to represent losses for higher temperature ranges.
- Use insights from RFCCDFs when extrapolations refer to macroeconomic losses at the global level or anyway at large geographical areas. Results can be less robust at higher spatial resolution levels.

- Better characterize climate change impacts affecting (directly or indirectly) those factors of production with a “pervasive” influence on production activities like capital and labour. These are more likely to translate in larger economic effects.

This also suggests a final reflection specific to ACCREU and COACCH RFCCDFs: in the range of 2 to 3°C and for large geographical areas the two sets of functions are similar. Although ACCREU adds new knowledge, it does not lead to a complete, but only incremental transformation of COACCH RFCCDFs. This result is encouraging, pointing to a progressive consolidation of macroeconomic estimates of (non-catastrophic) climate change damages. In summary, given the still existing uncertainty, keep on using the previous COACCH RFCCDFs would still be justifiable

REFERENCES

Boitier, B., Mekki, H., Le Mouël, P. *et al.* (2025). Projected climate impacts and impact-specific damage functions for EU countries: A review and estimation. *Climatic Change* **178**, 189 (2025). https://doi.org/10.1007/s10584-025-04049-5

Bosello, F. (2014), “The role of economic modelling for climate change mitigation and adaptation strategies”, in A. Markandya, I. Galarraga, E. Sainz de Murieta (eds.) “Routledge Handbook of the Economics of Climate Change Adaptation”, Routledge, Oxon and New York

Bosello F.; Parrado R. (2020). Macro-economic assessment of climate change impacts: Methods and findings. EKONOMIAZ, vol. 97, pp. 45-61 (ISSN 0213-3865)

Bosello F., and R. Parrado (2021), “Climate change impacts and market driven adaptation: The costs of inaction including market rigidities” in Dirk Rübbelke and Anil Markandya (eds.) "Climate and Development", World Scientific Publishing. https://doi.org/10.1142/12376

Dietz, S., Rising, J., Stoerk, T., Wagner, G. (2021). Economic impacts of tipping points in the climate system. *PNAS* 118(34): e2103081118. doi:10.1073/pnas.2103081118

Ignjačević, P., Botzen, W.J.W., Parrado, R., … Estrada, F. (2026). Spatially-Explicit Economic Impacts and Risks of Climate Change in Europe. Economics of Disasters and Climate Change 10(2): 21. doi:10.1007/s41885-026-00201-2

Keen, S., Lenton, T.M., Garrett, T.J., Rae, J.W.B., Hanley, B.P., Grasselli, M. (2022). Estimates of economic and environmental damages from tipping points cannot be reconciled with the scientific literature. *PNAS* 119(21): e2117308119.

Pindyck, R.S. (2017). The Use and Misuse of Models for Climate Policy. *Review of Environmental Economics and Policy* 11(1): 100–114

Rising, J., Tedesco, M., Piontek, F., Stainforth, D.A. (2022). The missing risks of climate change. *Nature* 610: 643–651. doi:10.1038/s41586-022-05243-6

Standardi, G., Dasgupta, S., Parrado, R., De Cian, E., & Bosello, F. (2023). Assessing Macro-economic Effects of Climate Impacts on Energy Demand in EU Sub-national Regions. Environmental and Resource Economics, 86(1–2), 173–201. https://doi.org/10.1007/s10640-023-00792-4

van der Wijst, K.-I., Bosello, F., Dasgupta, S., Drouet, L., Emmerling, J., Hof, A., Leimbach, M., Parrado, R., Piontek, F., Standardi, G., van Vuuren, D. (2023). New damage curves and multimodel analysis suggest lower optimal temperature. Nature Climate Change 13(5): 434–441. doi:10.1038/s41558-023-01636-1

Annex:

Regional Parameterization for the Climate Change Damage Functions (relative to 1995-2014)

Table 2: Damage function parameters: Non-SLR impacts – Linear Quantile Regression

Region	b1	b2	a0.05	a0.50	a0.95	fit	b1_0.05	b1_0.50	b1_0.95	b2_0.05	b2_0.50	b2_0.95	fit_var
BRA	6.15545	0	0.397717	1	1.418436	linear	2.448127	6.15545	8.731109	0	0	0	T_delta
CAN	-0.98303	0	1.823373	1	-0.24735	linear	-1.79244	-0.98303	0.243158	0	0	0	T_delta
CEU	1.127152	0	0.152707	1	2.467811	linear	0.172124	1.127152	2.781597	0	0	0	T_delta
CHN	3.870876	0	0.513072	1	1.370383	linear	1.986038	3.870876	5.304584	0	0	0	T_delta
EAF	16.80783	0	0.484122	1	1.806987	linear	8.137034	16.80783	30.37153	0	0	0	T_delta
INDIA	9.455702	0	0.619958	1.000001	2.230118	linear	5.862139	9.455715	21.08734	0	0	0	T_delta
JAP	2.573258	0	0.493471	1	1.294619	linear	1.269828	2.573258	3.331388	0	0	0	T_delta
ME	5.250994	0	0.460022	1	1.612956	linear	2.415574	5.250994	8.46962	0	0	0	T_delta
OCE	3.823174	0	0.552209	1	1.402194	linear	2.111193	3.823174	5.360833	0	0	0	T_delta
RSAM	5.607565	0	0.498616	1	1.248934	linear	2.79602	5.607565	7.003481	0	0	0	T_delta
RSAS	8.95565	0	0.162076	1	1.783891	linear	1.451492	8.95565	15.9759	0	0	0	T_delta
RUS	3.523063	0	0.500289	1	1.488723	linear	1.762548	3.523063	5.244866	0	0	0	T_delta
SAF	6.516844	0	0.465795	1	1.583299	linear	3.03551	6.516844	10.31811	0	0	0	T_delta
SEAS	8.335142	0	0.488695	1	1.516382	linear	4.073341	8.335142	12.63926	0	0	0	T_delta
USA	2.23397	0	-0.20586	1	1.548106	linear	-0.45989	2.23397	3.458423	0	0	0	T_delta
WEU	0.969828	0	0.34556	0.999999	2.24001	linear	0.335134	0.969828	2.172425	0	0	0	T_delta
KOR	2.573258	0	0.493471	1	1.294619	linear	1.269828	2.573258	3.331388	0	0	0	T_delta
INDO	8.95565	0	0.162076	1	1.783891	linear	1.451492	8.95565	15.9759	0	0	0	T_delta
MEX	5.607565	0	0.498616	1	1.248934	linear	2.79602	5.607565	7.003481	0	0	0	T_delta
RCAM	5.607565	0	0.498616	1	1.248934	linear	2.79602	5.607565	7.003481	0	0	0	T_delta
UKR	3.523063	0	0.500289	1	1.488723	linear	1.762548	3.523063	5.244866	0	0	0	T_delta
STAN	3.523063	0	0.500289	1	1.488723	linear	1.762548	3.523063	5.244866	0	0	0	T_delta
TUR	5.250994	0	0.460022	1	1.612956	linear	2.415574	5.250994	8.46962	0	0	0	T_delta
NAF	5.250994	0	0.460022	1	1.612956	linear	2.415574	5.250994	8.46962	0	0	0	T_delta
WAF	16.80783	0	0.484122	1	1.806987	linear	8.137034	16.80783	30.37153	0	0	0	T_delta
RSAF	16.80783	0	0.484122	1	1.806987	linear	8.137034	16.80783	30.37153	0	0	0	T_delta
World	4.562654	0	0.399228	1	1.62659	linear	1.821539	4.562655	7.421568	0	0	0	T_delta

Table 3: Damage function parameters: Non-SLR impacts – Quadratic Quantile Regression

Region	b1	b2	a0.05	a0.50	a0.95	fit	b1_0.05	b1_0.50	b1_0.95	b2_0.05	b2_0.50	b2_0.95	fit_var
BRA	1.175777	4.131337	0.655492	1	1.392482	quadratic	0.770712	1.175777	1.637248	2.708057	4.131336	5.752811	T_delta
CAN	-0.48675	-0.37343	2.197503	1	-0.22551	quadratic	-1.06963	-0.48675	0.109768	-0.82061	-0.37343	0.084213	T_delta
CEU	0.038782	0.968472	0.178048	1	2.842505	quadratic	0.006905	0.038782	0.110238	0.172434	0.968472	2.752886	T_delta
CHN	2.283733	1.399806	0.577719	1	1.38099	quadratic	1.319356	2.283733	3.153811	0.808695	1.399806	1.933118	T_delta
EAF	11.2622	4.04313	0.678678	1	1.845442	quadratic	7.643411	11.2622	20.78374	2.743985	4.04313	7.461363	T_delta
INDIA	6.719669	2.557179	0.639587	1	2.209985	quadratic	4.297812	6.719669	14.85037	1.635538	2.557179	5.651327	T_delta
JAP	1.425295	0.894857	0.661166	1	1.430805	quadratic	0.942357	1.425295	2.039319	0.591649	0.894857	1.280365	T_delta
ME	2.43679	2.332239	0.56406	1	1.310134	quadratic	1.374495	2.43679	3.192522	1.315522	2.332239	3.055546	T_delta
OCE	3.658855	0.128089	0.566432	1	1.415184	quadratic	2.072494	3.658855	5.177953	0.072554	0.128089	0.18127	T_delta
RSAM	4.666082	0.733902	0.554553	1	1.292864	quadratic	2.58759	4.666082	6.032609	0.406987	0.733902	0.948835	T_delta
RSAS	11.40726	-1.91107	0.146099	1	1.662172	quadratic	1.666594	11.40726	18.96082	-0.27921	-1.91107	-3.17653	T_delta
RUS	2.128018	1.167525	0.642456	1	1.515205	quadratic	1.367159	2.128018	3.224384	0.750084	1.167525	1.76904	T_delta
SAF	4.592016	1.483432	0.569732	1	1.305094	quadratic	2.61622	4.592016	5.993013	0.845159	1.483432	1.936019	T_delta
SEAS	6.952581	1.07773	0.543207	1	1.571078	quadratic	3.776689	6.952581	10.92305	0.58543	1.07773	1.693199	T_delta
USA	-1.23066	2.700736	-0.27001	1	2.624565	quadratic	0.332286	-1.23066	-3.22994	-0.72922	2.700736	7.088259	T_delta
WEU	-0.3752	1.262542	0.553629	1	1.579416	quadratic	-0.20772	-0.3752	-0.5926	0.69898	1.262542	1.994079	T_delta
KOR	1.425295	0.894857	0.661166	1	1.430805	quadratic	0.942357	1.425295	2.039319	0.591649	0.894857	1.280365	T_delta
INDO	11.40726	-1.91107	0.146099	1	1.662172	quadratic	1.666594	11.40726	18.96082	-0.27921	-1.91107	-3.17653	T_delta
MEX	4.666082	0.733902	0.554553	1	1.292864	quadratic	2.58759	4.666082	6.032609	0.406987	0.733902	0.948835	T_delta
RCAM	4.666082	0.733902	0.554553	1	1.292864	quadratic	2.58759	4.666082	6.032609	0.406987	0.733902	0.948835	T_delta
UKR	2.128018	1.167525	0.642456	1	1.515205	quadratic	1.367159	2.128018	3.224384	0.750084	1.167525	1.76904	T_delta
STAN	2.128018	1.167525	0.642456	1	1.515205	quadratic	1.367159	2.128018	3.224384	0.750084	1.167525	1.76904	T_delta
TUR	2.43679	2.332239	0.56406	1	1.310134	quadratic	1.374495	2.43679	3.192522	1.315522	2.332239	3.055546	T_delta
NAF	2.43679	2.332239	0.56406	1	1.310134	quadratic	1.374495	2.43679	3.192522	1.315522	2.332239	3.055546	T_delta
WAF	11.2622	4.04313	0.678678	1	1.845442	quadratic	7.643411	11.2622	20.78374	2.743985	4.04313	7.461363	T_delta
RSAF	11.2622	4.04313	0.678678	1	1.845442	quadratic	7.643411	11.2622	20.78374	2.743985	4.04313	7.461363	T_delta
World	1.384329	2.4023	0.738817	1	1.472127	quadratic	1.022766	1.384329	2.037908	1.774859	2.4023	3.536491	T_delta

Table 4: Damage function parameters: SLR impacts – Linear Quantile Regression

Region	b1	b2	a0.05	a0.50	a0.95	fit	b1_0.05	b1_0.50	b1_0.95	b2_0.05	b2_0.50	b2_0.95	fit_var
BRA	2.399666	0	0.47639	0.999999	1.423159	linear	1.143177	2.399664	3.415105	0	0	0	SLR
CAN	1.703589	0	0.394147	1	1.886774	linear	0.671464	1.703589	3.214288	0	0	0	SLR
CEU	2.640391	0	0.292335	1	1.818961	linear	0.771878	2.640391	4.802769	0	0	0	SLR
CHN	1.884873	0	0.458241	1.000001	3.388793	linear	0.863725	1.884875	6.387445	0	0	0	SLR
EAF	0.67048	0	0.283124	1	2.574701	linear	0.189829	0.67048	1.726286	0	0	0	SLR
INDIA	1.155478	0	0.434124	1	2.238202	linear	0.501621	1.155478	2.586194	0	0	0	SLR
JAP	5.814044	0	0.305732	0.999998	2.394948	linear	1.77754	5.814034	13.92433	0	0	0	SLR
ME	4.378659	0	0.280389	1	1.710501	linear	1.227728	4.378659	7.4897	0	0	0	SLR
OCE	2.16075	0	0.518693	1	1.396432	linear	1.120767	2.16075	3.017339	0	0	0	SLR
RSAM	5.178789	0	0.336668	1	2.089337	linear	1.743532	5.178789	10.82024	0	0	0	SLR
RSAS	1.542191	0	0.45005	1	2.197051	linear	0.694063	1.542191	3.388272	0	0	0	SLR
RUS	1.751767	0	0.345174	1	1.809807	linear	0.604664	1.751767	3.170361	0	0	0	SLR
SAF	1.002074	0	0.30792	1	1.752816	linear	0.308559	1.002074	1.756452	0	0	0	SLR
SEAS	5.915389	0	0.413883	1	1.568256	linear	2.448277	5.915389	9.276841	0	0	0	SLR
USA	1.997702	0	0.425114	1	1.71898	linear	0.849251	1.997702	3.43401	0	0	0	SLR
WEU	3.30879	0	0.377016	1.000003	2.986132	linear	1.247468	3.308799	9.880483	0	0	0	SLR
KOR	5.814044	0	0.305732	0.999998	2.394948	linear	1.77754	5.814034	13.92433	0	0	0	SLR
INDO	1.542191	0	0.45005	1	2.197051	linear	0.694063	1.542191	3.388272	0	0	0	SLR
MEX	5.178789	0	0.336668	1	2.089337	linear	1.743532	5.178789	10.82024	0	0	0	SLR
RCAM	5.178789	0	0.336668	1	2.089337	linear	1.743532	5.178789	10.82024	0	0	0	SLR
UKR	1.751767	0	0.345174	1	1.809807	linear	0.604664	1.751767	3.170361	0	0	0	SLR
STAN	1.751767	0	0.345174	1	1.809807	linear	0.604664	1.751767	3.170361	0	0	0	SLR
TUR	4.378659	0	0.280389	1	1.710501	linear	1.227728	4.378659	7.4897	0	0	0	SLR
NAF	4.378659	0	0.280389	1	1.710501	linear	1.227728	4.378659	7.4897	0	0	0	SLR
WAF	0.67048	0	0.283124	1	2.574701	linear	0.189829	0.67048	1.726286	0	0	0	SLR
RSAF	0.67048	0	0.283124	1	2.574701	linear	0.189829	0.67048	1.726286	0	0	0	SLR
World	3.150307	0	0.390043	1	1.732618	linear	1.228756	3.150307	5.458279	0	0	0	SLR

Table 5: Damage function parameters: SLR impacts – Quadratic Quantile Regression

Region	b1	b2	a0.05	a0.50	a0.95	fit	b1_0.05	b1_0.50	b1_0.95	b2_0.05	b2_0.50	b2_0.95	fit_var
BRA	2.060513	1.431372	0.516495	0.999999	1.404666	quadratic	1.064246	2.060512	2.894333	0.739297	1.431371	2.0106	SLR
CAN	0.7314	3.407293	0.43887	1	1.969629	quadratic	0.320989	0.7314	1.440587	1.495358	3.407293	6.711103	SLR
CEU	1.742667	3.497085	0.361205	1	1.841368	quadratic	0.62946	1.742667	3.20889	1.263165	3.497085	6.43942	SLR
CHN	1.170041	3.411595	0.443642	0.999995	3.004965	quadratic	0.519079	1.170035	3.515933	1.513527	3.411576	10.25172	SLR
EAF	2.068301	-5.44768	0.712914	1	1.2237	quadratic	1.474521	2.0683	2.53098	-3.88373	-5.44768	-6.66632	SLR
INDIA	0.995344	0.48533	0.442576	1.000001	2.305955	quadratic	0.440516	0.995346	2.29522	0.214796	0.485331	1.11915	SLR
JAP	2.915393	11.60917	0.265783	1	2.250236	quadratic	0.774863	2.915393	6.560322	3.085524	11.60917	26.12338	SLR
ME	5.463913	-4.22761	0.240477	1	1.541783	quadratic	1.313944	5.463913	8.424166	-1.01664	-4.22761	-6.51805	SLR
OCE	2.150755	0.038933	0.520115	1	1.39625	quadratic	1.11864	2.150755	3.002992	0.02025	0.038933	0.05436	SLR
RSAM	6.950465	-6.90156	0.276967	1	1.849809	quadratic	1.92505	6.950465	12.85703	-1.91151	-6.90156	-12.7666	SLR
RSAS	3.507817	-7.65709	0.634973	1	1.574318	quadratic	2.227367	3.507817	5.522418	-4.86204	-7.65709	-12.0547	SLR
RUS	0.729692	3.786629	0.417189	1	1.88446	quadratic	0.304419	0.729692	1.375075	1.579738	3.786629	7.13575	SLR
SAF	0.427499	2.144436	0.433386	1	1.821761	quadratic	0.185272	0.427499	0.778801	0.929368	2.144436	3.90665	SLR
SEAS	7.507166	-6.20077	0.354522	1	1.39835	quadratic	2.661457	7.507166	10.49765	-2.19831	-6.20077	-8.67084	SLR
USA	1.344848	2.543189	0.504828	1	1.69726	quadratic	0.678917	1.344848	2.282558	1.283872	2.543189	4.316454	SLR
WEU	1.119965	11.11571	0.341114	1	2.41524	quadratic	0.382036	1.119966	2.704985	3.791728	11.11571	26.8471	SLR
KOR	2.915393	11.60917	0.265783	1	2.250236	quadratic	0.774863	2.915393	6.560322	3.085524	11.60917	26.12338	SLR
INDO	3.507817	-7.65709	0.634973	1	1.574318	quadratic	2.227367	3.507817	5.522418	-4.86204	-7.65709	-12.0547	SLR
MEX	6.950465	-6.90156	0.276967	1	1.849809	quadratic	1.92505	6.950465	12.85703	-1.91151	-6.90156	-12.7666	SLR
RCAM	6.950465	-6.90156	0.276967	1	1.849809	quadratic	1.92505	6.950465	12.85703	-1.91151	-6.90156	-12.7666	SLR
UKR	0.729692	3.786629	0.417189	1	1.88446	quadratic	0.304419	0.729692	1.375075	1.579738	3.786629	7.13575	SLR
STAN	0.729692	3.786629	0.417189	1	1.88446	quadratic	0.304419	0.729692	1.375075	1.579738	3.786629	7.13575	SLR
TUR	5.463913	-4.22761	0.240477	1	1.541783	quadratic	1.313944	5.463913	8.424166	-1.01664	-4.22761	-6.51805	SLR
NAF	5.463913	-4.22761	0.240477	1	1.541783	quadratic	1.313944	5.463913	8.424166	-1.01664	-4.22761	-6.51805	SLR
WAF	2.068301	-5.44768	0.712914	1	1.2237	quadratic	1.474521	2.0683	2.53098	-3.88373	-5.44768	-6.66632	SLR
RSAF	2.068301	-5.44768	0.712914	1	1.2237	quadratic	1.474521	2.0683	2.53098	-3.88373	-5.44768	-6.66632	SLR
World	2.647871	1.957241	0.426352	1	1.727301	quadratic	1.128926	2.647871	4.57367	0.834474	1.957241	3.380745	SLR

7.5. Appendix E:

Identifying differences between direct and indirect damages in economic assessments with IAMs and CGEs

Direct damages result from monetising a specific impact by multiplying the expected material damage by its corresponding monetary cost and the result could be expressed as a percentage of GDP.
Indirect damages are the result of using the direct damages as inputs in economic models that provide indicators of production at the macro level and are usually expressed as percentage changes of GDP or sectoral output. These indirect damages represent additional (indirect) effects that could increase or decrease the magnitude of the initial direct damages.
The differences between direct and indirect damages within an economic assessment can be explained by considering two main aspects. The first one concerns damage propagation over time and across the economy, while the second one relates to the entry points used for the assessment, which vary depending on the economic model (IAM or CGE).

Damage propagation

Among indirect damages there are two main categories. The first one regards the indirect effects on production through changes in investments, which eventually have cumulative effects over time. The second category represents the economy-wide effects derived from the intertwined structure of an economic market where the product of one sector is used as an input by the rest of the sectors to produce other goods and services. Due to this explicit market structure, there is a propagation effect when one sector's output is reduced, which affects all other sectors using that product as an input. Therefore, this second category has effects both across the economy and over time.

Figure D1 depicts the production process for n sectors in the economy (Si to Sn) showing the inputs used to produce goods or services. On the input side there are primary factors (capital, labour, and land) that constitute the value added in the production process. These primary factors are then combined with other goods or services (intermediate inputs), provided by the rest of the sectors in the economy, to produce the final output of sector i.

This production chain is useful to identify the propagation of damages throughout the economy. The area of each rectangle in the output column (middle of Figure D1) represents the output of each sector with the red area representing production losses due to climate change. If climate change impacts only sector 1 of the economy, the reduction of its output could be interpreted as the direct damage, since the expected damage is measured as the reduction of sector 1 (S1) output. Given that S1 output is also used in the production processes of the rest of the sectors in the economy, the damage propagates as economy-wide indirect damages because S1 output cannot be replaced by other products. Therefore, total damages are the sum of the direct damages in S1 plus the indirect damages in the rest of the sectors. In addition, there are the cumulative effects over time derived from the reduced output in all sectors. To these effects we must add the corresponding changes

in investments (not depicted in Figure D1) which end up affecting the capital available for use by each sector and its growth in the future.

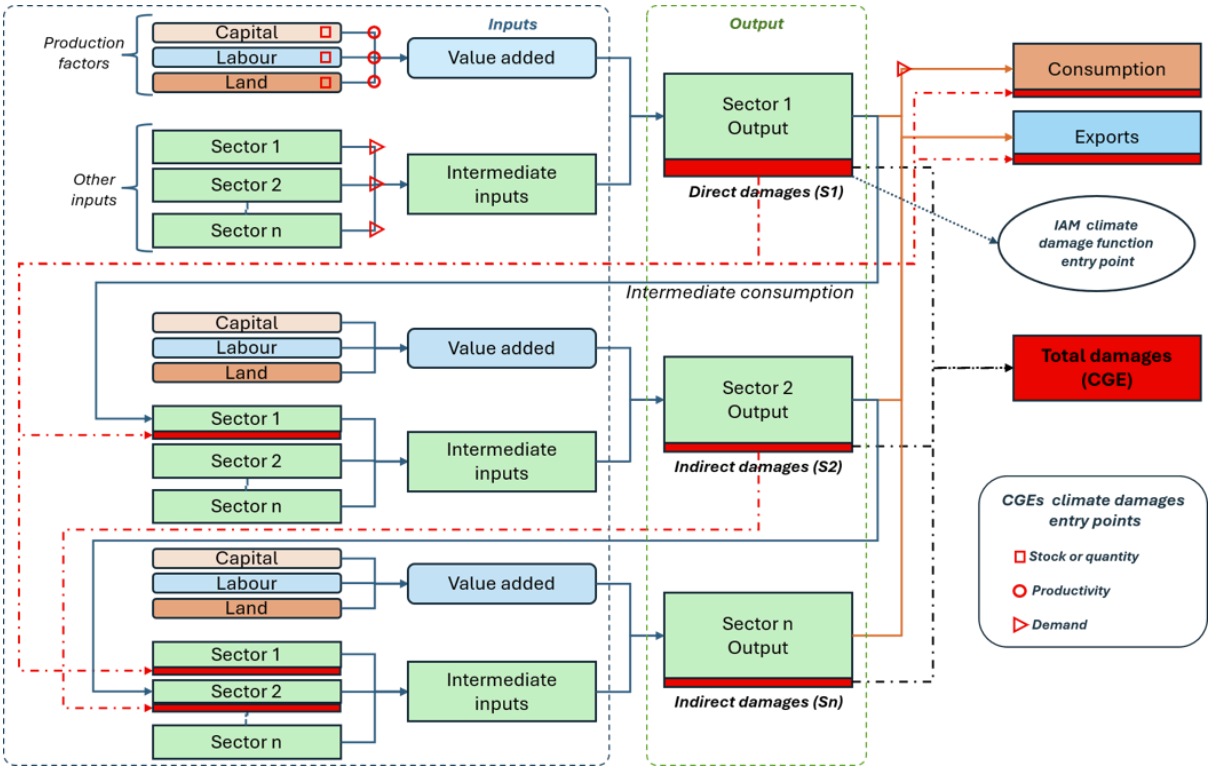

Figure D1: Economy-wide propagation of direct damages

Damage entry points and interlinkages

Figure 1 is useful for explaining the differences between the assessments produced by IAM and CGE models by identifying the entry points. An IAM is usually aggregated at the national or regional level and represents the economy as one sector or few sectors. To internalize climate change damages IAMs use a damage function that reduces GDP or final output. This could be roughly represented by assuming the economy is only sector 1 in Figure D1. The model uses direct damages as information to reduce output by means of a climate damage function as shown in the figure (see Direct cost S1) and produces indirect damages through the investment channel embedded in its aggregated economic structure. The CGE models used in ACCREU are multi-region and multi-sector models with several entry points depending on the impact, identified as red boxes, circles or triangles for S1. Most of the entry points are in the production process (supply), specifically as changes in the quantity (red box) or productivity (red circle) of primary factors or the demand for intermediate inputs (red triangles), which end up changing production. Other entry points are in the final demand for specific goods or services (see the red triangle for final consumption at the top right of Figure D1).

While changes in production are propagated as shown in Figure D1, there are also other interaction channels derived from the general equilibrium structure that adjust all prices to equalize supply and demand of products (goods/services) and production factors (capital, labour and land). The corresponding changes in prices will affect the cost structure of each

sector, which will adjust its demand for inputs to respect its budget constraint. The interaction of all these channels in the CGE framework can amplify or dampen the initial direct impacts depending on the magnitude and the interlinkages of the initially affected sector with the rest of the economy.

Take sea-level rise or riverine floods as examples. The direct damage is the expected annual damage estimated by specific models. In an IAM, such damage will enter as part of the climate damage function reducing GDP or consumption. In a CGE model, those damages could enter in the production process of all affected sectors through the following channels:

1. Reducing the availability of capital stock using information on expected annual damages to assets.
2. Reducing labour productivity by using information on affected people.
3. Reducing land stock due to flooding.

These three channels involve primary factors that are substitutable to a certain extent. This implies that the affected sector will demand more of the other primary factors to compensate for the reduced availability of one input. Given the limited supply of primary factors across the economy, their prices will rise inducing adjustments in the production and prices of the remaining sectors. This entire process generates a propagation of direct damages, which can be aggregated to estimate the total indirect damages, that will also be compounded over time.